MOLECULAR AND PHYSIOLOGICAL INTERACTIONS WITHIN THE DUCKWEED MICROBIOME AND WITH THE MODEL PLANT, *ARABIDOPSIS THALIANA*, VIA THE AUXIN PATHWAY

By

SARAH GILBERT

A dissertation submitted to

the School of Graduate Studies

Rutgers, The State University of New Jersey

In partial fulfillment of the requirements

For the degree of

Doctor of Philosophy

Graduate Program in Plant Biology

Written under the direction of

Eric Lam

And approved by

_____

_____

_____

_____

New Brunswick, New Jersey

October 2019

ABSTRACT OF THE DISSERTATION

Molecular and Physiological Interactions within the Duckweed Microbiome and with the Model plant, *Arabidopsis thaliana*, via the Auxin Pathway

by SARAH GILBERT

Dissertation Director:

Dr. Eric Lam

Duckweeds are small aquatic plants with applications in wastewater treatment, biofuel production and animal feed additive. Although duckweeds grow rapidly all over the world, man-made farming remains a challenge for large-scale production. Our growing world population requires sustainable agricultural practices that involve introduction of novel crops such as duckweeds and improved farming methods for existing crops. Beneficial microbes are of interest to improve plant health and yield. Thus, understanding interactions between plants and bacteria would be necessary for proper selection of bacterial strains and application procedures. Many bacteria are known to improve plant growth by production of phytohormones such as indole-3-acetic acid (IAA), an auxin commonly found in nature. In this thesis, we aim to 1) Characterize the duckweed microbiome by auxin production to identify potential growth promoting strains, 2) Determine the mechanisms of plant-bacteria interactions via the auxin pathway, and 3) Determine the mechanisms of auxin signaling within tripartite interactions.

Isolation of forty-seven strains of duckweed associated bacteria (DABs) from various duckweed clones provided an excellent resource for studying the diversity of interactions within the duckweed microbiome. Characterizing the duckweed microbiome by auxin production led to evidence for an association between the type of indole related compound produced by the DAB and the duckweed genus that it was isolated from. Binary association assays with DABs capable of producing indole related compounds revealed two genetically similar *Microbacterium* strains DAB 1A and DAB 33B. DAB 1A, but not DAB 33B, caused an auxin associated short root phenotype on the model plant *A. thaliana*. Yet both strains can cause similar, but not identical, transcriptional responses that included known auxin-responsive genes in the plant, indicating various roles of auxins in signaling between bacteria and the plant host. Co-inoculation of DAB 1A and *Herbaspirillum* strain DAB 5E onto *A. thaliana* resulted in suppression of the short root phenotype. Based on results from auxin-response reporter plant lines and auxin stability studies with bacteria culture, we propose that DAB 5E degrades IAA at high levels, which can enhance its growth and competition among other strains, while maintaining IAA response in the plant to escape detection. Altogether, these results suggest various roles of indole related compounds, such as IAA, in assembly of the plant microbiome.

ACKNOWLEDGMENTS

There are many people that I am extremely grateful to have supported me throughout my graduate studies. I would like to thank the various people who have made the completion of my degree possible.

I would like to express my deepest appreciation to my advisor, Dr. Eric Lam, for his mentorship from the beginning of my lab rotation through to completion of this degree. His enthusiasm for science and dedication to his lab drew my initial interest to duckweed research. Throughout my studies, he has taught me the importance of scientific storytelling.

I would also like to thank my committee members, Dr. Ilya Raskin, Dr. Juan Dong and Dr. Mohamed Donia. They have supported my research by collaborating on projects. I also appreciate their unique perspectives and feedback during committee meetings, which greatly improved my project scope and final dissertation.

I would like to thank my labmates, who have provided intellectual and emotional support. This experience would not have been as enjoyable and memorable without them. I would also like to thank Dr. Alexander Poulev for his mass spectrometry work, my lab mentees, Katie Scott, Jacob Armitage, and Jenny Xu who dedicated time to this dissertation and my collaborators at the DOE Joint Genome Institute and the Environmental Molecular Sciences Laboratory.

I am especially grateful for the funding and travel grants provided by the Rutgers Division of Life Sciences Undergraduate Instruction, the Robert and Lillian White-Stevens Graduate Fellowship, the Rutgers Graduate School, and the Rutgers Plant Biology Graduate Program.

Finally, a special thanks to my friends and family, particularly my parents and sister, who provided tremendous support throughout the entire process. I am very lucky to have them.

TABLE OF CONTENTS

LIST OF TABLES

Chapter 2

Chapter 3

Chapter 4

LIST OF FIGURES

Chapter 1

Chapter 2

Chapter 3

CHAPTER 1

Introduction

1.1 Thesis Goals

The specific goals of this thesis were to 1) Characterize the duckweed microbiome by auxin production to identify potential growth promoting strains, 2) Determine the mechanisms of plant-bacteria interactions via the auxin pathway, and 3) Determine the mechanisms of auxin signaling within tripartite interactions. The contributions of this work to our molecular and biochemical understanding of plant-bacteria interactions and the impact on improving plant health are discussed.

The outline of this thesis is as follows: A general introduction (Ch.1) on the biology and microbiome of the duckweed plant, the role of auxin in plant-bacteria interactions and current research on plant microbiome assembly and synthetic bacterial communities for improved plant health. The following chapters discuss characterization of the duckweed microbiome by auxin production (Ch.2), physiological and molecular effects of individual auxin-producing bacterial strains on the model plant, *Arabidopsis thaliana,* (Ch. 3) and physiological, molecular and biochemical effects of multiple auxin-producing bacterial strains on *A. thaliana* (Ch.4). A general summary (Ch.5) reiterates the overall findings and addresses the implications of this work for understanding plant microbiome assembly.

1.2 Biology of Duckweeds

Lemnaceae, more commonly known as duckweed, are aquatic plant species that grow in stagnant ponds. The subfamily Lemnoideae consists of *Lemna*, *Spirodela* and

Landoltia, whereas Wolffioideae consists of *Wolffia* and *Wolffiella*. The five genera are comprised of 37 species and over 1000 individual clones are stored in the Rutgers Duckweed Stock Cooperative (RDSC) at Rutgers University, New Brunswick, NJ. Duckweeds preferentially reproduce via asexual propagation and are found growing all over the world. The duckweed structure differs from soil-based plants in that it consists of a flat leaf-like structure called a frond. The frond can range in size from less than 0.1 mm^2 of *Wolffia globosa* to 39 mm^2 of *Spirodela polyrhiza* (Landolt and Kandeler, 1987). Duckweed genera vary in the number of roots and they lack lateral roots and root hairs. Dormant, starch-filled structures called turions overwinter at the bottom of ponds and then develop into fronds that grow rapidly during the summer months and cover the surface of the water.

Duckweeds are eaten and carried by fish, turtles, birds and humans. They have been eaten for thousands of years in Asian countries such as Thailand, Laos, and Cambodia. Certain clones can be up to 45 % (dry weight) protein and they contain more of the essential amino acids than other plant-based proteins (Appenroth et al., 2017; Landolt and Kandeler, 1987). In addition to being attractive for animal and human consumption, duckweeds have become of interest as a low-cost alternative in wastewater treatment since they are efficient in the removal of nitrogen and phosphate which allows for water reuse (Korner and Vermaat, 1998). Furthermore, the duckweed biomass can then be harvested for biofuel production since certain clones have been shown to reach 45% starch (dry weight) (Cheng and Stomp, 2009).

1.3 Microbiome of Duckweeds

Man-made duckweed systems have been developed by private companies around the world for wastewater treatment, biofuel/bioplastic production, and animal feed additive. In these systems and laboratory facilities, duckweeds often compete with algae and fungi contamination, but bacterial competition is less observed. Recent studies have revealed that duckweed associated bacteria (DABs) can improve the growth of duckweed by increasing frond production rate as well as higher chlorophyll content (Yamaga et al., 2010; Suzuki et al., 2014). Some duckweed associated bacterial strains were found to breakdown phenol contaminants or increase the removal of nitrogen and phosphate from wastewater by these aquatic plants, which may be correlated with their ability to promote plant growth (Yamaga et al., 2010; Suzuki et al., 2014). After inoculation of a PGPB isolated from the surface of the duckweed, *Lemna aoukikusa* (indistinguishable from *Lemna aequinoctialis* using atpF-atpH and psbK-psbI barcodes [Borisjuk et al., 2015]), there was an observed increase in chlorophyll content in the monocotyledon *Lemna minor* as well as the dicotyledon *Lactuca sativa* (Suzuki et al., 2014).

Clones brought to the Rutgers Duckweed Stock Cooperative (RDSC) from their natural environment are first sterilized for research purposes. During the sterilization process, it is often difficult to completely rid of all bacteria, with contamination sometimes appearing months later. Thus, we speculated that certain bacterial strains may have a strong association with the duckweed tissue. With over 1000 clones collected from all over the world, the Rutgers Duckweed Stock Cooperative (RDSC) provides an excellent resource of natural variation for studying the duckweed microbiome. In a preliminary study, Actinobacteria strain 1A and Firmicutes strain 3D were isolated from *Lemna* and *Spirodela* respectively, and then inoculated onto sterile *Lemna.* After being

grown in the greenhouse, fronds that were inoculated with bacteria appeared darker green, suggesting potential plant growth promotion abilities (Figure 1.1). Studying plant growth promotion by the duckweed microbiome may provide insight to how bacteria associate with plants, escape the host immune system and elicit morphological and molecular changes to induce a plant response.

1.4 Role of Auxin in Plant-Bacteria Interactions

In general, plant growth promoting bacteria (PGPB) have been shown to improve plant health by increasing nutrient availability, providing defense against pathogens, protection from abiotic stresses, and producing phytohormones such as auxin (Santoyo et al., 2016). To understand the plant growth promotion mechanism of Actinobacteria strain 1A we inoculated it onto sterile *Lemna* and grew the inoculated plant under sterile conditions in a growth chamber. Contrary to the greenhouse experiment, no phenotypic changes in plant tissue were observed (Figure 1.2a). However, inoculation onto the model plant, *Arabidopsis thaliana,* resulted in a short root phenotype (Figure 1.2b). Due to the differences in plant morphology between duckweeds and *A. thaliana,* particularly the root structure, we concluded that *A. thaliana* may provide a better plant system for studying the mechanisms of plant-bacteria interactions.

Observation of the short root phenotype by the Actinobacteria strain 1A under the microscope also revealed an increase in root hairs (Figure 1.3). Auxin is a plant hormone that is known to result in this phenotype. We inoculated various concentrations of indole-3-acetic acid (IAA) onto *A. thaliana* and observed a similar phenotype to that of inoculation with the Actinobacteria strain 1A (Figure 1.4). We hypothesized that strain 1A may be producing auxin, thus resulting in the short root phenotype.

The phytohormone IAA is the most commonly occurring auxin found in nature and is produced by both plants and bacteria through a similar biosynthetic pathway (Mano and Nemoto, 2012; Spaepen and Vanderleyden, 2011). It is suggested that over 80% of rhizosphere bacteria may be capable of synthesizing IAA (Spaepen and Vanderleyden, 2011). Production of IAA by microbes may affect plant health, through gall formation by pathogens or by increase in root nodules and root biomass by plant growth promoting bacteria (PGPB) (Spaepen and Vanderleyden, 2011). High concentrations of IAA produced by bacteria have been shown to increase overall root biomass, allowing the plant to better uptake water and minerals, which in turn can enhance bacteria colonization (Duca et al., 2014; Spaepen and Vanderleyden, 2011).

The many IAA biosynthesis pathways found in plants and bacteria indicate that IAA may have additional roles besides being involved in plant development (Spaepen et al., 2011). There is evidence that IAA may act as a signal molecule between bacteria and plants (Bianco et al., 2006; Lui and Nester, 2006; Spaepen et al., 2007). For example, one study found that IAA was downregulated by the plant to provide defense against pathogens (Navarro et al., 2006). A commonly studied PGPB is *Azospirillum brasilense* which produces IAA through the indole pyruvic acid pathway. An *A. brasilense ipdC* knockout mutant produced less than 10% the wild-type level of IAA, demonstrating that this gene is critical in IAA production by this strain (Broek et al., 1999). Furthermore, expression of *ipdC* was upregulated by IAA and synthetic auxins indicating that not only are genes regulated by IAA in plants but also in bacteria (Broek et al., 1999). Conversely, certain Proteobacteria strains have been shown to degrade IAA by the iac gene operon and convert it into catechol to be used as a carbon source (Greenhut et al., 2018).

Indole is a less common, naturally occurring compound that has been shown to be a signal molecule between microbes in biofilm formation and quorum sensing (Martino et al., 2003; Lee and Lee, 2010). However, in contrast to the case of IAA, the role of various indole related compounds during plant-microbe interactions is poorly understood.

1.5 Plant Microbiome Assembly

Soil based bacteria have been categorized into separate compartments in which they associate with the plant, the phyllosphere (the above ground region), rhizosphere (the surrounding soil) and endophytic region (the closely associated space between or within plant cells). Much research has been performed to survey the diversity of rhizosphere bacteria isolated from the surrounding soil of plants (Bai et al., 2015; Berendsen et al., 2012; Haney et al., 2015). Microbes living in the rhizosphere contribute to plant growth, carbon sequestration, and phytoremediation (Lundberg et al., 2012). Various studies have compared the microbial diversity in the different plant compartments as well as how plant genotype and soil type alter the microbiome (Bulgarelli et al., 2012; Edwards et al., 2015; Lundberg et al., 2012; van der Heijden et al., 2015). While host genotype, soil type, and cultivation practices play a role in shaping the microbiome, one study found that the largest variation in microbial diversity is seen across the three compartments of the plant (phyllosphere, endophytic region, and rhizosphere) (Lundberg et al., 2012). The plant microbiome undergoes a loss of diversity from the rhizosphere to the endophytic compartment, where strains become enriched or depleted (Lundberg et al., 2012). Enrichment and exclusion may take place by the plant immune system or other microbes however the exact mechanisms are poorly understood.

Most of our understanding of microbiome assembly by the plant immune system comes from studies on microbe-associated molecular patterns (MAMPs) and effector proteins, which recognition by plants leads to MAMP-triggered immunity (MTI) and effector-triggered immunity (ETI), respectively. In an evolutionary race, plants and microbes evolve receptors and signals to recognize one another or escape recognition as explained by the 'guard hypothesis' and 'zig zag model' (Jones and Dangl, 2006). However, the microbiome is composed of pathogens as well as beneficial microbes, and assembly can be shaped by the members themselves, whether it be through direct suppression or resource competition (Berg and Koskella, 2018; Helfrich et al., 2018). Furthermore, the plant can secret chemical signals to recruit beneficial microbes (Rudrappa et al., 2008). The mechanisms of how the microbiome is assembled are of increasing interest for deploying synthetic bacterial communities to improve plant health.

1.6 Synthetic Bacterial Communities

Conventional methods to improve plant health involve the use of herbicides, pesticides, and fertilizers. Increased use of these chemicals can result in leaching into waterways and disrupting the ecosystem. Synthetic bacterial communities, such as the probiotic medicines used for human health, may provide an alternative method to improve plant health. The methods of constructing synthetic bacterial communities traditionally consist of a bottom-up or top-down approach. The bottom-up approach involves first screening for a PGBP through binary interactions. Over the years, binary plant-bacteria interactions have provided insight to the mechanisms of plant immunity. Similarly, binary-association assays have shed light on the symbiotic relationship between nodule-forming bacteria and legumes (Oldroyd et al., 2009). However, these

findings do not always translate to an agricultural setting where plants are exposed to a range of different bacterial and fungal pathogens and symbionts. The top-down approach typically involves randomly selecting different combinations of bacterial communities to screen for a phenotype (Ristova et al., 2016). This process can be time consuming and costly by requiring a large amount of resources. Reproducing the effects of the community can also be challenging when the individual functions of each bacterial strain are unknown. Recently, synthetic bacterial communities have been successfully studied on *A. thaliana* using binary-association assays to inform construction of small communities that lead to predicted phenotypes (Paredes et al., 2018). While the study focused on phosphate accumulation in *A. thaliana*, in this thesis we have concentrated on the auxin pathway. Similarly, we used binary-association assays to inform construction of tripartite interactions. Individual strains from this work can then be incorporated into natural plant microbiomes and compared in a large community setting. Hopefully by understanding both plant-bacteria interactions and bacteria-bacteria interactions, we can successfully deploy a synthetic community in an agricultural setting.

1.7 Figures

Figure 1.1. Inoculation of RDSC duckweed associated bacteria onto sterile *Lemna.*

Inoculation of Actinobacteria strain 1A and Firmicutes strain 3D improved the health of *Lemna* compared to the sterile control as demonstrated by darker frond color, suggesting increased chlorophyll content.

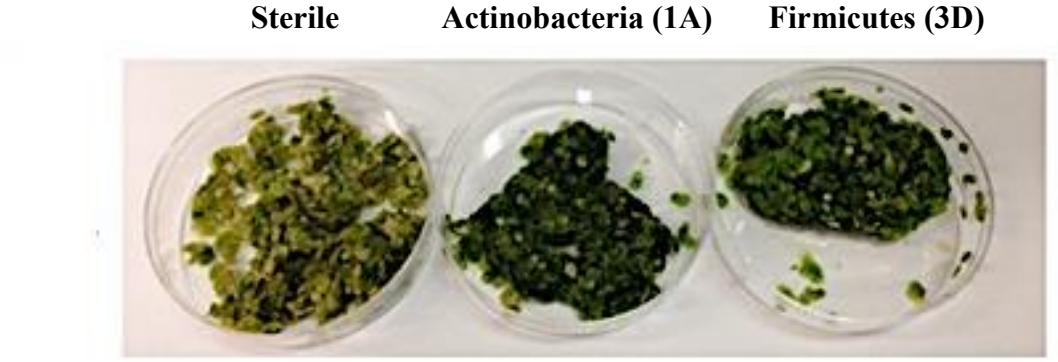

Photo courtesy of Lam Lab.

Figure 1.2. Effect of Actinobacteria strain 1A on duckweed and *Arabidopsis* root morphology. Inoculation of 1A onto **A)** *Lemna* and **B)** *A. thaliana*. Plate gridlines represent 13 mm.

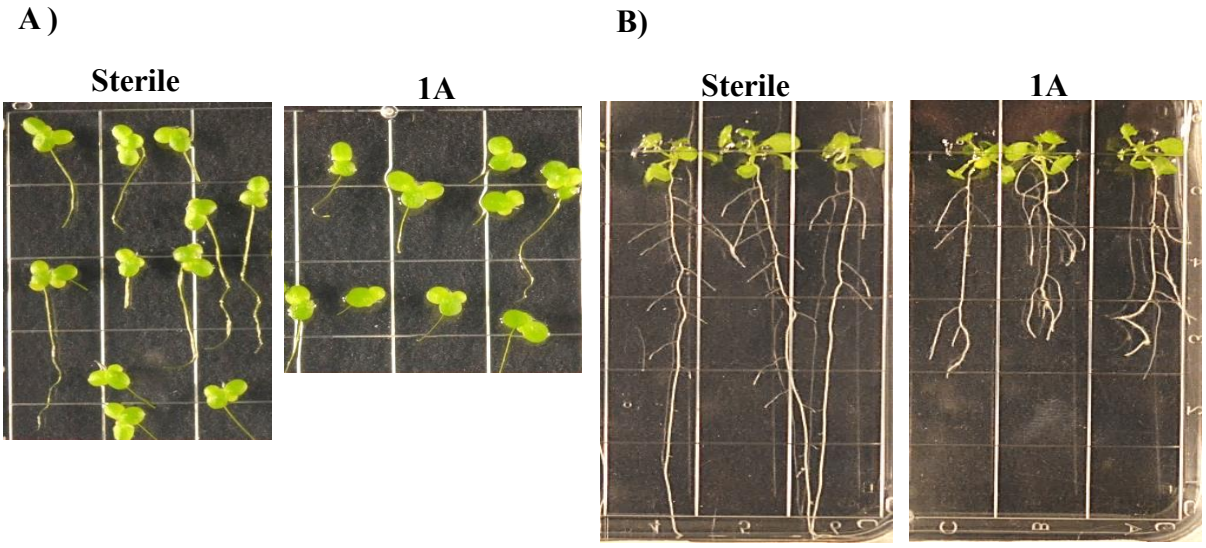

Figure 1.3. Effect of Actinobacteria strain 1A on *Arabidopsis* root hairs. Inoculation of 1A caused an increase in *A. thaliana* root hairs compared to the sterile control. Phase contrast microscopy was performed using the Olympus FSX100 microscope at 1/90 second exposure time with the 10x objective lens.

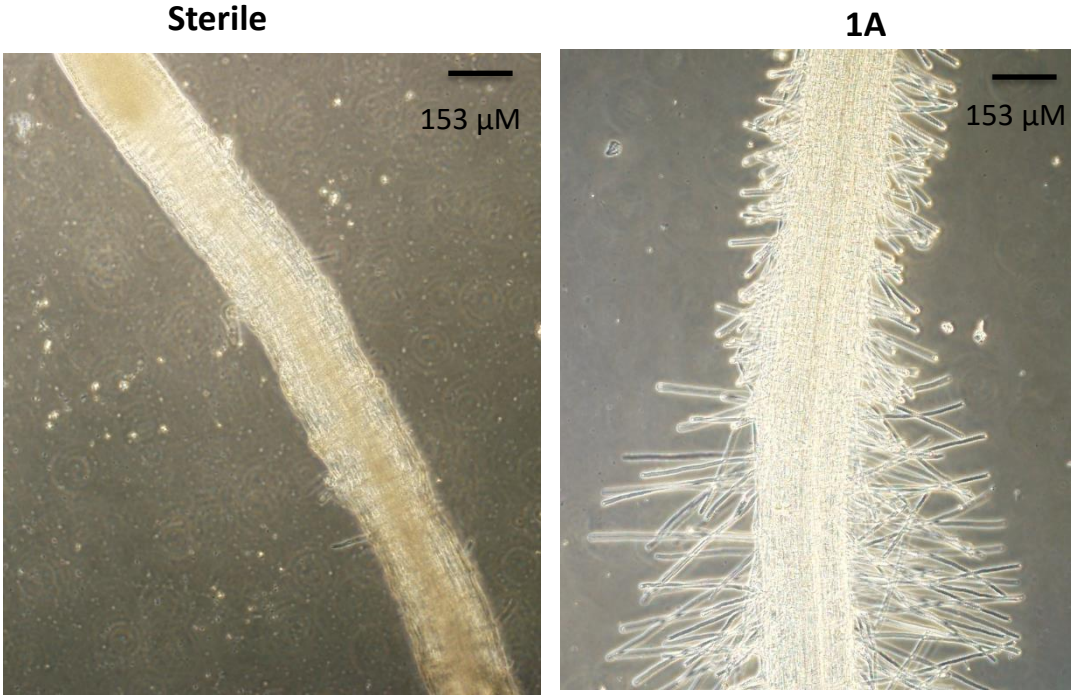

Figure 1.4. Effect of indole-3-acetic acid (IAA) on *Arabidopsis* roots. Increasing concentrations of IAA were applied to Col-0, which stunted primary root growth while increasing the length and number of lateral roots.

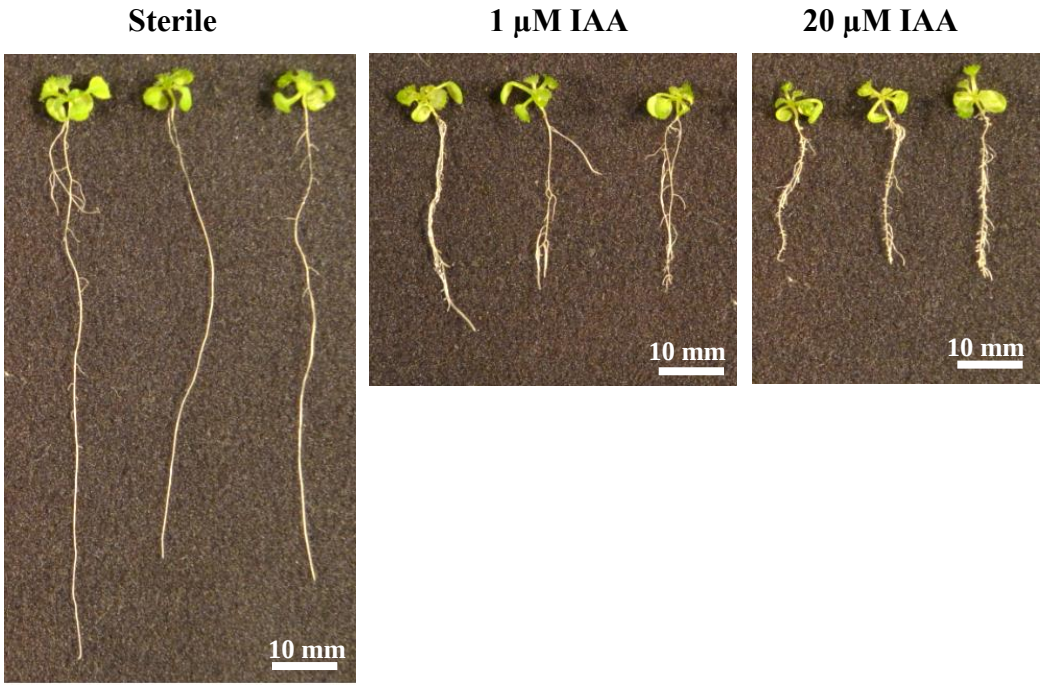

CHAPTER 2

Bacterial production of indole related compounds reveals their role in association between duckweeds and endophytes

Front Chem. 2018 Jul 12; 6:265

2.1 Abstract

Duckweed farming can be a sustainable practice for biofuel production, animal feed supplement and wastewater treatment, although large scale production remains a challenge. Plant growth promoting bacteria have been shown to improve plant health by producing phytohormones such as auxin. While some of the mechanisms for plant growth promotion have been characterized in soil epiphytes, more work is necessary to understand how plants may select for bacterial endophytes that have the ability to provide an exogenous source of phytohormones such as auxin. We have isolated and characterized forty-seven potentially endophytic bacteria from surface-sterilized duckweed tissues and screened these bacterial strains for production of indole related compounds using the Salkowski colorimetric assay. Indole-3-acetic acid (IAA), indole-3-lactic acid (ILA), and indole produced by various bacterial isolates were verified by mass spectrometry. Using the Salkowski reagent, we found that 79% of the isolated bacterial strains from our collection may be capable of producing indole related compounds to various extents during *in vitro* growth. Of these bacteria that are producing indole related compounds, 19% are producing both IAA and indole. There is an apparent correlation between the type of indole related compound produced by a particular bacteria and the duckweed genus from which the bacterial strain is derived. These results suggest the possible association between different duckweed genera and endophytes that are

producing distinct types of secondary metabolites. Understanding the role of indole related compounds during interaction between endophytes and the plant host may be useful to help design synthetic bacterial communities that could target specific or multiple species of duckweed in the future to sustainably enhance plant growth.

2.2 Introduction

In this work, we have characterized a set of 47 duckweed-associated bacteria (DABs) based on their production of indole related compounds by using the Salkowski reagent and mass spectrometry. The Salkowski reagent consists of ferric chloride and perchloric acid that when mixed with IAA produces a pink color (Gordon and Weber, 1951). Well characterized *Azospirillum brasilense* strains Sp7 and Sp245, originally isolated as plant-associated bacteria from wheat tissues (Bashan and de-Bashan, 2010), were used in our work as positive controls since they are known to produce IAA and one is an epiphyte (Sp7) while the other is an endophyte (Sp245) in wheat. Analysis of duckweed associated endophytes reveals that the production of indole is correlated with the DAB being associated with the *Wolffia* genus whereas the production of indole related compounds such as IAA is correlated with those DABs that were isolated from the *Lemna* genus. Indole and indole related compounds, IAA and indole-3-lactic acid (ILA), were detected from cultures of a subset of DABs in our collection and their potential role in improving duckweed plant health is discussed. Future work may involve screening for effects on the production of other plant hormones such as gibberellin or modulation of host ethylene production by strains in our collection.

2.3 Methods

2.3.1 Duckweed Tissue

Plant material was obtained from the Rutgers Duckweed Stock Cooperative at Rutgers University, New Brunswick, NJ, USA. Plant strains were maintained in 60 mm x 15 mm Petri dish on 0.5X Schenk and Hildebrandt (SH) Basal Salt Mixture (pH 5.7) supplemented with 0.8% w/v Difco Agar, granulated. Plants were additionally maintained on 0.5X SH medium (pH 5.7) with 0.8% w/v agar and 0.5% sucrose with and without the addition of 100 mg/L cefotaxime. The plants were grown at a temperature of 15°C under illumination of 40-44 µmol m^{-2} s^{-1} light. Duckweed strains stored at the Rutgers Duckweed Stock Cooperative originate from various locations in the world. Duckweed strains were also collected June 2015 from various locations in New Jersey, USA.

2.3.2 Isolation of Bacteria

To isolate duckweed associated bacterial strains, duckweed tissue was surface sterilized before placing on LB (Miller) agar medium or Tryptic Soy Agar (TSA). Duckweed tissues were rinsed in 1.5 mL eppendorf tubes with sterile Rinse Solution (0.1% Triton-X, 137 mM NaCl, 2.7 mM KCl, 10 mM Na_2HPO_4•$7H_20$, 1.8 mM KH_2PO_4, 0.5 mM $MgSO_4$, 1 mM $CaCl_2$, pH 7.4) for one minute and then decanted. For isolation using bleach, an extra step was performed by washing the tissue in 0.6% (v/v) sodium hypochlorite until only the meristem retained chlorophyll and then washing with 2% $Na_2S_2O_3$ for one minute to neutralize the bleach. The solution was decanted and the tissue was washed in sterile Millipore water for one minute. The tissue was then homogenized using a plastic drill and then spread onto LB agar plates or TSA plates. The plates were incubated at 28°C for up to 72 hrs. Colonies on the plates were picked and re-streaked

several times on LB or TSA plates for single colonies to obtain pure isolates. Bacterial strains were stored at -80°C in LB or Tryptic Soy Broth (TSB) supplemented with 40% sterilized glycerol.

2.3.3 Fluorescent Microscopy

To confirm the bleach treatment that we employed to isolate candidate endophytic bacteria from duckweed can effectively remove most if not all surface-associated bacteria, fluorescent microcopy was performed on *Lemna minor* strain 370-DWC112 inoculated with DAB 1A. Plant tissue was treated with 0.3% (v/v) sodium hypochlorite for 2 minutes using the method described for isolation of bacteria, which left only the meristem to retain chlorophyll. The tissue was placed in a microcentrifuge tube with 100 µL of 6 µM Syto 9 stain (ThermoFisher Scientific, Waltham, MA). The Syto 9 stain was removed after 3 minutes and the tissue was washed twice with 200 µL of sterile water. The tissue was then placed on a microscope slide and observed using an Olympus FSX100 epifluorescence microscope (460-495 nm excitation/510-550 nm emission). To image the surface of the plant tissue, the 10x objective lens was first used to focus on the guard cells of the stomates before switching to higher magnification objectives to resolve stained bacteria on the same focal plane.

2.3.4 Genotyping Duckweed Strains

Plant DNA was isolated by grinding 100 mg fresh weight of the tissue in liquid nitrogen and 500 µL of 1x CTAB buffer with 5 µL of 2-mercaptoethanol. The extract was incubated at 65°C for 30 minutes. 1x volume of phenol/chloroform/isoamyl alcohol (25:24:1) was added. The extract was centrifuged at 10,000x g for 5 minutes and then the aqueous phase was transferred into a new tube. 2 µL of RNase A (10 mg/mL) was added

and the sample was incubated at room temperature for 30 minutes. The phenol/chloroform/isoamyl alcohol step was repeated one more time before adding 0.5x volume of 7.5 M ammonium acetate and 2.5x volume of 100% ethanol to the aqueous phase. The sample was centrifuged at 16,000x g for 30 minutes at room temperature. The supernatant was decanted and 500 µL of 70% ethanol was added. The sample was centrifuged at 10,000x g for 5 minutes and the supernatant was decanted. The pellet was air dried and then resuspended in 5 µL of sterile Millipore water. Concentration and quality of DNA was determined with a Nanodrop-1000 UV/Vis Spectrophotometer (Thermo Scientific, Waltham, MA) and then by running an aliquot of the sample on a 1% agarose gel with ethidium bromide followed by visualization on a transilluminator, respectively.

PCR amplification of the *atpH* and *psbK* regions of the plastid genome was performed to identify duckweed collected from the environment (Borisjuk et al., 2015). For the *atpH* gene the forward primer was ACTCGCACACACTCCCTTTCC and the reverse primer was GCTTTTATGGAAGCTTTAACAAT. For the *psbK* locus, the forward primer was TTAGCATTTGTTTGGCAAG and the reverse primer was AAAGTTTGAGAGTAAGCAT. 100 ng of DNA was added to the amplification mixture containing 1x buffer, 0.25 mM dNTPs, 0.4 µM forward primer, 0.4 µM reverse primer, 4 mM $MgCl_2$, and 2 U of Taq polymerase. The PCR condition was Stage 1 at 95°C for 5 minutes, Stage 2 with 35 cycles at 95°C for 30 seconds, 51°C for 30 seconds, 72°C for 1 minute, and Stage 3 at 72°C for 5 minutes.

2.3.5 Sequencing of 16S rRNA Gene

PCR amplification of the 16S rRNA gene was performed on single bacterial colonies using the bacterial universal primers e9f forward (GAGTTTGATCCTGGCTCAG) and e926r reverse (CCGTCAATTCCTTTGAGTTT) (Baker et al., 2003; Chakravorty et al., 2007). DNA was added to the amplification mixture containing 1x buffer, 0.2 mM dNTPs, 0.4 µM forward primer, 0.4 µM reverse primer and 2 U of Taq polymerase. The PCR condition was Stage 1 at 95°C for 5 minutes, Stage 2 with 25 cycles at 95°C for 1 minute, 50°C for 30 seconds, 72°C for 1 minute, and Stage 3 at 72°C for 5 minutes.

2.3.6 Sequence Analysis

Sanger sequencing of the *atpH*, *psbK* and 16S rRNA genes was performed by Genewiz Co. (Piscataway, New Jersey) and sequences were analyzed using Serial Cloner and UGENE programs. With the support by the Joint Genome Institute (JGI)-Environmental Molecular Sciences Laboratory (EMSL) Collaborative Science program, the complete genome sequences for thirty-three of our DAB collection have been determined. Analysis of complete genome sequences was performed using JGI, KEGG Mapper and RAST annotation service (Aziz et al., 2008; Overbeek et al., 2013; Brettin et al., 2015). Amino acid sequence alignment of tryptophanase and % identity matrix was performed using Clustal Omega version 1.2.4 with default parameters.

2.3.7 Colorimetric Detection of Indole Related Compounds

Bacterial strains from glycerol stocks were streaked onto either an LB agar plate or a TSA plate, depending on the medium of their original isolation and grown at 28°C. For each strain, a single colony was used to inoculate 6 mL of liquid LB medium, with and without 5 mM L-tryptophan. For DAB 33B and DAB 39B, liquid TSB (with and

without 5 mM L-tryptophan) was used instead due to difficulty growing these two strains on LB medium. After 48 hours of growing at 28°C with shaking at 240 rpm, 1 mL of culture was centrifuged for 5 minutes at 14,000 rpm to collect the supernatant. The original Salkowski assay based on the Gordon and Weber protocol was adapted for a 96-well format (Gordon and Weber, 1951). In a Corning 96-well clear bottom white plate, 100 µL of the supernatant was added to 200 µL of Salkowski reagent (10 mM $FeCl_3$, 97% reagent grade, and 34.3% perchloric acid, ACS grade) in duplicate. After incubating samples with the Salkowski reagent at room temperature for 30 minutes, the color change was recorded. A BioTek Synergy HT microplate reader was used to determine the absorbance (O.D.) at a single wavelength of 530 nm. To estimate the amount of indole related compounds at 530 nm, an IAA standard curve was generated by suspending IAA (Gibco Laboratories, Life Technologies, Inc., New York, USA) in 100% acetonitrile at a concentration of 1 mg/mL and diluting in LB medium or TSB to a concentration of 100 µg/mL, 50 µg/mL, 20 µg/mL, 10 µg/mL, 5 µg/mL and 0 µg/mL. Sterile LB medium (with and without 5 mM L-tryptophan) and sterile TSB (with and without 5 mM L-tryptophan) were used as controls. The concentration of indole related compounds at 530 nm of the sterile control sample, either LB or TSB depending on the bacterial medium used, was subtracted from the concentration of indole related compounds at 530 nm of the bacterial samples to obtain a background subtracted concentration.

A full spectrum analysis from 440-600 nm, using a 1 nm interval, was performed to identify the wavelength of maximum absorbance. Full spectrum analysis was performed on bacterial samples grown in liquid LB medium supplemented with 5 mM L-tryptophan whereas free indole and free IAA (as references) were suspended in 100%

acetonitrile. The wavelength of maximum absorbance (λ_{max}) was calculated between 460 nm and 600 nm due to the high background signal observed at wavelengths shorter than 460 nm from addition of the Salkowski reagent to LB medium.

For determining the specificity of the Salkowski reagent, we tested IAA, indole-acetamide (IAM), indole-3-pyruvatic acid (IPA), ILA, indole-3-butyric acid (IBA), indole, indoxyl sulfate, tryptophol, and tryptophan. The compounds were suspended in 100% acetonitrile, HPLC grade, before diluting in LB medium, which did not contain 5 mM L-tryptophan due to the high absorbance background tryptophan generates when performing a spectrum analysis from 440 nm to 600 nm wavelength.

2.3.8 Extraction of Indole Related Compounds

For extraction of indole related compounds, bacterial strains from glycerol stocks were streaked onto an LB agar plate and grown at 28°C. A single colony was used to inoculate a starter culture of 6 mL liquid LB medium, supplemented with 5 mM L-tryptophan, and grown at 28°C and 240 rpm. After 24 hours, the starter culture was used to make a 60 mL culture of liquid LB medium, supplemented with 5 mM L-tryptophan, at OD_{600} 0.01. The cultures were grown at 28°C and 240 rpm. After 24 hours, the supernatant was collected by centrifugation at 10,000x g for 5 minutes. For the spike sample, 300 µg of free IAA was added to 60 mL of LB medium supplemented with 5 mM L-tryptophan. All of the samples were then acidified with 1 N HCl to a pH of 2.7. The samples were then separated into 20 mL aliquots for biological triplicates. A Sep-Pak C18 cartridge (360 mg sorbent, 55-105 µm particle size) was prepared for each sample by washing with 10 mL of 100% acetonitrile followed by 10 mL of water. The acidified supernatant was passed through the C18 cartridge. The C18 cartridge was then washed

with 10 mL of water and eluted with 5 mL of 80% (v/v) acetonitrile. The eluate was vacuum concentrated and then stored at -20°C until ready for LC/MS. Concentrated samples were dissolved in 1 mL of 100% acetonitrile. The samples were sonicated twice for 15 minutes and then centrifuged at 14,000 rpm for 5 minutes to remove any solid particles. A standard curve was generated by making IAA solutions of 0.5 ng/µL, 1 ng/µL and 10 ng/µL in 100% acetonitrile. Acetonitrile of HPLC grade and HCl of ACS grade was used for the experiment and water was prepared from Millipore Synergy 185.

2.3.9 Detection of IAA by LC/MS

Samples were separated and analyzed by a UPLC/MS system including the Dionex® UltiMate 3000 RSLC ultra-high pressure liquid chromatography system, consisting of a workstation with ThermoFisher Scientific's Xcalibur v. 4.0 software package combined with Dionex®'s SII LC control software, solvent rack/degasser SRD-3400, pulseless chromatography pump HPG-3400RS, autosampler WPS-3000RS, column compartment TCC-3000RS, and photodiode array detector DAD-3000RS. After the photodiode array detector the eluent flow was guided to a Q Exactive Plus Orbitrap high-resolution high-mass-accuracy mass spectrometer (MS). Mass detection was full MS scan with low energy collision induced dissociation (CID) from 100 to 1000 m/z in either positive or negative ionization mode with electrospray (ESI) interface. Sheath gas flow rate was 30 arbitrary units, auxiliary gas flow rate was 7, and sweep gas flow rate was 1. The spray voltage was 3500 volts (-3500 for negative ESI) with a capillary temperature of 275°C. The mass resolution was 140,000 and the isolation window was 0.4 mDa. Substances were separated on a Phenomenex™ Kinetex C8 reverse phase column, size 100 x 2 mm, particle size 2.6 mm, pore size 100 Å. The mobile phase consisted of 2

components: Solvent A (0.5% ACS grade acetic acid in LCMS grade water, pH 3-3.5), and Solvent B (100% Acetonitrile, LCMS grade). The mobile phase flow was 0.20 ml/min, and a gradient mode was used for all analyses. The initial conditions of the gradient were 95% A and 5% B; for 30 minutes the proportion reaches 5% A and 95% B which was kept for the next 8 minutes, and during the following 4 minutes the ratio was brought to initial conditions. An 8 minutes equilibration interval was included between subsequent injections. The average pump pressure using these parameters was typically around 3,900 psi for the initial conditions.

Putative formulas of IAA metabolites and other indole related compounds were determined by performing isotope abundance analysis on the high-resolution mass spectral data with Xcalibur v. 4.0 software and reporting the best fitting empirical formula. Database searches were performed using reaxys.com (RELX Intellectual Properties SA) and SciFinder (American Chemical Society).

2.4 Results

2.4.1 Isolation of Bacterial Endophytes

Duckweed tissues that were selected from the RDSC or collected from various locations in New Jersey, USA are of the genera *Wolffia, Lemna, Spirodela* and *Landoltia*. Forty-seven strains of bacteria were isolated from 16 strains of surface sterilized duckweed tissue. Of the bacterial isolates, 62% belong to the Proteobacteria phylum, 23% belong to the Firmicutes phylum, 11% belong to the Actinobacteria phylum, and 4% belong to the Bacteroidetes phylum.

2.4.2 Specificity of the Salkowski Reagent

We tested the Salkowski reagent on various commercially available indole related compounds to determine the specificity of the assay (Table 2.1). IAA, IAM and IPA, resulted in a color change to pink when these compounds were mixed with the Salkowski reagent. The wavelength which resulted in the maximum absorbance increase was 530 nm. IBA resulted in a color change to orange with a wavelength of maximum absorbance increase at around 450 nm. Indoxyl sulfate resulted in a purple color change with a wavelength of maximum absorbance increase at around 560 nm and indole resulted in a brown color change with a wavelength of maximum absorbance increase at around 490 nm. Tryptophan, ILA and tryptophol resulted in no observable color change.

2.4.3 Colorimetric Detection of Indole Related Compounds

Using the Salkowski reagent as a colorimetric assay, we determined that 78.7% (37 out of 47) of the isolated DABs are capable of producing indole related compounds. Of those DABs producing indole related compounds, 81.1% are pink-type as observed by a color change from yellow to pink at a maximum absorbance increase at around 530 nm and 18.9% are brown-type as observed by a color change from yellow to brown at a maximum absorbance increase at around 480 nm (Table 2.2). As a positive control, we performed the Salkowski assay on *Azospirillum brasilense* strains Sp7 and Sp245, which are well-studied IAA-producing PGPBs. When the Salkowski reagent was applied to the supernatant of Sp7 and Sp245, there was a color change to pink with an increase in absorbance that peaks at 530 nm. The concentration of indole related compounds in the sample was estimated using an IAA standard curve. The concentration of indole related compounds produced by pink-type bacteria, as compared to no color change bacteria, are listed in Table 2.2.

2.4.4 Synthesis of Indole Related Compounds without Exogenous L-Tryptophan

A subset of 19 pink-type and 5 brown-type bacterial strains were further screened for their ability to synthesize indole related compounds without 5 mM L-tryptophan supplemented into the growth medium. The full absorption spectrum from 400-600 nm of an IAA standard curve from the Salkowski assay reveals that a wavelength of maximum absorbance (λ_{max}) cannot be detected at ≤5 µg/mL of IAA when no exogenous L-tryptophan is supplemented into the medium. A λ_{max} cannot be detected at ≤10 µg/mL of IAA when 5 mM L-tryptophan is supplemented into the medium due to a high background absorbance. Four pink-type strains and one brown-type strain were able to synthesize indole related compounds without exogenous 5 mM L-tryptophan as determined by the color change after addition of the Salkowski reagent to the supernatant (Figure 2.1). This suggests that most of the DABs in our collection require an exogenous source of tryptophan to produce indole related compounds when cultured alone.

Using KEGG Mapper to analyze the complete genome sequences for thirty-three strains of our DAB collection, we identified tryptophan metabolism genes present in a subset of these bacterial genomes. Based on the estimated quantity of indole related compounds from the Salkowski assay, we compared the genomes of a pink-type top producer, a pink-type moderate producer and one that did not change color (DAB 37A, 1A and 3D). We found that the pink-type top producer contained the most tryptophan metabolism-related genes of the three genomes compared. All three DABs contain a gene encoding a potential amidase enzyme, which may be able to convert IAM to IAA. Interestingly, the genome of DAB 3D which did not change color in the Salkowski assay, also appears to have this gene present, suggesting it may have the ability to convert IAM

to IAA. However, based on the Salkowski assay, DAB 3D is not a producer of indole related compounds when grown alone in culture medium with or without addition of tryptophan.

2.4.5 Potential Correlation between Production of Indole Related Compounds and Duckweed Genus

Because of the large proportion of pink-type DABs and an unexpected proportion of DABs that turned brown, we wanted to determine whether there was an association between the type of indole related compound produced by the DABs and the duckweed genus from which these DABs were isolated. We calculated that of the 30 pink-type DABs, 19 or 63.3% are derived from *Lemna* species and of the 6 brown-type DABs that were isolated from genotyped duckweed strains, 4 or 66.7% are derived from *Wolffia* species. Pearson's chi square test of independence was used to calculate the null hypothesis that production of indole related compounds from DABs is independent of the duckweed genus that the DAB was isolated from. The obtained chi square value from the 3 by 4 contingency table is 20.3 with a degree of freedom of 6 and a p value of 0.002. The p value is less than the critical value of 0.05 and therefore we reject our null hypothesis.

To determine which categories of the 3 by 4 contingency table are associated, two 2 by 2 contingency tables were created. The first 2 by 2 contingency table was used to test the null hypothesis that pink-type DABs are independent of the duckweed genus *Lemna*. The obtained chi square value is 4.30 with a degree of freedom of 1 and a p value of 0.038. The p value is less than the critical value of 0.05 and therefore we reject our null hypothesis. The second 2 by 2 contingency table was to test the null hypothesis that

brown-type DABs are independent of the duckweed genus *Wolffia*. The obtained chi square value is 14.16 with a degree of freedom of 1 and a p value of 0.0001. The p value is much less than the critical value of 0.05 and therefore we reject our null hypothesis and conclude that there is a strong association between the brown-type DABs and the *Wolffia* genus, analogous to the association observed between the pink-type DABs and the *Lemna* genus. These results suggest that there is a significant correlation between the type of indole related compound produced by a particular DAB and the duckweed genus from which the DAB was isolated.

2.4.6 Identification of Indole Related Compounds by LC-MS

To more precisely validate the identity of the indole related compounds that are produced by the DABs, we first used LC-MS to determine whether the pink-type DABs were producing free IAA. The molecular weight of free IAA is 175 g/mol with positive ionization resulting in molecular ion at m/z 176 [M+H] and a fragment at m/z 130 (Figure 2.2). Negative ionization also resulted in molecular ion at m/z 174 [M-H] and a fragment at m/z 130. MS/MS was not performed due to the CID IAA fragmentation into an m/z 130 species representing the indole CH_2 bridge component of IAA. Furthermore, fragmentation into an m/z 130 species from a larger compound at a different retention time from that of IAA led us to identify indole-lactic-acid (ILA) in one of the bacterial samples, indicating that the method could resolve specific indole related compounds.
A solution of 5 ng/µL of free IAA in 100% acetonitrile was used to determine the retention time of free IAA in our LC-MS system, which was approximately 9.84 minutes (Figure 2.3A) in extracted single ion chromatogram. The extracted ion chromatogram peak areas of m/z 176 are shown in Figure 3C - 3I for pink-type strains (Sp7, DAB 1A,

DAB 37A and DAB 5E), brown-type strains (DAB 34D and 39B), and no color change strain DAB 3D. The extracted ion chromatograms demonstrate that the brown-type strains, DAB 34D and DAB 39B, produce small but detectable amounts of free IAA compared to the higher amounts observed in the pink-type strains. The background signal from the species with an m/z value of 176 in the medium with a shorter retention time of 8.0-8.1 minutes is not observed in the Sp7 and DAB 37A samples since the amount of IAA is much higher in these cases and the scale of the Y-axis is for a larger range. A free IAA standard was used to determine the HPLC UV absorbance signal at 280 nm for quantification. Using a spike sample of 5 µg/mL free IAA in LB medium added just before our extraction and concentration protocol, we calculated a 61.5% recovery from the extraction process. Estimation of IAA production based on the Salkowski assay method suggested that our *Azospirillum* strain, DAB 37A, was a top IAA producer. However, quantification using HPLC, which has better resolution and sensitivity for IAA detection, suggests that *Microbacterium* strain, DAB 1A, and control *Azospirillum* strain, Sp7, produce higher levels of free IAA.

Further LC-MS analysis revealed not only production of free IAA by the pink-type *Herbaspirillum* strain, DAB 5E, but also production of free ILA. This was detected by an m/z 130 fragment at a different retention time than IAA. Free ILA did not result in a color change after addition of the Salkowski reagent (Table 2.1) and therefore, was only detectable using LC-MS. To verify the identity of the suspected ILA compound, a solution of 100 ng/µL of free ILA in 100% acetonitrile was used to determine the retention time of free ILA in our LC-MS system, which was approximately at 8.35 minutes (Figure 2.4A). Detection of free ILA with negative ionization resulted in a major

peak at m/z 204 in extracted ion chromatogram. Extracted ion chromatograms at m/z 204 demonstrate that pink-type *Herbaspirillum* strain, DAB 5E produced free ILA in LB medium culture as well as a pink-type *Microbacterium* strain, DAB 1A, though at a much lower level (Figure 2.4D and E). These two DABs thus have an inverse ratio of IAA/ILA production with DAB 1A having a high IAA/ILA ratio while DAB 5E has a low IAA/ILA ratio (compare Figure 2.3 to Figure 2.4).

2.4.7 Identification of the Major Salkowski-positive Molecule in Brown-Type DABs as Indole

When using KEGG Mapper to identify tryptophan metabolism genes present in the DAB bacterial genomes, we noted the presence of a gene encoding tryptophanase in all of the brown-type DABs, excluding DAB 34D which does not have the complete genome sequenced yet. This enzyme produces indole from tryptophan and this product could react in the Salkowski assay to produce a brown color that would be consistent with our observations. We BLASTed the amino acid sequence of the *E. coli* tryptophanase provided by KEGG Mapper (K-12 MG1655) to the amino acid sequence database of our DAB genomes. The sequence was 84% identical to the predicted homolog in the brown-type *Aeromonas* strain, DAB 39B, with an E value of 0.0. The other brown-type DABs with genome sequence available also contain a predicted coding sequence that is similar to the *E. coli* typtophanase, although the percent identity was lower.

To determine whether the Salkowski assay result of a brown color change is due to indole, we performed the Salkowski assay on *E. coli*, strain DH5-alpha, which is a well-studied indole-producing bacterium. The result was a color change from yellow to

brown with a wavelength of maximum absorbance increase at 490 nm (Figure 2.5B). When the Salkowski reagent was added to LB medium containing 1 mg/mL of free indole compound, the color change was from yellow to brown with a wavelength of absorbance maximum at 487 nm (Figure 2.5D). The full spectra from reaction with supernatants from brown-type *Aeromonas* strain, DAB 39B, brown-type *Chryseobacterium* strain, DAB 37D, and brown-type *Vogesella* strain, DAB 34D, are shown in Figure 2.5 along with the full spectrum of LB medium containing both 1 mg/mL of free indole and 0.1 mg/mL of free IAA. There appear to be two peaks of absorbance corresponding to indole and IAA for DAB 39B, DAB 34D and DAB 37D. Some of the DAB strains thus appear to be producing multiple indole related compounds during *in vitro* growth with potentially indole being one of them.

2.4.8 Extraction and Detection of Indole from DAB Strains by LC-MS

We used LC-MS to more precisely validate the identity of the suspected indole compound produced in the brown-type DABs. A solution of 100 ng/µL of free indole in 100% acetonitrile was used to determine the retention time of free indole in our LC-MS system, which was approximately 13.30 minutes (Figure 2.6). Sample preparation and extraction of free indole were performed identically to the extraction of free IAA. Detection of free indole with positive ionization resulted in a major peak at m/z 118 in extracted ion chromatogram. Using the peak area at m/z 118 of the samples, we detected free indole present in the supernatants of the brown-type *Vogesella* strain, DAB 34D, and the brown-type *Aeromonas* strain, DAB 39B (Figure 2.6). No indole was detected with supernatant from the pink-type *Microbacterium* strain, DAB 1A. A peak corresponding to IAA was also detected in the supernatants of brown-type strains DAB 34D and DAB

39B, but at much lower levels compared to the pink-type strain, DAB 1A (Figure 2.3). Our results thus provided strong evidence for the identity of indole as the major compound produced by the brown-type DABs and not produced by the pink-type DABs.

2.5 Discussion

The Salkowski colorimetric assay is traditionally used to detect the bacterial production of IAA. However, after testing various indole related compounds, IAM and IPA also resulted in a color change to pink with an absorbance maximum at 530 nm. Similar findings were previously reported in which IAA, IPA and IAM all reacted with the Salkowski reagent to cause a pink color change, however sulfuric acid was used rather than hydrochloric acid (Glickmann and Dessaux, 1994). We used hydrochloric acid based on a previous report that it results in greater color intensity than sulfuric acid and thus could be more sensitive (Gordon and Weber, 1951). Our present study, along with a previous report, indicates that the Salkowski assay alone is not sufficient to distinguish which indole related compounds are produced by bacteria (Glickmann and Dessaux, 1994). This is also evident by the mass spec detection of ILA produced by pink-type *Herbaspirillum* strain, DAB 5E, which could not have been detected by the Salkowski reagent since it does not react with this particular indole related compound to produce a visible color change. Studies using the Salkowski assay should thus be cautious of these limitations and employ additional techniques such as mass spectrometry for specific detection and positive identification of the indole related compounds.

The isolated endophytic DABs were primarily from the phyla Proteobacteria, Firmicutes, and Actinobacteria, which has been similarly reported for the land plant, *Arabidopsis thaliana* (Bulgarelli et al. 2012; Lundberg et al. 2012). This indicates that the

core microbiome of duckweeds may be quite similar to those of land plants such as the dicot *A. thaliana* and highlights the conservation of plant-microbe association mechanisms as far back as the divergence between monocots and dicots about 150 million years ago (Chaw et al., 2004). Of the 47 endophytic DABs used for the Salkowski assay in this study, 79% were capable of producing indole related compounds. This is similar to the suggested 80% of epiphytic bacteria reported in literature capable of producing IAA (Spaepen and Vanderleyden, 2011). However, the result in a brown color change after addition of the Salkowski reagent has not been widely reported. Mass spectrometry confirmed the presence of free IAA in the pink-type DABs and the presence of free indole in addition to free IAA in the brown-type DABs, although the levels of IAA in the latter cases are substantially lower. In addition, our genome analysis of non-Salkowski-reactive *Bacillus* strain, DAB 3D, revealed the presence of a potential amidase gene, which may convert IAM to IAA. However, the Salkowski assay and mass spectrometry did not detect the presence of free IAA in the DAB 3D supernatant. One explanation could be that the gene is not expressed when the bacteria is grown as a monoculture *in vitro*. Whether this is a pseudogene or if it is tightly regulated in DAB 3D to respond to specific cues remains to be determined. Future work is thus needed to determine whether some DABs are capable of producing free IAA when interacting with the duckweed hosts or in a community context.

In this study, we have also found that exogenous tryptophan is necessary for 79% of the tested DABs to produce indole related compounds during *in vitro* growth. The majority of the DABs may thus require exogenous tryptophan supplied by the plant to produce indole related compounds or they may have to be induced by the plant host to

produce more tryptophan themselves. A previous study supports this notion that tryptophan-like compounds secreted by the plant root may stimulate IAA synthesis of PGPBs (Kamilova et al., 2006). Regardless of the cause for this requirement, our observation suggests that the DAB's phytohormone production capability during *in vitro* growth per se does not necessarily result in phenotypic effects of heightened auxin levels when inoculated onto the plant. Future experiments studying interactions of these DABs with various duckweed genera and environments will be necessary to better understand the dynamic control for this trait in different context of plant-microbe interaction. Our present results thus serve as a necessary foundation to better interpret future studies comparing the phenotypic output of different combinations of DAB and plant hosts. In this context, the availability of whole genome sequences for both DABs and high quality reference genomes for duckweed such as *Spirodela polyrhiza* (Michael et al., 2017) should enable the application of molecular tools to begin to characterize the signaling pathways involved.

The need to more closely examine mechanisms used by endophytic DABs to associate with the plant is further supported by the finding of an apparent correlation between the production of specific indole related compounds and the duckweed genus that the DAB was isolated from. Specifically, pink-type DABs are more likely to be associated with DABs isolated from *Lemna* species whereas brown-type DABs are overrepresented in DABs that were isolated from *Wolffia*. Enrichment of specific bacteria phyla by different plant host genotypes has been previously reported (Edwards et al, 2015; Haney et al., 2015; Lundberg et al., 2012). Our present work indicates one additional selection factor could be the particular type of genes for indole related

compounds that the bacteria may be able to synthesize. The effect of IAA on plant root development has been well characterized and more recently studies have demonstrated that it could function as a signal molecule between bacteria in a community as well as between bacteria and the plant host (Spaepen and Vanderleyden, 2011). On the other hand, indole production by bacteria has been shown to be involved in a number of microbial processes including quorum sensing and biofilm formation (Lee and Lee, 2009). However its effect on plant health and development is poorly understood compared to that of IAA. *Wolffia* plants are morphologically distinct from *Lemna* species in that they are usually comprised of a more spherical frond and are rootless. Thus, architecturally, colonization of *Wolffia* plants by DABs may pose different challenges and different strategies/mechanisms, such as formation of a biofilm, could be needed in the bacteria. One possible explanation for our findings is that either the duckweed or the endophytic bacteria is selecting for a symbiont in which the appropriate resources it requires, whether it may be a specific indole related compound or a particular plant morphology, could be utilized and enable colonization of the microbe on the plant host. More studies will be necessary to uncover the role of indole producing DABs on the health of different duckweed genera and to delineate the function for the indole that could be produced by these bacteria.

Finally, we believe that understanding a potential coevolution between duckweeds and their associated endophytes is critical for selecting the appropriate combination of bacteria when designing synthetic bacterial communities. We may utilize bacteria to target specific or multiple duckweed species and therefore, it will be useful to understand how the different duckweed genera interact with various bacterial strains in order to

distinguish general and species-specific rules and pathways. This will be important for researchers trying to improve large scale duckweed farming in open, non-sterile conditions for wastewater treatment, biofuel or bioplastic production, and animal feed supplement, which currently remains important challenges to overcome.

2.6 Tables and Figures

Table 2.1. Specificity of the Salkowski reagent was determined by testing indole related compounds. A color change indicates detection of one or more indole related compound(s). The wavelength recorded indicates the wavelength of maximum absorbance. ILA: Indole-3-lactic acid; IAA: Indole-3-acetic acid; IAM: Indole-acetamide; IPA: Indole-3-pyruvic acid; IBA: Indole-3-butyric acid. N/a indicates not applicable result.

Compound	Color Change	Wavelength of Maximum Absorbance (nm)
Tryptophan	No color change	N/a
ILA	No color change	N/a
Tryptophol	No color change	N/a
IAA	Pink	530
IAM	Pink	530
IPA	Pink	530
IBA	Orange	450
Indole	Brown	490
Indoxyl Sulfate	Purple	560

Table 2.2. Estimation for the amount of indole related compounds detected by the Salkowski reagent in bacterial culture supernatants grown with 5 mM L-tryptophan. Background subtracted concentrations were obtained by taking the average concentration as calculated from the standard curve and subtracting the concentration of either the sterile TSB or sterile LB sample, depending on the medium used to culture the bacteria. Means and standard deviation were calculated using 3 biological replicates. **(A)** Mean concentration (ng/µL) of indole related compound and standard deviation of Sp7, Sp245 and pink-type DABs. **(B)** Mean concentration (ng/µL) of indole related compound and standard deviation of DABs resulting in no color change.

A)	Pink-Type		
Bacteria Genus	Strain	ng/µL of Indole Related Compound	Standard Deviation
	Sterile TSB	0.000	0.425
	Sterile LB	0.000	0.187
Pseudomonas	DAB D4EL2	3.485	0.973
Pseudomonas	DAB D2FKM1	3.666	1.918
Pseudomonas	DAB D2EKK1	4.376	0.125
Paenibacillus	DAB 26A	4.392	1.280
Rhodanobacter	DAB D4FL3	4.458	0.913
Microbacterium	DAB 19B	4.959	1.378
Paenibacillus	DAB 5M	5.036	1.929
Microbacterium	DAB 33B	5.182	2.873
Azospirillum	Sp7	5.396	3.024
Pseudacidovorax	DAB 35E	5.696	3.406
Paenibacillus	DAB 5A	6.967	1.586
Janthinobacterium	DAB D4EL3	7.484	3.200
Rhizobium	DAB 36D	7.533	2.690
Azosprillum	Sp245	7.764	1.333
Herbaspirillum	DAB 5O	8.424	3.206
Microbacterium	DAB 19A	8.564	2.154
Pseudomonas	DAB 36E	9.541	0.178
Rhizobium	DAB 35A	10.911	4.830
Herbaspirillum	DAB 5S	10.957	2.858
Paenibacillus	DAB 4T	11.196	2.501
Paenibacillus	DAB 4X	11.452	2.154
Paenibacillus	DAB 15A	11.719	0.818
Pseudomonas	DAB 38C	12.660	0.797
Herbaspirillum	DAB 5E	18.581	0.578
Bosea	DAB D4EK4	19.739	4.463
Microbacterium	DAB 1A	20.693	3.059
Microbacterium	DAB 1D	21.972	3.802
Acidovorax	DAB 35F	22.071	5.571
Azospirillum	DAB 38E	53.204	17.241
Rhizobium	DAB 20A	54.233	6.825
Rhizobium	DAB 33A	77.145	9.031
Azospirillum	DAB 37A	78.160	5.183

B)	No Color Change		
Genus	Strain	ng/µL of Indole Related Compound	Standard Deviation
Bacillus	DAB 3D	0.586	0.459
Bacillus	DAB 27A	0.878	0.216
Staphylococcus	DAB 1B	0.746	0.273
Bacillus	DAB 2C	2.660	1.119
Bacillus	DAB 36A	1.868	0.198
Bacillus	DAB 36C	1.076	0.618
Pseudomonas	DAB 38D	1.521	0.524
Rhodanobacter	DAB D4EH1	2.016	0.729
Rhodanobacter	DAB D4FH1	0.729	0.792
Rhodanobacter	DAB D4EL1	1.125	0.374

Figure 2.1. Production of indole related compounds from duckweed associated bacteria strains. Addition of Salkowski reagent to the bacterial supernatant of a subset of the pink-type and brown-type bacteria strains grown in medium with and without 5 mM L-tryptophan to measure the absorbance of indole related compounds at 530 nm. *Indicates that the supernatant without 5 mM L-tryptophan resulted in an observable color change.

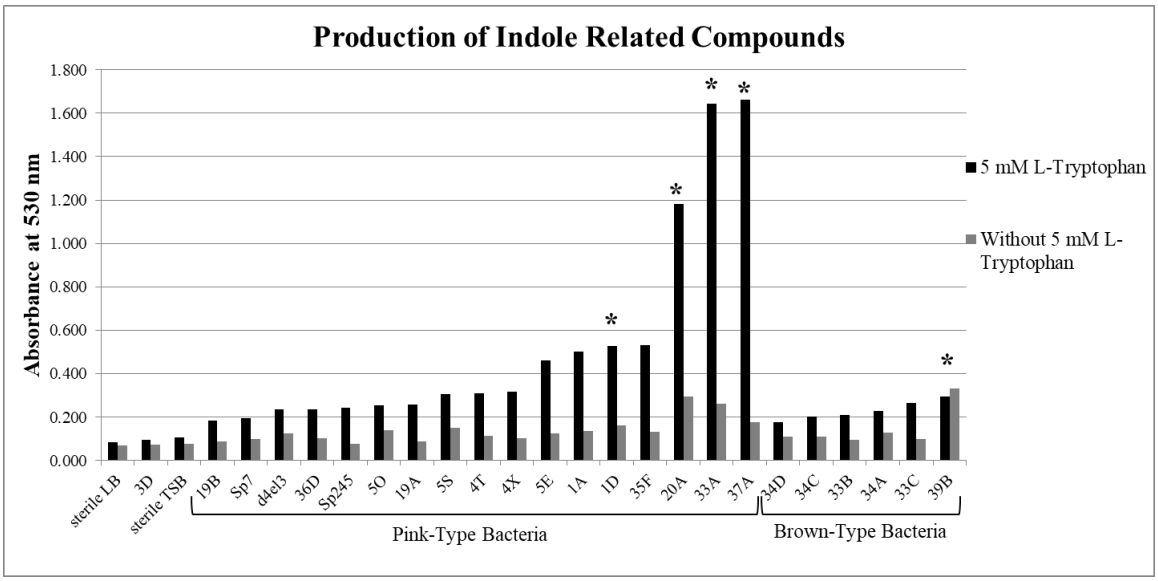

Figure 2.2. LC-MS positive ion scan spectrum of free IAA. 100 ng/µL of free IAA in 100% acetonitrile at a retention time of 9.94 minutes.

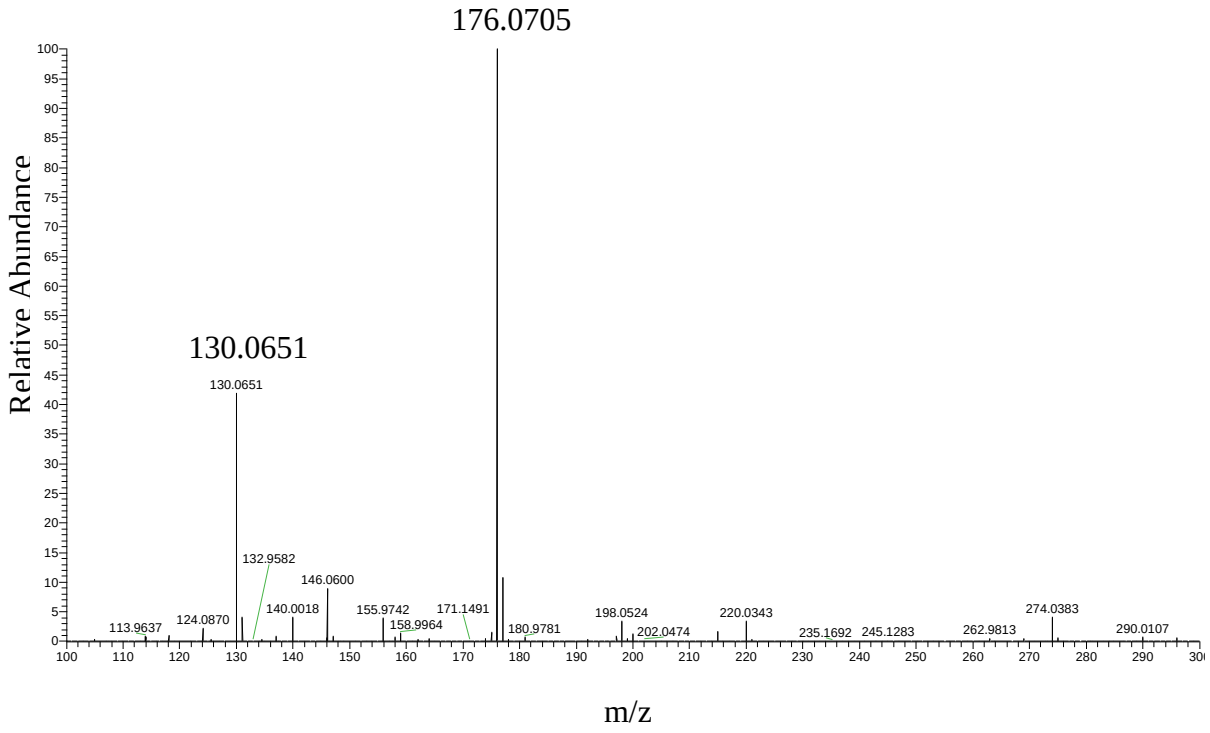

Figure 2.3. Validation of IAA production in DABs by mass spectrometry. LC-MS extracted positive ionization ion chromatograms at m/z 176.06 to m/z 176.08 ([M+H] of IAA). RT: Retention Time; AA: Automatic Area under peak; MA: Manual Area under peak.

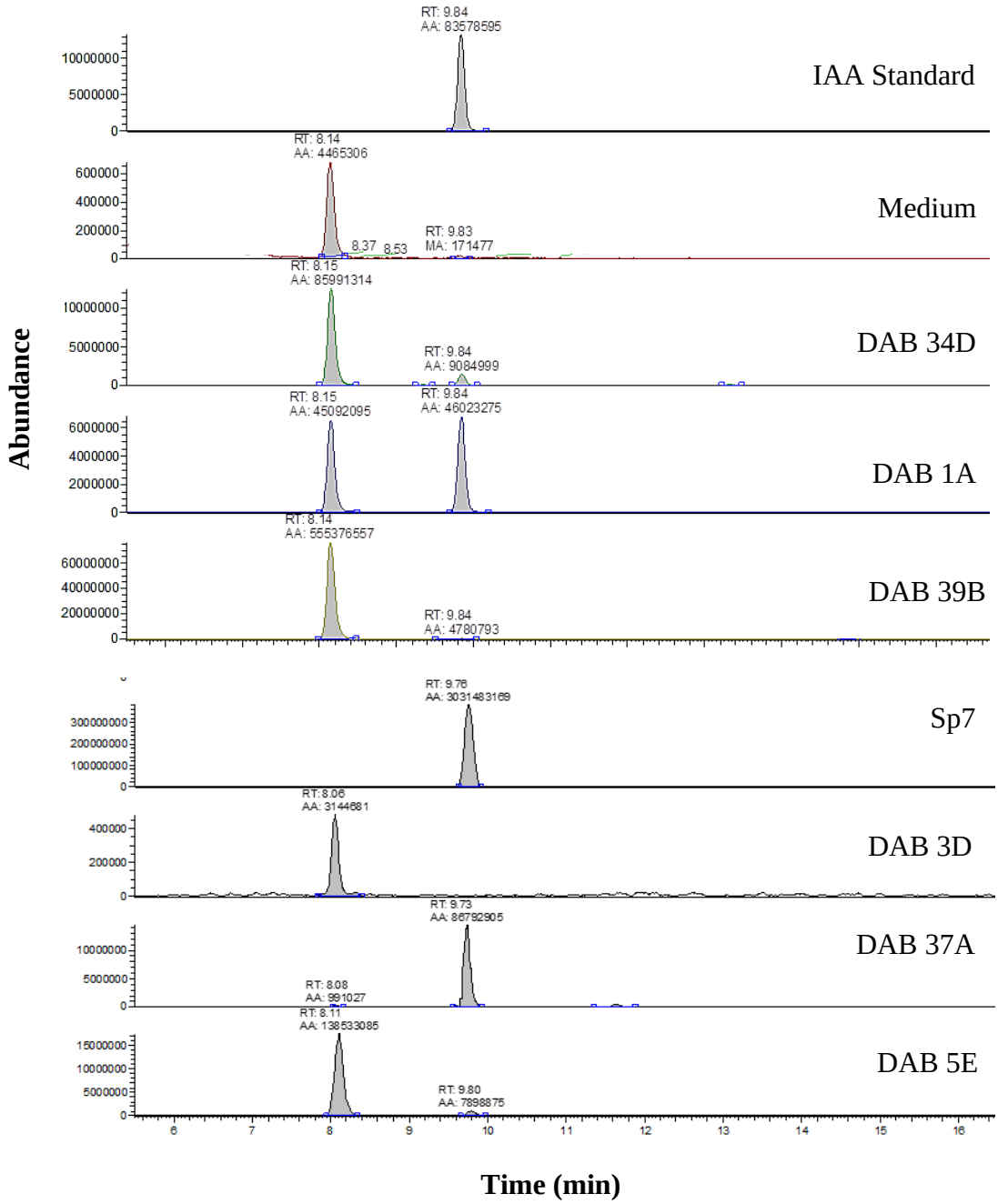

Figure 2.4. Detection of indole-3-lactic acid production in two DABs by mass spectrometry. LC-MS extracted negative ionization ion chromatograms at m/z 204.06 to m/z 204.07 ([M-H] of ILA). RT: Retention Time; AA: Automatic Area under peak.

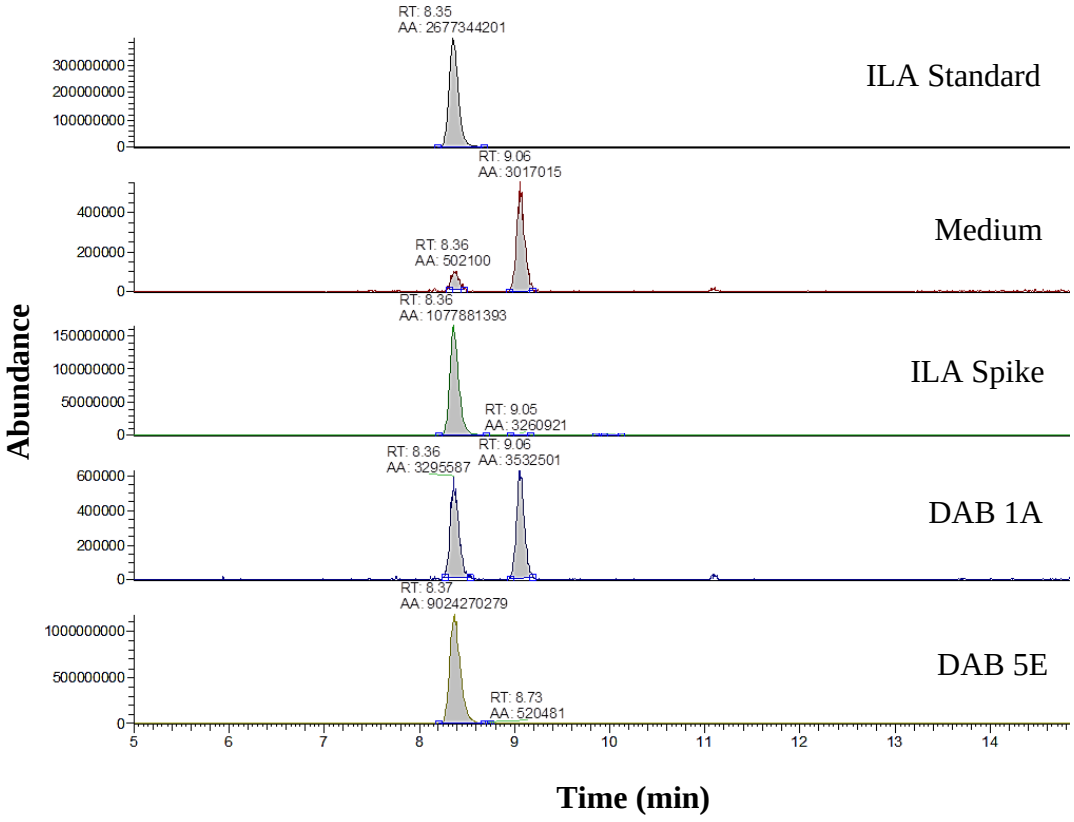

Figure 2.5. Comparison of absorbance spectra between DABs and other reference samples with the Salkowski assay. Absorbance spectrums from 440-600 nm to determine the wavelength at the maximum OD (λ_{max}).

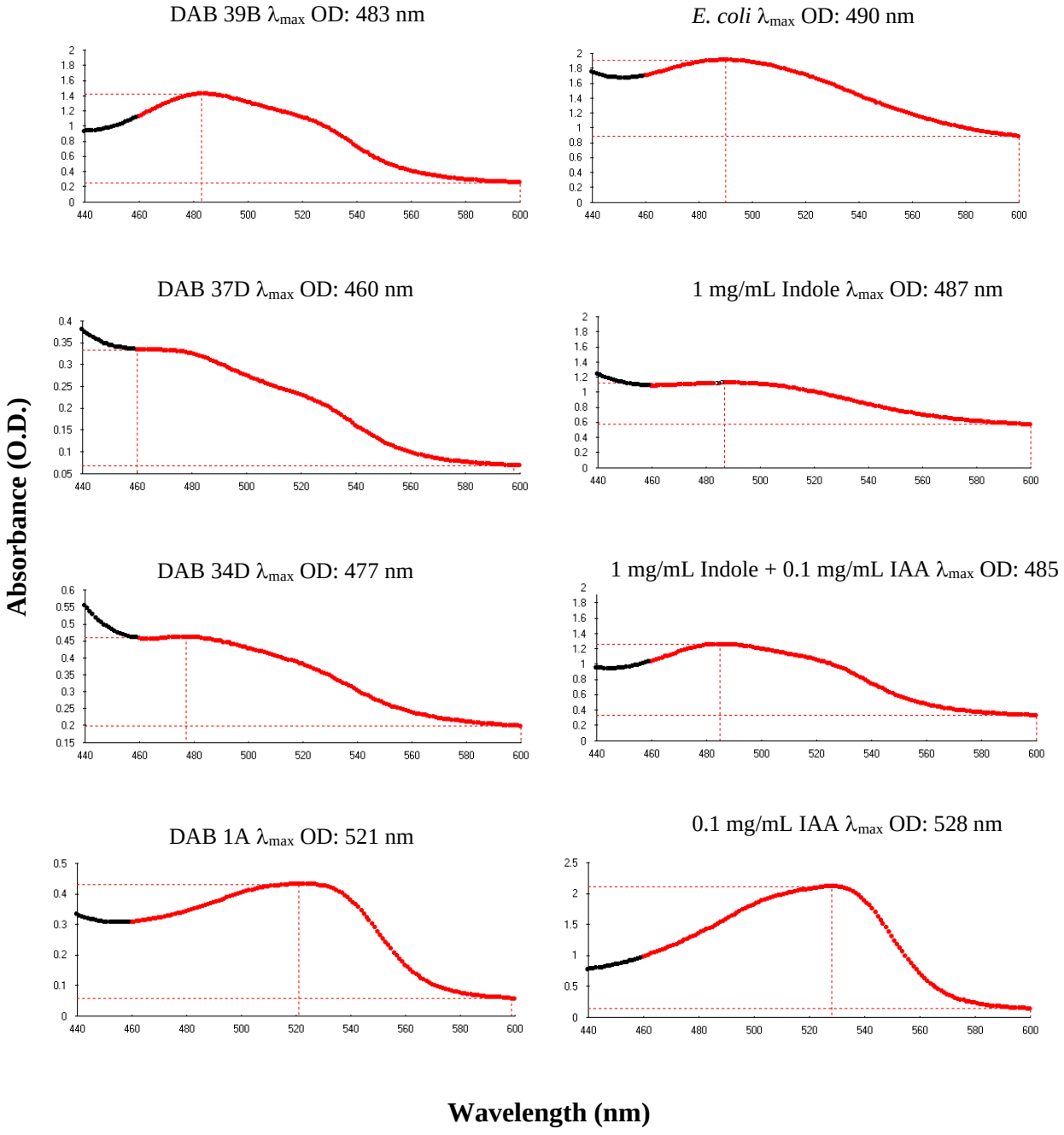

Figure 2.6. Identification of indole production in brown-type DABs by mass spectrometry. LC-MS extracted positive ionization ion chromatograms at m/z 118.06 to m/z 118.07 ([M+H] of indole). RT: Retention Time; AA: Automatic Area under peak; MA: Manual Area under peak.

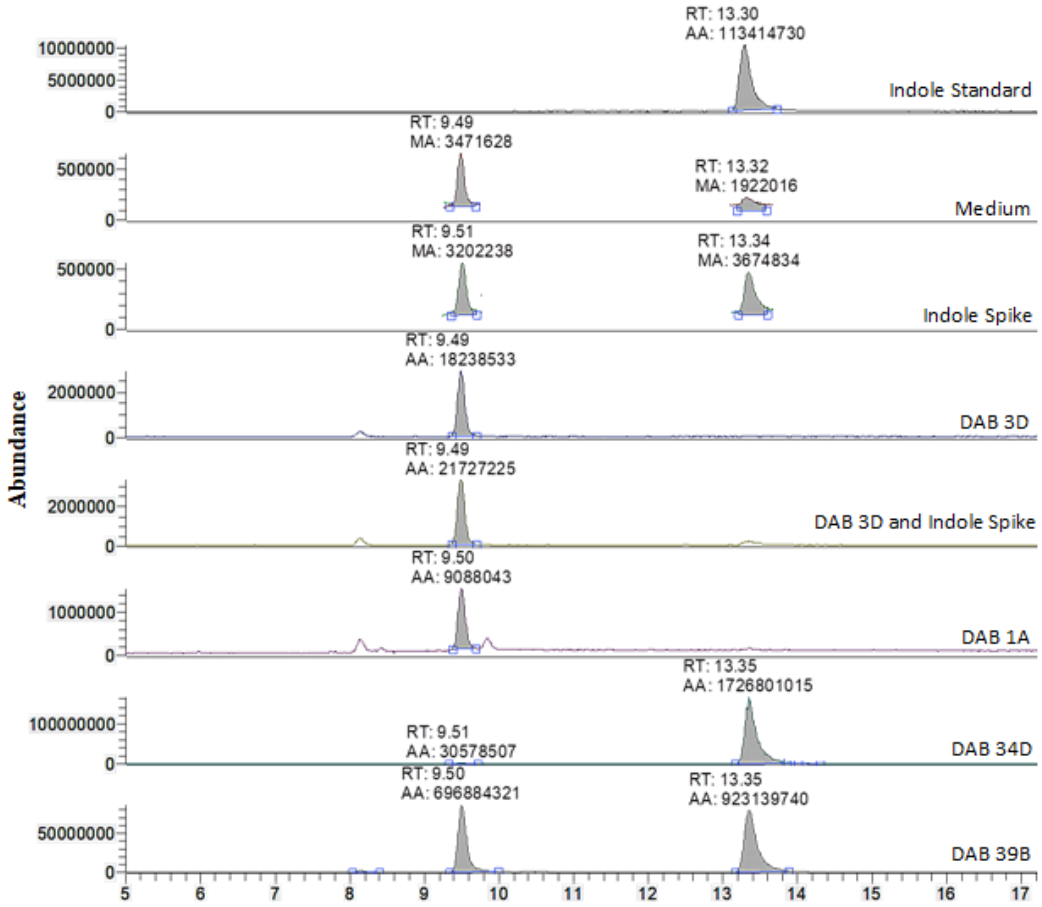

CHAPTER 3

Natural variation in phenotypic and molecular responses of *Arabidopsis thaliana* to bacterial strains producing indole related compounds.

3.1 Abstract

The role of IAA in plant-microbe interactions has been primarily studied using soil-based epiphytes. With an interest in using bacteria in agricultural farming, there is a need for understanding IAA's role in a variety of environmental settings, such as aquatic and endophytic relationships. Thus, using our collection of duckweed associated endophytes, we performed binary-association assays to evaluate physiological and transcriptomic responses of *A. thaliana* to strains capable of producing indole related compounds. High quantity IAA-producing *Microbacterium* strains caused a short root phenotype on *A. thaliana*, while a lower quantity IAA-producing *Microbacterium* strain affected auxin response genes but caused no obvious root phenotype. Use of the auxin insensitive mutants *axr1-3* and *tmk1,3,4/+* revealed potentially diverse functions of the AXR1 gene that may be related to bacterial interaction in addition to IAA response. Our findings provide insight to additional roles of auxin signaling between endophytes and plant hosts.

3.2 Introduction

The phytohormone, indole-3-acetic acid (IAA), is the most commonly occurring auxin found in nature and is produced by both plants and bacteria through a similar biosynthetic pathway (Mano and Nemoto, 2012; Spaepen and Vanderleyden, 2011). In addition to its role in plant gravitropism and cell elongation, IAA can change the root architecture to increase nutrient availability or it may be downregulated by the plant to

optimize defense against pathogens (Duca et al., 2014; Navarro et al., 2006). Production of IAA by microbes may also affect plant health, such as gall formation by pathogens or an increase in root nodules and root biomass by plant growth promoting bacteria (PGPB) (Spaepen and Vanderleyden, 2011). The multiple biosynthesis pathways of IAA suggest that it has many additional unknown roles in plant-bacteria interactions (Spaepen and Vanderleyden, 2011).

With the largest duckweed collection in the world, we were able to utilize this resource to survey auxin production within the duckweed microbiome. We extend from our previous work in Chapter 2 by studying the phenotypic and molecular responses of *A. thaliana* to our isolates capable of producing indole related compounds, in order to reveal potential mechanisms of auxin signaling between plants and bacterium. We have chosen to use *A. thaliana* because of the vast resources of auxin mutant lines available in this plant. Furthermore, we found that the majority of our isolates from bleach treated duckweed were of the phyla Proteobacteria, Firmicutes and Actinobacteria, which is similar to reports in land plants such as the dicot *A. thaliana*, suggesting possible conservation of plant-microbe association mechanisms (Lundberg et al., 2012; Gilbert et al., 2018). DABs capable of producing indole containing compounds were individually inoculated onto sterile wild type (Col-0) and auxin mutant lines, *axr1-3* and *tmk 1,3,4/+*. Physiological and transcriptomic responses were assessed to evaluate auxin signaling as well as other response pathways and various aspects of plant development. Of the DABs capable of producing indole related compounds, high quantity IAA-producing *Microbacterium* strains caused a short root phenotype. Comparison of a high vs. low quantity IAA-producing *Microbacterium* strain revealed similarities and differences in

transcriptomic response by the plant. Decreased transcriptome response in non-auxin pathways of the *axr1-3* mutant line suggests additional functions of the AXR1 gene that may be related to bacterial interaction.

3.3 Methods

3.3.1 Bacterial Strains and Media

Bacillus sp. RU 3D (DAB 3D), *Microbacterium* strains RU 1A (DAB 1A), RU 33B (DAB 33B), and RU RRCA (DAB 19A), *Herbaspirillum sp.* RU 5E (DAB 5E), *Rhizobium* strains RU 20A (DAB 20A) and RU 33A (DAB 33A), and *Azospirillum sp.* RU 37A (DAB 37A) were isolated from duckweed strains as described in Gilbert et al. 2018. Well characterized IAA-producing *Azospirillum brasilense* strain Sp245 from wheat tissue was used as a control. Bacterial strains were stored at -80°C in LB (Miller's, CA, USA) or Tryptic Soy Broth (TSB) (Hardy Diagnostics, OH, USA), depending on the medium of isolation, and supplemented with 40% sterilized glycerol. To isolate single colonies, bacteria from a glycerol stock was spread onto an agar plate (LB or TSB depending on the medium of isolation) using a sterile loop and then stored at 28ºC for 2 days or until single colonies were grown. Liquid cultures were made by taking a single colony using a pipet tip and placing the pipet tip in 6 mL of LB or TSB broth. Cultures were grown for 1 day at 28ºC and 240 rpm except for DAB 33B cultures which were grown for 2 days at the same temperature and rpm due to slower growth.

3.3.2 Arabidopsis thaliana Growth Assay

The *A. thaliana* growth assay was performed in a similar manner for observation of root lengths and morphology, microscopy, GUS activity, and RNA isolation. For each assay, 200 *Arabidopsis thaliana* (Col-0 ecotype) seeds (wild-type, *axr1-3* and

tmk1,3,4/+) were sterilized using 50% (v/v) bleach solution (0.3% sodium hypochlorite) in a 1.5 mL microcentrifuge tube for 4 minutes with continuous shaking using a vortex (Fisher Genie 2) shake setting 6. The bleach solution was removed and the seeds were washed four times in 1 mL of sterile water. After removing the water, the seeds were suspended in 0.1% (w/v) Difco Agar, Granulated (Becton Dickinson, MD, USA). Seeds were placed onto circular 100 x 15 mm plates containing 0.5x Murashige & Skoog (MS) Modified Basal Medium with Gamborg Vitamins (Phyto Technology Laboratories, KS, USA), 1% sucrose, pH 5.7, 0.25% phytagel (Sigma-Aldrich, MO, USA). The seeds were vernalized at 4°C in the dark for 2 days and then stored vertically in a growth chamber at 22 °C under 100 µmol m^{-2} s^{-1} of 12 h light. After 6 days, previously grown bacterial cultures were prepared by taking 1 mL of culture and centrifuging at 14,000 rpm for 5 minutes. The supernatant was discarded and the bacterial pellet was suspended in sterile water to an OD_{600}/cm of 0.7. Bacterial cultures for heat killed samples were autoclaved, centrifuged at 8,000 rpm for 5 min and the pellet diluted to an OD_{600}/cm of 0.7 before plating 100 µL onto an LB plate to check vitality. 100 µL of heat killed or living bacterial solution (or sterile water as a negative control) was spread onto square 100 x 15 mm plates containing 0.5x MS, pH 5.7, 0.5% Gellan Gum powder (Phyto Technology Laboratories, KS, USA). Plates containing 1 µM IAA (Gibco Laboratories, USA) were previously prepared by adding IAA dissolved in DMSO (Sigma-Aldrich, MO, USA) directly to the media before pouring and solidifying. For assays using *tmk1,3,4/+*, 100 µL of 1 µM IAA was spread onto the media after it solidified. For GUS staining assay, 2,4-D and IAA plates were prepared by spreading 100 µL of 50 µg/mL 2,4-D (Gibco Laboratories, USA) or IAA. Six to 12 seedlings (depending on the assay) were

transferred onto each plate, which were then sealed with self-adherent wrap, 3M, Micropore surgical tape (Coban, USA). Plates were then placed in the same growth chamber under the same conditions as previous for 7 days until processing for all subsequent experiments. Pictures of plants were taken with a Nikon D5200 camera and roots were measured using ImageJ. Water was prepared from Millipore Synergy 185 and sterilized using a 0.2 micron polyethersulfone syringe filter.

3.3.3 Genome Analysis

Whole genome sequencing was performed by DOE Joint Genome Institute (Project ID 1055648). Analysis of complete genome sequences was performed using JGI Genome Portal, KEGG Mapper and RAST annotation service (Aziz et al., 2008; Overbeek et al., 2013; Brettin et al., 2015).

3.3.4 Confocal Microscopy

Five whole seedlings of sterile or bacterial treated Col-0 and *axr1-3* were each placed in a 1.5 mL microcentrifuge tube containing 1 mL of 4% paraformaldehyde. The tissue was fixed overnight at room temperature and then the solution was removed followed by washing twice with 1 mL of sterile phosphate buffer saline (1.37M NaCl, 26mM KCl, 10mM Na_2HPO_4•$7H_20$, 17.6mM KH_2PO_4,pH 7.4) and then storing at 4°C. Images were acquired by EMSL (Richland, WA) using a Zeiss LSM 710 scanning confocal microscope. The channels used were blue (Calcofluor White), green (Sybrgold DNA), red (chlorophyll autofluorescence) and grey (transmitted light).

3.3.5 Quantification of IAA by LC/MS

Extraction of IAA

From glycerol stocks, bacterial strains were streaked onto an LB or TSA (for DAB 33B) agar plate and grown at 28°C. A single colony was used to inoculate a starter culture of 6 mL liquid LB medium, supplemented with 5 mM L-tryptophan (Sigma-Aldrich, MO, USA), and grown at 28°C and 240 rpm. After 24 h, the starter culture was used to make a 60 mL culture of liquid LB medium, supplemented with 5 mM L-tryptophan, at OD_{600} 0.01. The cultures were grown at 28°C and 240 rpm for 24 h. The supernatant was collected at 8,000 g at 4°C. For IAA spike samples, 300 µg of IAA was added to the culture by first generating a 1 mg/mL IAA solution in 100% acetonitrile and diluting to 100 µg/mL IAA solution in LB medium, supplemented with 5 mM L-tryptophan. Samples were then acidified with 1N HCl to a pH of 3.0. The samples were then separated into 20 mL aliquots for biological triplicates.

A Sep-Pak C18 cartridge (360 mg sorbent, 55-105 µm particle size) was prepared for each sample by washing with 10 mL of 100% acetonitrile followed by 10 mL of water. The acidified supernatant was passed through the C18 cartridge. The C18 cartridge was then washed with 10 mL of water and eluted with 5 mL of 80% (v/v) acetonitrile. The eluate was centrifuged at 12,000 rpm for 5 min at 4°C to remove solid particles. A 20 ng/µL solution of IAA was suspended into 100% acetonitrile for use as a standard in mass spectrometry. Acetonitrile of HPLC grade and HCl of ACS grade was used for the experiment and water was prepared from Millipore Synergy 185.

LC-MS

Samples were separated and analyzed by a UPLC/MS system including the Dionex® UltiMate 3000 RSLC ultra-high pressure liquid chromatography system, consisting of a workstation with ThermoFisher Scientific's Xcalibur v. 4.0 software

package combined with Dionex®'s SII LC control software, solvent rack/degasser SRD-3400, pulseless chromatography pump HPG-3400RS, autosampler WPS-3000RS, column compartment TCC-3000RS, and photodiode array detector DAD-3000RS. After the photodiode array detector the eluent flow was guided to a Q Exactive Plus Orbitrap high-resolution high-mass-accuracy mass spectrometer (MS). Mass detection was full MS scan with low energy collision induced dissociation (CID) from 100 to 1000 m/z in positive ionization mode with electrospray (ESI) interface. Sheath gas flow rate was 30 arbitrary units, auxiliary gas flow rate was 7, and sweep gas flow rate was 1. The spray voltage was 3500 volts (-3500 for negative ESI) with a capillary temperature of 275°C. The mass resolution was 140,000 and the isolation window was 0.4 mDa. Substances were separated on a Phenomenex™ Kinetex C8 reverse phase column, size 100 x 2 mm, particle size 2.6 mm, pore size 100 Å. The mobile phase consisted of 2 components: Solvent A (0.5% ACS grade acetic acid in LCMS grade water, pH 3-3.5), and Solvent B (100% Acetonitrile, LCMS grade). The mobile phase flow was 0.20 ml/min, and a gradient mode was used for all analyses. The initial conditions of the gradient were 95% A and 5% B; for 30 minutes the proportion reaches 5% A and 95% B which was kept for the next 8 minutes, and during the following 4 minutes the ratio was brought to initial conditions. An 8 minutes equilibration interval was included between subsequent injections. The average pump pressure using these parameters was typically around 3,900 psi for the initial conditions.

Putative formulas of IAA metabolites were determined by performing isotope abundance analysis on the high-resolution mass spectral data with Xcalibur v. 4.0 software and reporting the best fitting empirical formula. Database searches were

performed using reaxys.com (RELX Intellectual Properties SA) and SciFinder (American Chemical Society).

Using the external standard of IAA with concentrations of 2.5 ng/µL, 5 ng/µL, 50 ng/µL and 100 ng/µL, with 0.2 µL injections, we calculated the concentration of free IAA in the samples using the peak area of UV280 in single ion chromatograms at positive ionization and subtracting the peak area of UV280 appearing at the same retention time of the LB or TSB medium only samples. To calculate the concentration in the original culture, the concentration was then divided by four to account for the original culture volume being 20 µL and the final elution volume being 5 µL.

3.3.6 Quantitative GUS Activity Assay

Sterile and bacteria treated DR5:GUS seedlings were harvested for GUS enzyme activity assay. 36 seedlings were separated into roots and vegetative tissue (including hypocotyl and leaves). The tissue was then placed into a 2 mL polypropylene disruption tube containing 1.0 g of 100 µm silica beads, 0.5 g of 1.7 mm zirconium beads, a single 14 mm silica bead. Tissue was disrupted by adding 500 µL of GUS extraction buffer (50 mM sodium phosphate pH 7.0, 10 mM EDTA pH 8.0, 0.1% SDS, 0.1% Triton X-100, 10 mM mercaptoethanol) and grinding at 4°C for 8 min, until homogenized, at 4000 rpm using HT Mini (OPS Diagnostics LLC, NJ, USA). The tissue was centrifuged at 4°C for 5 min at 12,000 rpm and the amount of protein in the supernatant was measured with Bradford assay. 50 µL volume of each sample was added (in 4 replicates) to a 96-well plate. 50 µL of 4-MUG reaction (25 mM 4-MUG in GUS extraction buffer) was added to each well and the plate was incubated at 37 °C and shaking at 100 rpm. After 30 min, 50 µL of 1 M sodium carbonate was added to stop the reaction. A standard curve was

generated with 100 nM, 250 nM and 500 nM 4-MU in sodium carbonate stop reagent. The fluorescence was measured using a BioTek Synergy HT microplate reader at an excitation wavelength of 365 nm, an emission wavelength of 455 nm and a sensitivity of 50. GUS activity was measured in nmol 4-MU/min/mg protein.

3.3.7 Transcriptome Analysis

RNA Isolation

Total RNA isolation was performed on Col-0 ecotype, wildtype, *axr1-3* and *tmk 1,3,4/+* lines using a modified protocol of the mirVana miRNA Isolation kit (Thermo Scientific, MA, USA). For RNA-Seq, 6 seedlings were used for whole seedling extraction and 25 seedlings were used for root-specific extraction. For qRT-PCR and RT-PCR, seedlings were cut into roots and vegetative tissue (including hypocotyl and leaves). Roots from 60 seedlings were used and vegetative tissue from 12 seedlings were used. Tissue was placed into a 2 mL polypropylene disruption tube containing 1.0 g of 100 µm silica beads, 0.5 g of 1.7 mm zirconium beads, and a single 14 mm silica bead. Tissue was disrupted by adding 1 mL of lysis buffer, supplied by the RNA isolation kit, and grinding at 4°C for 2-16 min, until homogenized, at 4000 rpm using HT Mini (OPS Diagnostics LLC, NJ, USA). Tubes were left on ice for 5 min and then 100 µL of Homogenenate Additive, supplied by the RNA isolation kit, was added. After 10 min on ice, the tubes were centrifuged at 10,000 rpm for 5 min at 4°C. The supernatant was removed and used for the remaining extraction following the RNA isolation kit manual. RNA was eluted with 50 µL of elution buffer, supplied by the RNA isolation kit, and stored at -20°C for short-term use or -80°C for long-term.

Concentration and quality of RNA was determined with a Nanodrop-1000 UV/Vis Spectrophotometer (Thermo Scientific, MA, USA) and then by running an aliquot of the sample on 2100 Bioanalyzer (Agilent Technologies, Inc., USA). Samples were then treated with TURBO DNA-free kit (Thermo Scientific, MA, USA).

RNA-Seq

Sequencing and analysis were performed by EMSL (Richland, WA) on 3 biological replicates. DeSeq2 was used to calculate the $\log_2$ change of the treated samples vs. the sterile control. Functional enrichment analysis was performed to illustrate pathways that are enriched among up and down regulated genes. Principal coordinate analysis was performed to evaluate the similarity between biological replicates.

RT-PCR

1 µg of DNase treated RNA was used to make cDNA with SuperScript III reverse transcriptase (Thermo Scientific, MA, USA). Primer sequences for the genes of interests (GH3.2, SAUR26, and Extensin12) and the housekeeping gene (Actin2) are located in Table 1. 0.7 µL- 2 µL of cDNA was added to the amplification mixture containing 1x buffer, 0.2 mM dNTPs, 0.2mM forward primer, 0.2 mM reverse primer, and 1 U of Taq polymerase. The quantity was determined by the housekeeping gene, Actin2. The PCR condition was Stage 1 at 95°C for 1 min, Stage 2 with 32 cycles for GH3.2 (37 cycles for SAUR26 and Extensin 12, and 30 cycles for Actin2) at 95°C for 30 sec, 65°C for 30 sec for GH3.2 and Actin2 (55°C for SAUR 26 and Extensin 12), 72°C for 30 sec, and Stage 3 at 72°C for 5 minutes. PCR products were analyzed on a 1% (w/v) agarose gel. Due to sequence similarity within the GH3 gene family, specificity of GH3.2 primers was confirmed by sequencing of the PCR product by Genewiz Co. (New Jersey, USA).

Sequences were analyzed using Serial Cloner and UGENE programs and RT-PCR was performed on samples treated without reverse transcriptase as a control.

RT-qPCR

cDNA from vegetative tissue samples was generated using 1 µg of DNase treated RNA with SuperScript III reverse transcriptase (Thermo Scientific, MA, USA). Primer sequences were generated using Primer Express 3.0.1. A standard curve and melt curve analysis were performed on each primer set to calculate efficiency and ensure specificity. Four 1:10 dilutions were used for Actin2 and five 1:10 dilutions were used for GH3.2. Efficiencies and primer sequences are located in Table 2. qPCR was performed using 3 µL of sterile autoclaved water, 1 µL of forward primer, 1 µL of reverse primer, 10 µL of Power SYBR Green Master Mix (Thermo Scientific, MA, USA), and 5 µL of cDNA (diluted 1:100). The PCR condition was Stage 1 at 95° C for 10 min and Stage 2 (40 cycles) at 95° C for 15 s and 60° C for 1 min. For melt curve analysis, there was an added Stage 3 at 95° C for 15 s, 60° C for 1 min and 95° C for 15 sec. Relative gene expression was calculated with StepOne Software v2.2.2 using comparative C_T analysis. Each sample was analyzed using three technical replicates, and three biological replicates for Col-0 treatments and five biological replicates for *axr1-3* treatments. Actin2 was used as an endogenous control and the sterile Col-0 sample was used as a reference. Data is presented as the mean relative quantity (2^-ddCt) and error bars represent the minimum and maximum relative quantity. Student's T-test was performed using dCt values to determine significant difference ($P<0.05$) relative to the sterile control.

3.4 Results

3.4.1 Comparison of the Salkowski Assay and A. thaliana Auxin Phenotype

Of the bacteria isolated from duckweed that were able to produce indole containing compounds in culture (Gilbert et al. 2018), we asked whether all strains were able to produce a short root phenotype on *A. thaliana,* resembling that of an auxin response. Of the 23 tested pink-type and brown-type bacteria, only 6 pink-type caused a short root phenotype as demonstrated by primary root length inhibition (Figure 3.1 and 3.2). Two of these were the control strains *Azospirillum brasilense,* Sp7 and Sp245, from wheat. The remaining 4 strains, DAB 1A, DAB 1D, DAB 19A and DAB 19B, were of the genus *Microbacterium* and were derived from the duckweed genus *Lemna.* Only one other bacterial strain of the 23 tested was of the genus *Microbacterium*, and this strain, DAB 33B, which was derived from the duckweed genus *Wolffia,* did not cause a short root phenotype (Figure 3.2). None of the brown-type strains which produce indole displayed a short root phenotype. Thus, although the Salkowski assay detects production of indole containing compounds, a positive result does not always lead to a short root phenotype.

Exogenous tryptophan was not added to the bacteria growth medium before inoculation onto the plant. Exogenous tryptophan would thus be supplied by the plant if any was taken up by the bacterial strains. Of the five strains that tested positive in the Salkowski assay without exogenous L-tryptophan (Gilbert et al. 2018), only one caused a short root phenotype (Figure 3.1). Therefore, the ability to produce indole containing compounds, including IAA, without exogenous L-tryptophan is insufficient for the bacteria to cause a short root phenotype.

To determine whether the short root phenotype of *Microbacterium* strain DAB 1A was specifically related to IAA, we tested a subset of bacteria on two auxin insensitive *A.*

thaliana mutants in the TMK and AXR1 genes. The TMK gene family consisting of 4 genes encodes a transmembrane kinase. The *tmk1,3,4/+* mutant has altered early responses to auxin, but normal responses to other hormones such as ethylene, ABA and cytokinin (Dai et al., 2013). In roots, TMK genes are involved in cell expansion whereas in leaves, they are involved in cell number as well (Dai et al., 2013). The AXR1 gene is related to a ubiquitin-activating E1 enzyme and *axr1-3* mutant shows reduced sensitivity to IAA in the roots along with various other tissues (Lincoln et al., 1990). It has also been demonstrated that AXR1 mutants show reduced induction of ethylene biosynthesis by exogenous auxin (Lincoln et al., 1991). Negative control strain DAB 3D, which does not produce IAA, did not cause short roots on Col-0 nor *axr1-3* but inhibited the root length of *tmk 1,3,4/+* (Figure 3.2, Figure 3.3, and Figure 3.4). However, the difference in root phenotype may be due to increased colony growth because of sucrose added to the medium needed to grow this mutant line. No other DABs showed increased colony growth on the medium with added sucrose. Exogenously applied 1 µM IAA no longer inhibited root length on both mutants (Figure 3.3 and Figure 3.4). DAB 1A no longer inhibited root length in *axr1-3* and showed partial inhibition in *tmk 1,3,4/+* (Figure 3.3 and Figure 3.4). One possible explanation may be DAB 1A is producing more than 1 µM IAA, which is the concentration used for the exogenous control. The AXR1 mutant and TMK triple mutant appear to be involved in root response to DAB 1A.

3.4.2 Genome Comparison of Microbacterium strains

Since *Microbacterium* strains DAB 1A and DAB 19A resulted in a short root phenotype and DAB 33B did not, we asked how similar the genomes are to potentially identify genes responsible for the difference in phenotype. The average nucleotide

identity (ANI) for DAB 1A compared to DAB 33B, DAB 19A, and DAB 3D are 78.45, 83.49, and 59.78 respectively. The alignment fraction (AF) for DAB 1A compared to DAB 33B, DAB 19A and DAB 3D are 42.78, 66.76, and 0.392 respectively. An auxin related gene that encodes monoamine oxidase (EC 1.4.3.4) was present in the genome of DAB 1A and DAB 19A, but not DAB 33B. This enzyme converts tryptamine to indole-3-acetaldehyde in the IAA biosynthesis pathway. Interestingly, this gene was also present in the genome of *Azospirillum* strain, DAB 37A, which does not cause a short root phenotype, however whether it is expressed or not is unknown.

3.4.3 Localization of DABs on A. thaliana

We asked whether DAB 1A was localized to certain plant tissues in Col-0 as well as how this compared to localization of DAB 33B and negative control strain DAB 3D which does not produce indole related compounds. Positive control strain Sp245 showed endophytic colonization and formed biofilms (Figure 3.5A). Sp245 is an endophyte isolated from wheat tissues, therefore its ability to strongly colonize *A. thaliana* suggests a conserved mechanism of attachment on plant tissue. DAB 1A showed endophytic colonization on the leaves and roots, whereas DAB 33B showed epiphytic colonization on the leaves and roots (Compare Figure 3.5B and Figure 3.5C). DAB 33B was found in higher abundance on the leaves compared to the roots (Figure 3.5C). DAB 3D, which does not produce indole related compounds, showed epiphytic colonization on the leaves and roots and low abundance in these tissues (Figure 3.5D). Except for Sp245, all strains showed no observed differences in abundance or location on wild type (Col-0) vs. *axr1-3*. Endophytic colonization of Sp245 was not observed on *axr1-3* suggesting a different mode of attachment by this strain compared to DAB 1A. More specifically, Col-0 leaves

showed Sp245 colonization of stomata which was not observed with *axr1-3* (Figure 3.5A). Thus, AXR1 function in stomatal movement may be influencing Sp245 colonization on the plant.

3.4.4 Quantification of IAA from DAB Strains by LC-MS

We next asked whether the short root phenotype caused by *Microbacterium* strains was associated with the ability to produce high levels of IAA in culture. LC-MS was used to identify and quantify the amount of free IAA produced by various strains tested positive in our Salkowski assay. The retention time of free IAA in our LC-MS system was determined to be approximately 9.7 min (Gilbert et al., 2018). The molecular weight of free IAA is 175 g/mol with positive ionization resulting in a molecular ion at m/z 176 [M+H] and a fragment at m/z 130, as previously determined (Gilbert et at., 2018). The resulting standard curve equation was generated; y=5,722x-193.47 with an R^2 value of 1.00. Using three biological replicates of 1 µL injections each, we calculated the % recovery of free IAA in our extraction with 5 ng/µL spike samples. The free IAA spike in the LB medium was 2.408 ng/µL ± 0.173 ng/µL (48% recovered) and the amount of free IAA spike in the TSB medium was 2.750 ng/µL ± 0.184 ng/µL (55% recovered). The amount of free IAA in the bacterial supernatant of control strain DAB 3D was 0.014 ng/µL ± 0.007 ng/µL, of DAB 33B, was 0.344 ng/µL ± 0.017 ng/µL and of DAB 1A, was 20.709 ng/µL ± 1.970 ng/µL. Thus, of the two pink-type *Microbacterium* strains, DAB 1A which causes a short root phenotype, can produce higher levels of free IAA than DAB 33B which does not cause a short root phenotype.

We next compared the amount of free IAA in the supernatant of various DAB strains that were top producers of indole related compounds based on the Salkowski

assay. Three other strains capable of producing a short root phenotype (DAB 19A, Sp7 and Sp245) were screened for IAA quantification, as well as four strains not capable of producing a phenotype, yet based on the Salkowski assay were top producers of indole related compounds (DAB 5E, DAB 20A, DAB 33A and DAB 37A). The strains not capable of producing a short root phenotype all produced lower than 1 ng/µL of free IAA (Figure 3.6). Control strain Sp245 produced a similar level of IAA as previously reported (Ona et al., 2005).

3.4.5 Quantification of IAA response in the Plant

We next asked whether IAA response in the plant was greater upon treatment of DAB 1A compared to DAB 33B. Furthermore, we wanted to know whether the IAA response was stronger in the roots or vegetative tissue. We used the DR5:GUS reporter system to measure GUS activity in response to the IAA-responsive synthetic promoter, DR5. GUS activity in nmol 4-MU/min/mg protein was measured using MUG as a substrate. *A. thaliana* roots and vegetative tissue were evaluated separately to compare tissue specific GUS activity in response to *Bacillus* strain DAB 3D, *Microbacterium* strain DAB 1A, *Microbacterium* strain DAB 33B, and exogenous 1 µM IAA. In the vegetative tissue, relative to the sterile control, GUS activity increased in response to 1 µM IAA and DAB 1A, decreased in response to DAB 33B and was not changed in response to DAB 3D (Figure 3.7). In the roots, the sterile control sample showed high background levels of GUS activity and there was minimal increase in GUS activity in response to the IAA control. This suggests the biochemical activity of the reporter system may be saturated by endogenous IAA. GUS activity decreased in response to all bacterial treatments indicating that endogenous levels of IAA may have decreased.

3.4.6 Transcriptome of A. thaliana in Response to DABs

RNA-Seq Analysis

We asked to what extent the plant showed a transcriptomic response when treated with DAB 3D, DAB 1A, DAB 33B and exogenous 1 µM IAA. Functional enrichment analysis of RNA-Seq was performed to show which pathways were enriched among genes that were upregulated and downregulated. The response to auxin pathway (indicated in the heatmap with an arrow) was significantly upregulated by DAB 1A, DAB 33B and exogenous 1 µM IAA (Figure 3.8). This suggests that although DAB 33B did not cause an auxin associated short root phenotype, it nevertheless induced an auxin response in the plant.

We clustered the remaining pathways into three groups based on the pattern of regulation (Figure 3.8). Group 1 contains most pathways that were enriched by our treatments. They were either significantly upregulated or downregulated by treatment of 1 µM IAA but not in the bacterial treatments, which suggests many pathways were significantly changed by exogenous IAA without enrichment by IAA-producing *Microbacterium* strains DAB 1A and DAB 33B. Based on microscopy, DAB 3D does not strongly attach to the plant tissue and transcriptomics suggests that the plant has less overall enrichment of pathways compared to DAB 1A and DAB 33B (Figure 3.8). However, the ‘response to bacterium’ pathway (indicated in the heatmap with an arrow), showed significant upregulation by treatment with all three DABs, but not exogenous IAA, suggesting that the plant is still responsive to DAB 3D. Conversely, Group 2 contains pathways that were upregulated in response to only DAB 1A and DAB 33B and contains pathways such as ‘peroxidase activity’, ‘endoplasmic reticulum’ and

'phosphorylation' (Figure 3.8). Specifically, FRK1 (FLG22-induced receptor-like kinase 1) and wall associated kinase genes, WAK5 and WAKL10, were significantly upregulated by DAB 1A and DAB 33, but not DAB 3D and exogenous 1 µM IAA. Group 3 contains pathways that were upregulated in response to only DAB 1A and are comprised of 'cell cycle' and 'microtubule' pathways, which may be correlated with the short root phenotype (Figure 3.8).

RNA-Seq on auxin insensitive mutants, *axr1-3* and *tmk1,3,4/+*, was used to determine whether the transcriptome changes in auxin response genes were dependent or independent of an IAA response mechanism. Mutants were treated with DAB 1A, DAB 33B and 1 µM IAA. In addition to the 'response to auxin' pathway (indicated in the heatmap with an arrow), various other pathways showed a loss of significant regulation in *axr1-3* to all three treatments, suggesting the AXR1 locus may be affecting other plant processes besides auxin (Figure 3.9). In all three treatments, the 'response to auxin' pathway was still significantly upregulated in *tmk 1,3,4/+* and various other pathways were also still enriched (Figure 3.9). In particular, Group 1 pathways were upregulated and Group 2 pathways were downregulated in response to DAB 1A and DAB 33B (Figure 3.9). However, treatment with exogenous IAA showed less pathways enriched by comparison to the functional enrichment analysis of the wild type plants (Compare Figure 3.8 and Figure 3.9). Along with the root length data, transcriptomics on auxin insensitive mutants suggest that the AXR1 and TMK loci are involved to a different extent in auxin response to DAB 1A. Furthermore, although no root phenotype was observed by treatment with DAB 33B, the plant nevertheless is responding to auxin.

Differential expression analysis was performed to determine which genes were upregulated and downregulated within a pathway. Auxin biosynthesis genes were not upregulated by DAB 1A or DAB 33B in Col-0, suggesting that an auxin response is most likely not due to endogenous IAA produced by the plant. Within the auxin response pathway, Gretchen Hagen 3 genes, GH3.2 and GH3.3, were significantly upregulated by DAB 1A on Col-0 (Figure 3.10). GH3 enzymes are known to conjugate free IAA as an early response mechanism for reducing high amounts of IAA in the plant. GH3.2 and GH3.3 genes were not as significantly upregulated by DAB 33B and 1 µM IAA treatments (Figure 3.10). One explanation may be that induction of these genes require higher levels of free IAA or another possible explanation may be that the exogenous IAA was already conjugated by 7 days at which the tissue was harvested. By comparison to DAB 1A treated Col-0, GH3.2 had increased upregulation in *tmk1,3,4/+* but not in *axr1-3*, whereas GH3.3 had increased upregulation in *axr1-3* but not in *tmk1,3,4/+* (Figure 3.10). This further indicates that the TMK genes and the AXR1 gene have different functions in auxin response.

To determine which genes have a change in expression by DAB 1A and not DAB 33B, we compared the $\log_2$ change of DAB 1A vs DAB 33B on Col-0. Genes that had significant differential expression were proline-rich extensins which were more strongly upregulated by DAB 1A than DAB 33B relative to the sterile control. In *tmk 1,3,4/+* but not *axr1-3,* expression of extensin genes were downregulated by DAB 1A (Figure 3.11). As previously mentioned, the TMK gene family is known to be involved in auxin sensitivity resulting in cell expansion in roots and leaves (Dai et al., 2013). Treatment with DAB 33B and exogenous IAA resulted in different gene expression patterns of

extensin genes in wild-type (Col-0) and auxin mutant lines compared to DAB 1A treatment (Figure 3.11). These results indicate that upregulation of extensin genes by DAB 1A is dependent on the TMK locus.

We next asked which pathways were enriched specifically in the root tissue of Col-0 and *axr1-3*, to find pathways potentially associated with the short root phenotype of DAB 1A. Overall, many pathways in the roots of Col-0 and *axr1-3* were not significantly enriched by our treatments, except for treatment of *axr1-3* with DAB 33B (Figure 3.12). In particular, the 'response to auxin' pathway was not significantly enriched in the roots by any of the treatments. This suggests a more homogenous gene expression between root tissue samples compared to whole seeding samples. The difference in pathway enrichment in the root tissue compared to whole seedling tissue of Col-0 may be due to a time dependent or dosage dependent effect (Compare Figure 3.8 and Figure 3.12). Of the few pathways that were significantly enriched, we clustered them into two groups (Figure 3.12). Group 1 contains pathways that were upregulated only in *axr1-3* by treatment with DAB 3D and DAB 33B, but not DAB 1A. These include 'response to bacterium', 'plant-type hypersensitive response', and regulation of 'systemic acquired resistance' pathways. This suggests that the AXR1 gene may function to suppress plant immune response in the root, specifically to DAB 3D and DAB 33B. Group 2 contains pathways that were upregulated in Col-0 by treatment with DAB 1A, but not 1 µM IAA, and was not upregulated in *axr1-3* (Figure 3.12). These are 'manganese ion binding' and 'nutrient reservoir activity' pathways. These pathways appear to be dependent on the AXR1 gene and suggests DAB 1A has additional signaling pathways besides IAA.

RT-PCR

To validate RNA-Seq analysis, RT-PCR was performed on GH3.2, SAUR 26 and Extensin12 before more sensitive gene expression quantification with RT-qPCR. In the sterile control sample, GH3.2 and Extensin12 genes were expressed more in the roots whereas SAUR26 was expressed more in the vegetative tissue (Figure 3.13). GH3.2 showed upregulation in the roots in response to DAB 1A and DAB 33B. Contrary to expected, upregulation of SAUR26 by DAB 1A, DAB 33B and exogenous IAA was not detectable with RT-PCR, but appeared to be upregulated in the roots and vegetative tissue by DAB 3D. Extensin12 showed upregulation in the roots by both DAB 1A and DAB 33B. However, expression in the vegetative tissue appeared to be greater by DAB 1A than DAB 33B, suggesting that the RNA-Seq, which was performed on whole seedlings, better reflected that of the vegetative tissue.

RT-qPCR

RT-qPCR was performed on Col-0 and *axr1-3* to quantify the degree of upregulation of GH3.2. Root tissue data had high variability between biological replicates making accurate quantification difficult. In vegetative tissue, upregulation of GH3.2 relative to the sterile control was significant in DAB 1A and DAB 33B treatments of Col-0 but not *axr1-3* (Figure 3.14). This suggests that DAB 1A as well as DAB 33B caused a response in the plant for conjugation of auxin, a known mechanism of responding to excess levels of IAA.

3.5 Discussion

In order to utilize auxin-producing bacteria in an agricultural application, such as through the use of synthetic bacterial communities, the mechanisms of auxin signaling in the plant microbiome need to be studied. Out of the 21 tested DAB strains capable of producing indole related compounds in our previous study (Gilbert et al., 2018) we identified four *Microbacterium* strains that resulted in a short root phenotype on *A. thaliana*, one being DAB 1A. By comparison of various DAB strains with LC-MS, the capacity to produce high levels of IAA appears to be associated with the short root phenotype. Strains that were top producers of indole related compounds using the Salkowski assay, which in many cases did not correspond to IAA, did not cause a short root phenotype. Thus, this commonly used assay for detecting auxin-producing strains does not necessarily result in an auxin phenotype.

We used the DR5:GUS reporter line to quantify IAA response in the plant. High background levels of GUS activity in the sterile roots and minimal increase by the exogenous IAA control indicates that the DR5 reporter system was responsive to endogenous IAA and biochemical activity was already saturated. Thus, significant increase in GUS activity was observed only in the vegetative tissue not the roots upon treatment with DAB 1A.

Auxin insensitive mutants were used to determine whether the short root phenotype caused by DAB 1A was dependent on IAA response in the plant. Although the short root phenotype caused by DAB 1A in the wild type plant was no longer observed in the auxin insensitive mutant *axr1-3*, there was still a small, but significant, level of root inhibition in *tmk 1,3,4/+* indicating that the TMK and AXR1 genes respond to auxin differently. Furthermore, our data indicates that AXR1 may have additional roles in plant-bacterial

interactions besides auxin signaling. Transcriptomics on the auxin mutant whole seedlings revealed that regulation of other non-auxin pathways was also affected in *axr1-3*. Transcriptomics on Col-0 and *axr1-3* roots suggests that the AXR1 gene may function to suppress the plant immune system in the roots in response to DAB 3D and DAB 33B, but not DAB 1A. The AXR1 gene has been previously reported to be involved in cytokinin and jasmonic acid signaling as well (Tiryaki and Staswick, 2002; Li et al., 2013). In wild type (Col-0) whole seedlings, treatment with DAB 33B caused significant upregulation of the 'response to cytokinin' pathway which was no longer observed in *axr1-3.* The 'response to jasmonic acid' pathway was significantly downregulated in wild type plants by DAB 1A and DAB 33B, which was also no longer observed in *axr1-3.* Furthermore, *axr1-3* has been reported to have accelerated stomatal response compared to wild-type in red and blue light exposure (Eckert and Kaldenhoff, 2000). Sp245 formed biofilms on wild type roots and leaves, specifically localizing to stomata and endophytic colonizing the plant. Plant defense response to bacteria may occur through stomata closure which prevents the entry of pathogens (Melotto et al., 2006). Endophytic colonization and stomata localization were not observed in *axr1-3,* suggesting AXR1 may additionally function to reduce bacterial colonization.

Transcriptome analysis revealed similarities and differences between plant responses to two IAA-producing *Microbacterium* strains. Treatment with DAB 1A caused enrichment of 'cell cycle' and 'microtubule' pathways which may be associated with the short root phenotype that also display a proliferation of lateral roots and root hairs. Furthermore, treatment with DAB 1A caused upregulation of extensin genes in the wild type but not in *tmk 1,3,4/+*. This was not observed with DAB 33B and exogenous

IAA, indicating a potential role of the TMK locus in extension gene expression specifically due to DAB 1A. Despite the low levels of IAA produced by DAB 33B in culture, this strain was not capable of causing a short root phenotype, but nevertheless caused a change in gene expression of auxin response genes as illustrated by upregulation of GH3.2 expression in the vegetative tissue of Col-0. The plant may be responding to low levels of IAA, other indole related compounds, or displaying a non-auxin related response. Lastly, there were observed differences in the transcriptome of plants treated with exogenous IAA compared to IAA-producing strains. The observed pathways enriched by only exogenous IAA may be dependent on time, dosage or be specific to non-bacterial derived IAA. There was significant upregulation of FRK1, WAK5 and WAKL10 genes in response to DAB 1A and DAB 33B, but not exogenous IAA and DAB 3D. FRK1 is a well-studied defense response gene involved in pathogen-associated molecular pattern-triggered immunity (PTI) and WAK genes, specifically WAK1 and WAKL10, are known to be expressed during pathogen response (He et al., 1998; Meier et al., 2010). Thus, DAB 1A and DAB 33B may be inducing a defense response in the plant.

Microscopy on roots and leaves suggest that DAB 1A is endophytic whereas DAB 33B and DAB 3D are epiphytic. This could explain the difference in root phenotype and transcriptomics upon treatment of the three strains. DAB 33B was primarily abundant on the leaves, suggesting a tissue specific niche for this strain. DAB 3D was not abundant on the leaves nor roots, which may explain the overall lower transcriptome response to this strain, despite having gene expression changes in a subset of bacterial response genes.

Therefore, the differences in location and abundance of these strains may contribute to the varying physiological and molecular responses in the plant.

Overall, this work demonstrates the similarities and differences in phenotypic and molecular responses of *A. thaliana* to two genetically similar *Microbacterium* strains that are capable of producing different levels of IAA. While the intellectual merit of this work includes limitations of the Salkowski assay and differences in wild-type and auxin mutant plant response to IAA-producing strains, further studies are necessary to determine whether the responses we found in this study are similar or different in duckweeds. This would provide information on the degree of conserved plant-bacteria interaction mechanisms and contribute to existing studies demonstrating that DABs can improve the health of duckweed through a variety of mechanisms, such as increasing frond production rate, chlorophyll content and the plant's ability to remove nitrogen and phosphate from wastewater (Korner and Vermaat, 1998; Yamaga et al., 2010; Suzuki et al., 2014).

3.6 Tables and Figures

Table 3.1. Primer sequences for RT-PCR. Primer sequences used in reverse transcription-polymerase chain reaction (RT-PCR) performed on Actin2, GH3.2, Extensin12 and SAUR26 genes. Actin2 was used as an endogenous control.

Locus	Gene	Polarity	Sequence
AT3G18780	Actin2	Forward	GTCTTGTTCCAGCCCTCGT
		Reverse	GAGATCCACATCTGCTGGAATG
AT4G37390	GH3.2	Forward	GCCTGTGATGAATCTCTACGTG
		Reverse	CCCTTCCCAATTCTCTTGTG
AT4G13390	EXT12	Forward	ATGAAAGGGCTTGGTCATTG
		Reverse	GTGGGGGTGATTCTGAGAGA
AT3G03850	SAUR26	Forward	AAGCAAAAAGCTACCGCAAC
		Reverse	TCTCAGCTCCAAGGATGAAGA

Table 3.2. Primer sequences and percent efficiency for RT-qPCR. Primer sequences and percent efficiency used in reverse transcription-quantitative polymerase chain reaction (RT-qPCR) on Actin2 and GH3.2 genes. Actin2 was used as an endogenous control.

Locus	**Gene**	**Polarity**	**Sequence**	**% Efficiency**
AT3G18780	Actin2	Forward	GATTCAGATGCCCAGAAGTCTTG	86.0
		Reverse	TGGATTCCAGCAGCTTCCAT	
AT4G37390	GH3.2	Forward	TCGTCCGGTTCTCACGAGTT	86.9
		Reverse	ACGGATCGTACGGTCGTCTCT	

Figure 3.1. Comparison of Salkowski assay and Col-0 auxin root phenotype.

Modified figure from Gilbert et al. 2018. Addition of Salkowski reagent to the bacterial supernatant of a subset of the pink-type and brown-type bacteria strains grown in medium with and without 5 mM L-tryptophan to measure the absorbance of indole related compounds at 530 nm. An asterisk indicates bacterial strains that induce a short root phenotype on Col-0. A "+" symbol indicates the strain has a Salkowski color change in the absence of supplemented 5mM L-tryptophan.

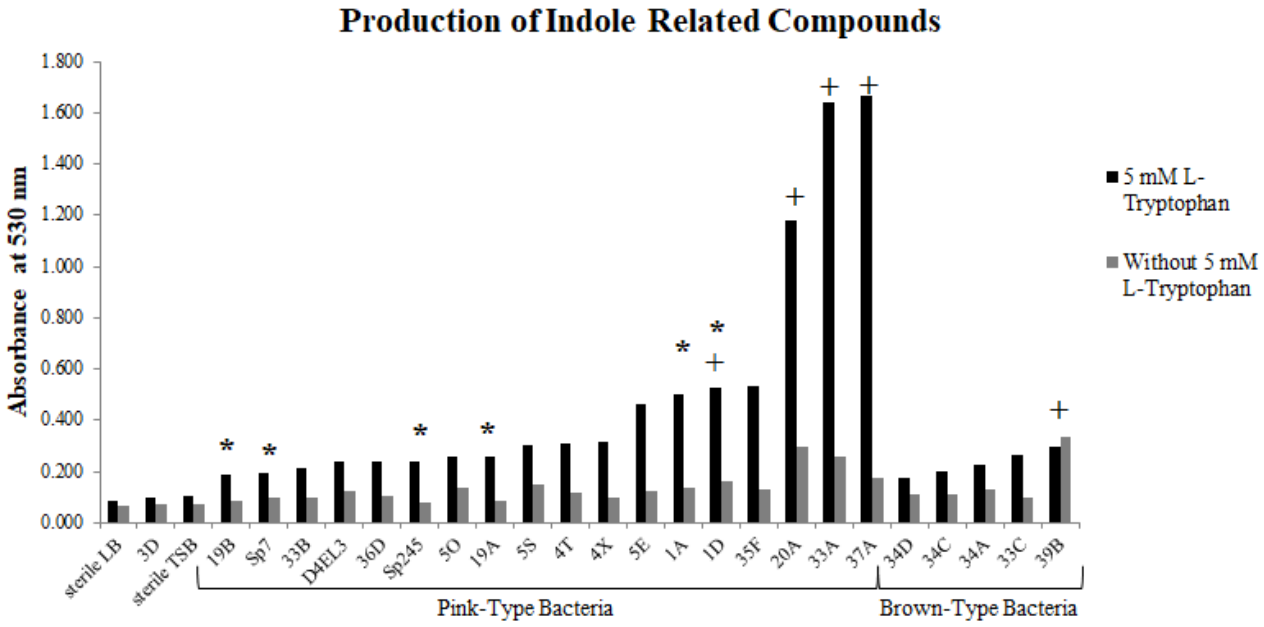

Figure 3.2. Effect of DABs on Col-0 primary root length. Box plot for change in primary root length in millimeters (mm) after 7 days. Horizontal lines represent the median, with the box representing the 25th and 75th percentiles, the whiskers representing the minimum and maximum. 1 µM IAA and well characterized IAA-producing *Azospirillum* strain Sp245 were used as positive controls. HT = Heat treated. Student's T-test ($P<0.05$) was performed (n=18) and an asterisk indicates significant difference compared to the sterile control.

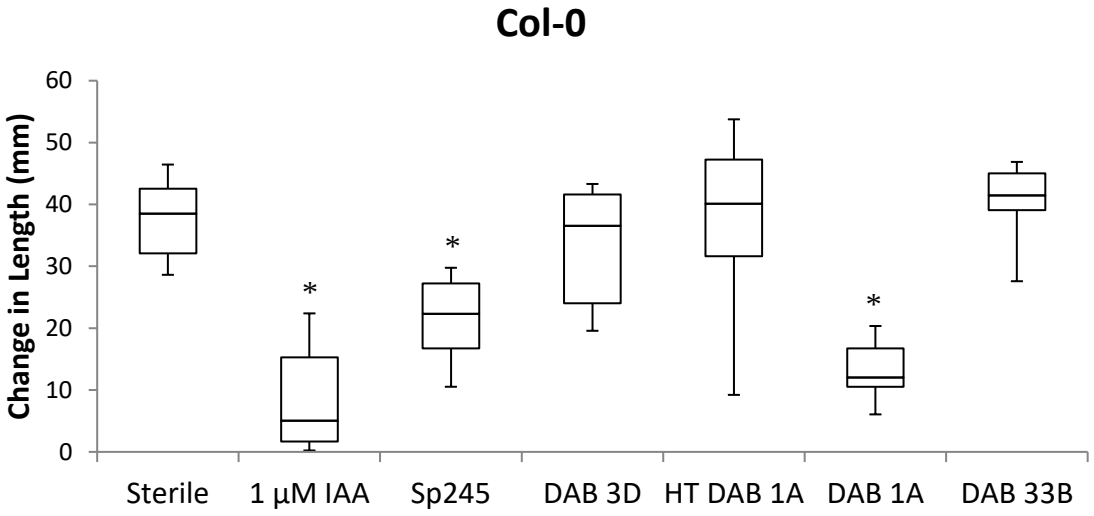

Figure 3.3. Effect of DABs on *axr1-3* primary root length. Box plot for change in primary root length in millimeters (mm) after 7 days. Horizontal lines represent the median, with the box representing the 25th and 75th percentiles, the whiskers representing the minimum and maximum. 1 µM IAA and well characterized IAA-producing *Azospirillum* strain Sp245 were used as positive controls. Student's T-test ($P<0.05$) was performed (n=18) and no treatments were significantly different compared to the sterile control.

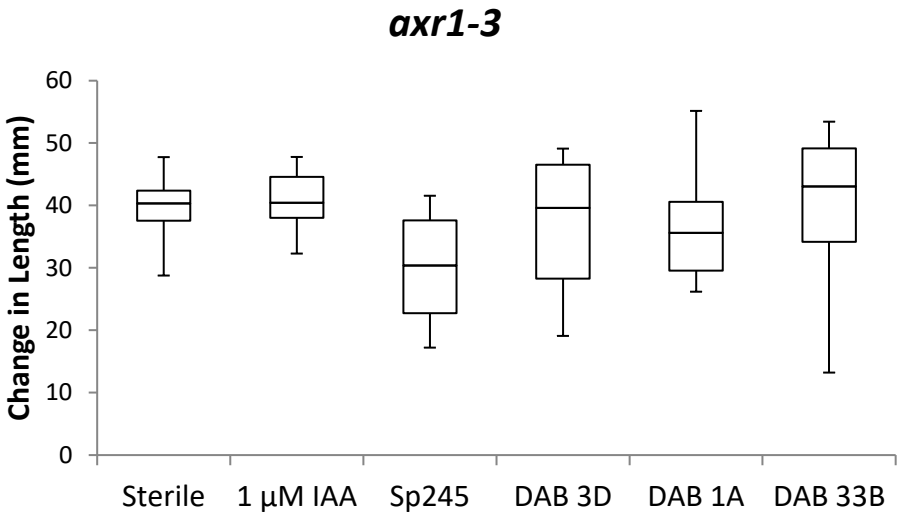

Figure 3.4. Effect of DABs on *tmk 1,3,4/+* primary root length. Box plot for change in primary root length in millimeters (mm) after 7 days. Horizontal lines represent the median, with the box representing the 25th and 75th percentiles, the whiskers representing the minimum and maximum. 1 µM IAA was used as a positive control. Student's T-test ($P<0.05$) was performed (n=18) and an asterisk indicates significant difference compared to the sterile control.

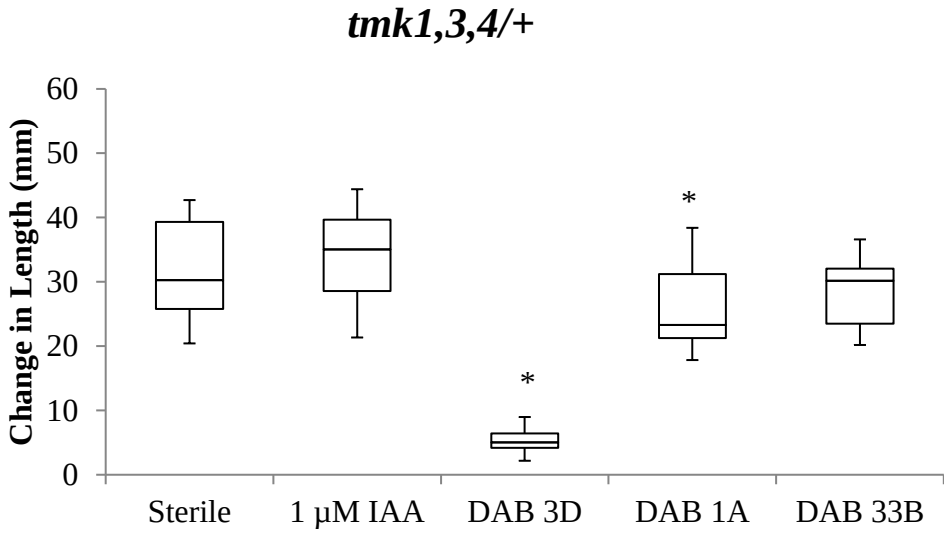

Figure 3.5. Localization of bacteria on Col-0 tissue. Confocal microscopy showing 3D structure of Col-0 leaves and roots, and orthogonal (ortho) view of Col-0 roots upon treatment with **A)** endophytic control strain *Azospirillum* Sp245, **B)** *Microbacterium* DAB 1A, **C)** *Microbacterium* DAB 33B, **D)** *Bacillus* DAB 3D and **E)** no bacteria. The microscopy channels are blue (Calcofluor White), green (Sybrgold DNA), red (chlorophyll autofluorescence) and grey (transmitted light). White arrows indicate bacteria location.

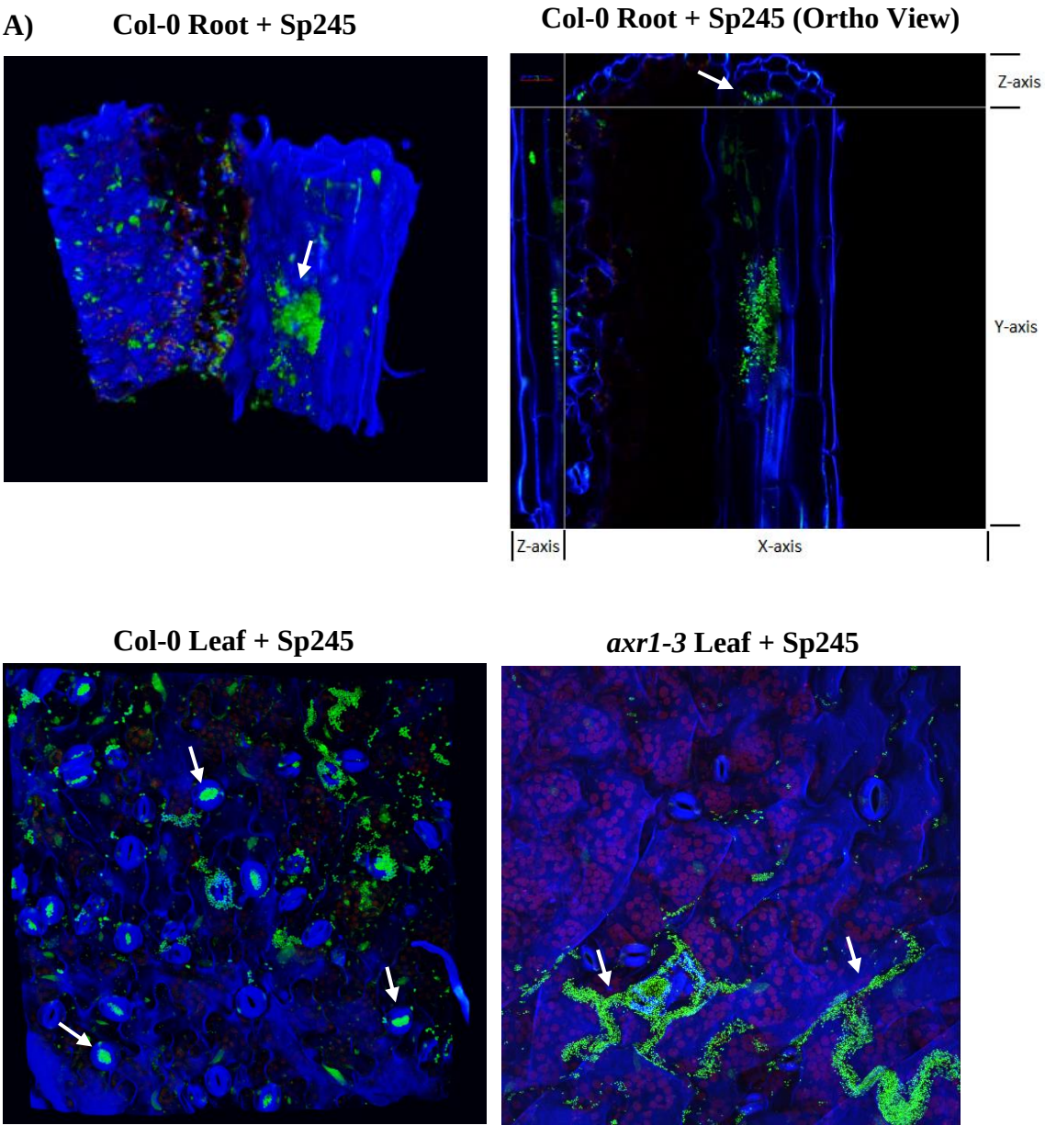

B)

Col-0 Root + DAB 1A

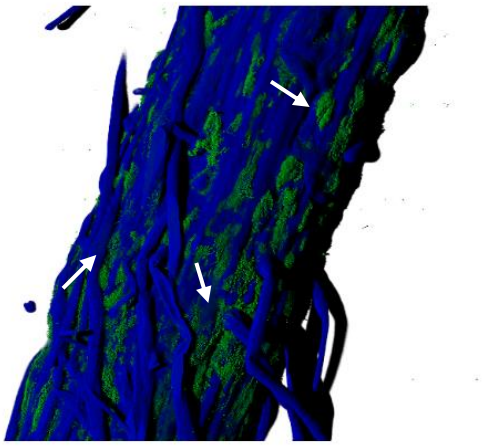

Col-0 Root + DAB 1A Ortho View

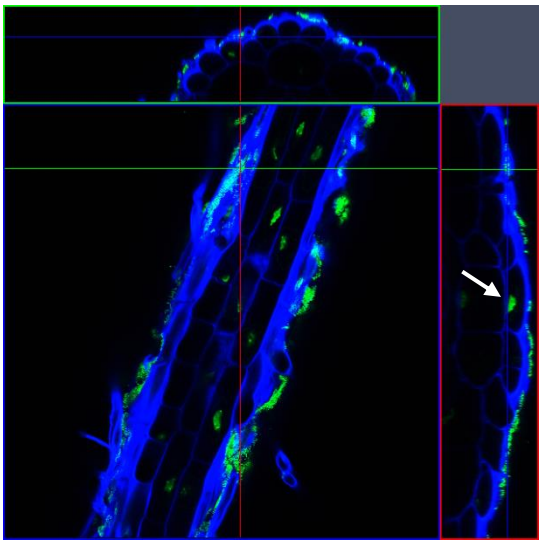

Col-0 Leaf + DAB 1A

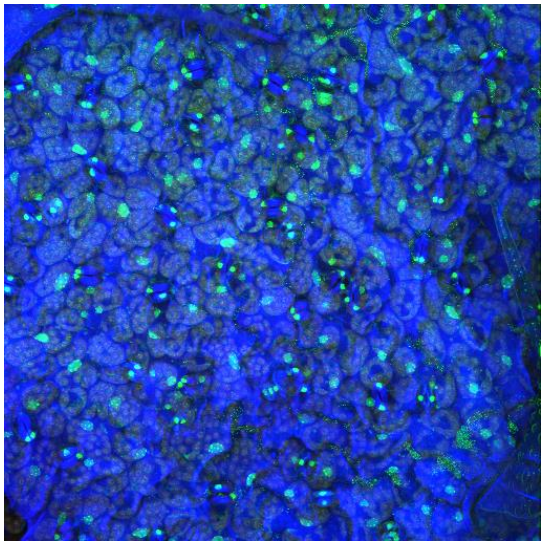

C)

Col-0 Root + DAB 33B

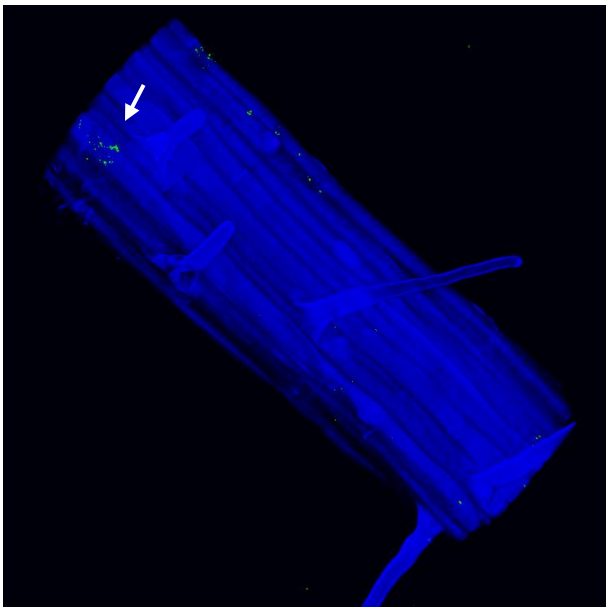

Col-0 Root + DAB 33B Ortho View

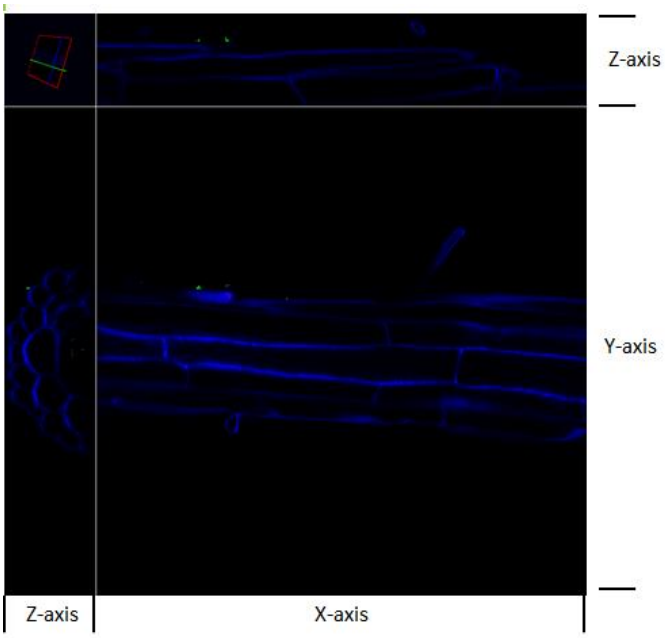

Col-0 Leaf + DAB 33B

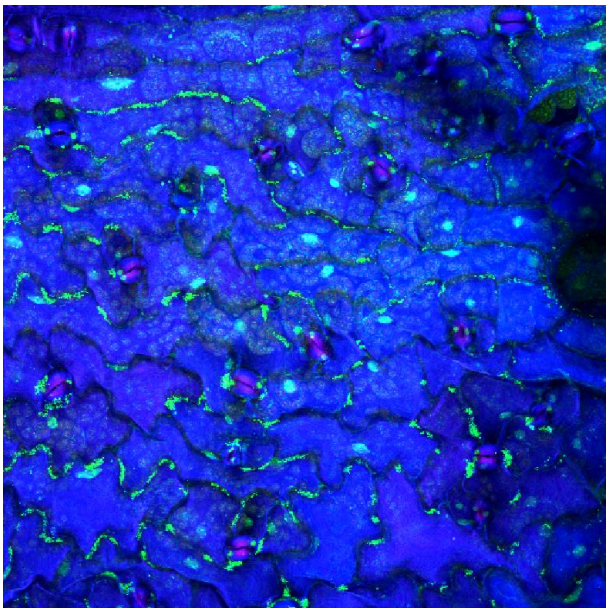

D)

Col-0 Root + DAB 3D

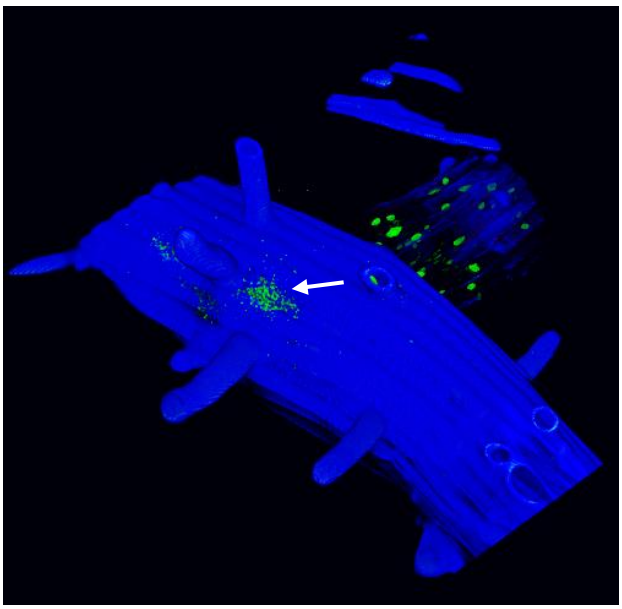

Col-0 Root + DAB 3D Ortho View

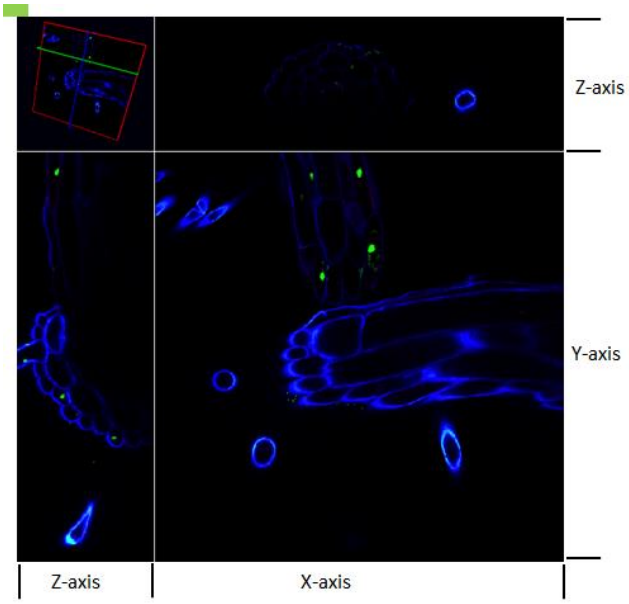

Col-0 Leaf + DAB 3D

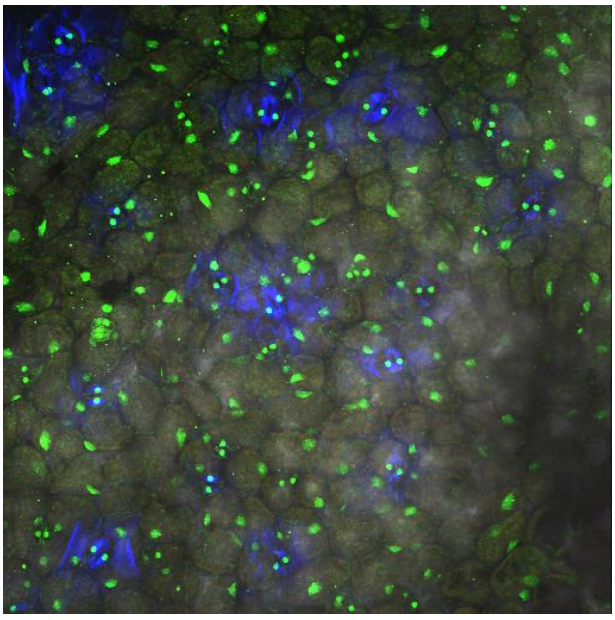

E)

Col-0 Root + No bacteria

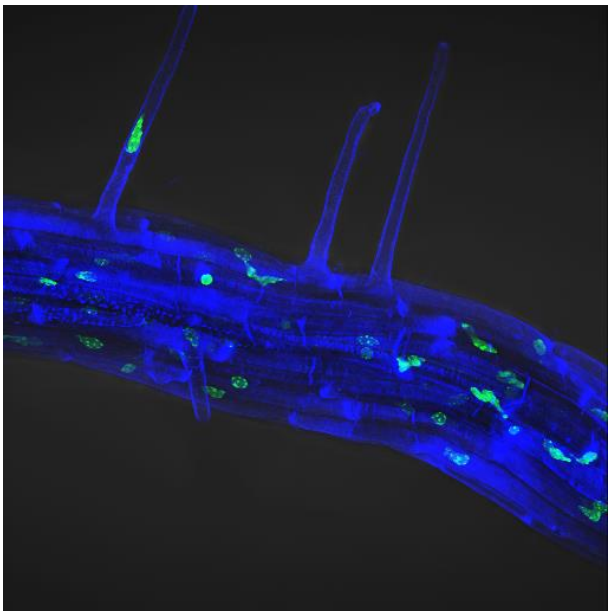

Col-0 Leaf + No bacteria

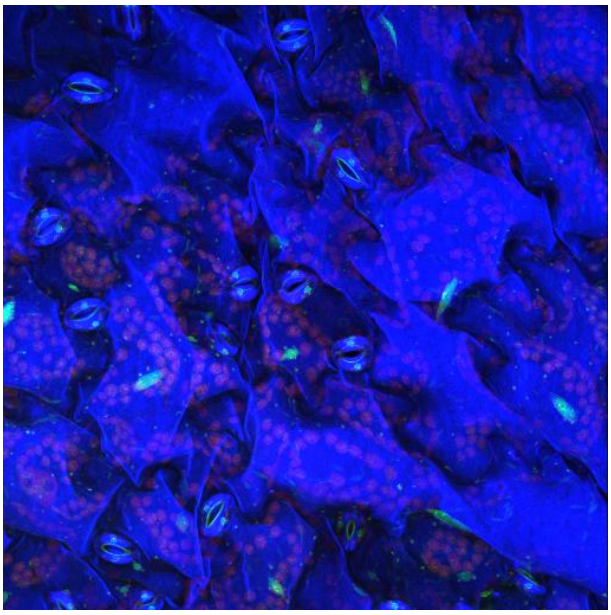

Figure 3.6. Quantification of IAA in bacterial supernatants by LC-MS. Data represents mean values of UV280 and SE (n=3). Bars with different letters are significantly different (One-way ANOVA p-value = 1.9E-09, Fisher's LSD = 3.7). Samples are listed in order of increasing Salkowski assay result for comparison.

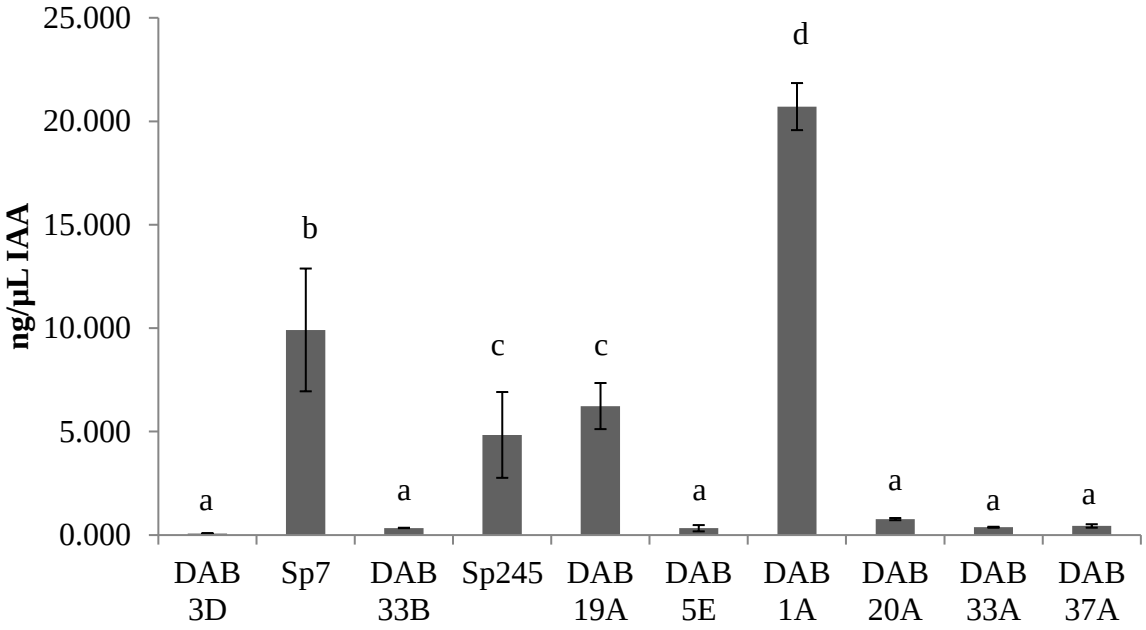

Figure 3.7. Effect of DABs on GUS activity in DR5:GUS. GUS activity in vegetative tissue (One-way ANOVA p-value= 2.42E-14, Fisher's LSD = 7.78) and in root tissue (One-way ANOVA p-value= 4.21E-11, Fisher's LSD= 27.32). Data represent mean values and SE are calculated from 4 replicates for vegetative samples and 3 replicates from root samples. Bars with different letters/numbers are significantly different.

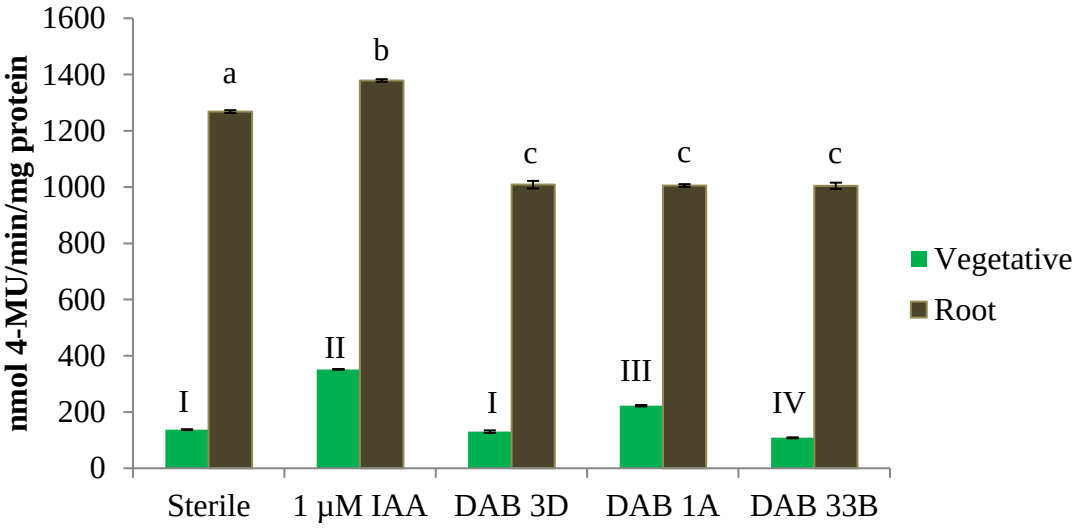

Figure 3.8. Functional enrichment analysis of RNA-Seq on wild-type whole seedlings. Pathways significantly regulated in Col-0 treated with *Bacillus* DAB 3D, *Microbacterium* DAB 1A, *Microbacterium* DAB 33B, or 1 µM IAA. Columns represent treatments whereas rows represent pathways significantly enriched. Enrichment score indicates statistical strength of the enrichment relative to the sterile control, with red indicating upregulation and blue indicating downregulation. Split cells indicate significant enrichment of the pathway's genes among both up- and down-regulated genes. Pathways are grouped based on the observed pattern of regulation.

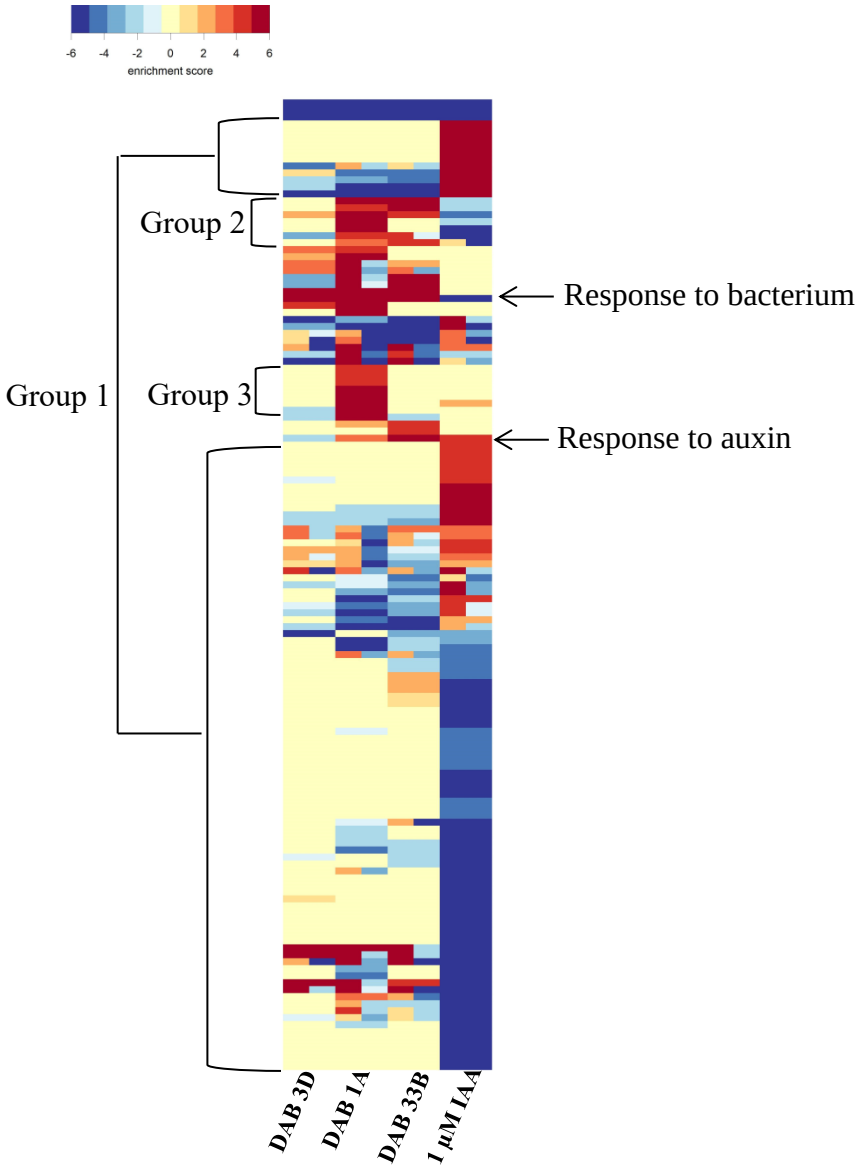

Figure 3.9. Functional enrichment analysis of RNA-Seq on auxin mutant whole seedlings. Pathways significantly regulated by *Microbacterium* DAB 1A, *Microbacterium* DAB 33B and 1µM IAA in *axr1-3* and *tmk1,3,4/+*. Columns represent treatments whereas rows represent pathways significantly enriched. Enrichment score indicates statistical strength of the enrichment relative to the sterile control, with red indicating upregulation and blue indicating downregulation. Split cells indicate significant enrichment of the pathway's genes among both up- and down-regulated genes. Pathways are grouped based on the observed pattern of regulation.

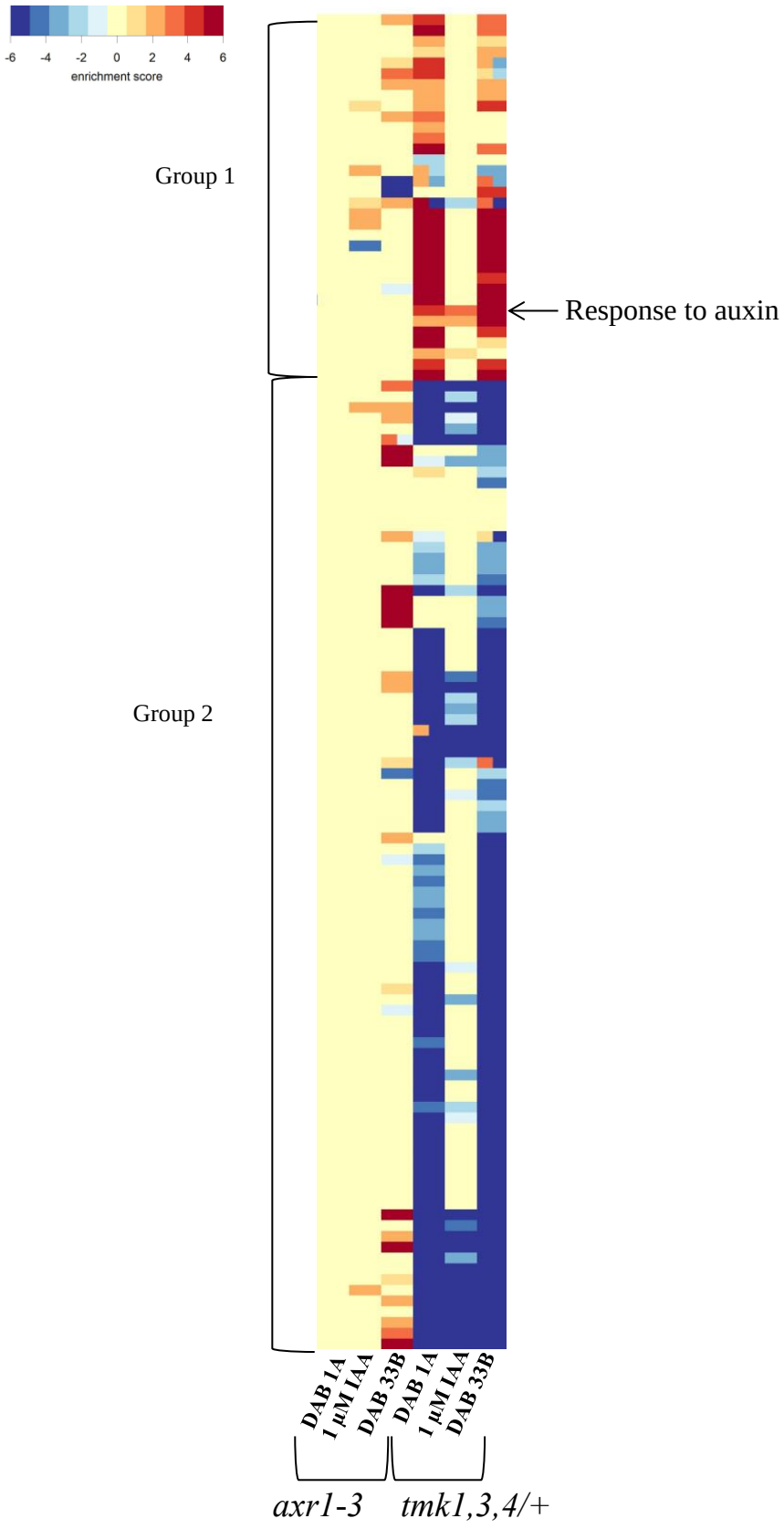
-6 -4 -2 0 2 4 6
enrichment score
Group 1
Response to auxin
Group 2
DAB 1A
1 μM IAA
DAB 33B
DAB 1A
1 μM IAA
DAB 33B
axr1-3
tmk1,3,4/+

Figure 3.10. Differential expression of auxin response genes in wild-type and auxin mutant whole seedlings. Select genes in the auxin response pathway that showed a significant change in regulation by treatment with *Microbacterium* DAB 1A, *Microbacterium* DAB 33B or 1 µM IAA in Col-0, *axr1-3* and *tmk1,3,4/+*. Genes not shown were not significantly regulated in all three plant lines. Value represents the $\log_2$ change in the treated samples relative to the sterile control, with red indicating upregulation and blue indicating downregulation.

		DAB 1A			DAB 33B			1 µM IAA		
Locus	**Gene**	**Col-0**	***tmk1,3,4/+***	***axr1-3***	**Col-0**	***tmk1,3,4/+***	***axr1-3***	**Col-0**	***tmk1,3,4/+***	***axr1-3***
AT4G37390	GH3.2	3.020	4.340	2.492	1.774	2.757	1.186	-0.042	0.823	0.136
AT2G23170	GH3.3	2.900	1.293	5.518	0.718	-0.557	0.524	-0.697	-0.135	-0.367
AT5G66700	HB53	1.569	2.335	0.172	0.339	1.841	0.554	1.397	0.554	1.295
AT5G20810	SAUR70	1.389	0.350	-0.469	1.158	1.338	-0.353	0.210	0.260	-0.247
AT5G65980	PILS7	1.244	0.878	0.190	1.087	0.213	0.045	-1.704	-0.417	-1.505
AT3G03840	SAUR27	1.026	1.306	-0.327	1.169	2.190	-0.930	2.660	0.994	-0.980
AT1G48690	GH3	0.930	0.624	-0.512	0.485	1.442	-0.829	0.411	0.719	-0.367
AT3G03820	SAUR29	0.919	0.376	-0.188	1.047	1.233	-0.467	0.659	0.338	-0.489
AT5G18080	SAUR24	0.837	0.971	-0.301	1.053	1.539	-0.180	0.922	0.993	-0.672
AT4G14560	IAA1	0.750	0.397	0.131	0.735	0.911	-0.298	0.074	0.892	-0.162
AT1G29510	SAUR68	0.641	0.592	0.291	0.734	1.317	-0.721	0.028	0.630	-0.352
AT4G31910	BAT1	0.639	0.748	0.373	0.335	1.148	0.723	1.178	0.931	0.703
AT1G29460	SAUR65	0.607	1.009	0.014	0.768	1.528	-0.298	1.705	0.742	-0.750
AT1G19850	MP	0.604	0.816	-0.052	0.113	0.450	0.264	0.240	0.093	-0.240
AT5G57090	EIR1	0.591	0.567	1.292	0.351	1.107	1.402	0.918	0.784	1.346
AT4G34790	SAUR3	0.564	0.716	-0.198	0.044	1.085	-0.437	1.623	0.318	-0.455
AT1G29430	SAUR65	0.540	0.634	-0.017	0.701	1.313	-0.546	1.052	0.848	-0.563
AT2G47460	MYB12	0.537	0.491	0.500	0.161	0.646	0.761	1.101	0.560	1.447
AT1G74660	MIF1	0.445	0.328	0.189	0.051	0.628	0.324	0.642	0.355	0.554
AT1G77690	LAX3	0.370	-0.035	0.271	0.130	0.296	0.211	0.449	0.415	0.117
AT3G16500	PAP1	0.358	0.317	-0.002	0.308	0.075	-0.089	0.140	-0.062	-0.193
AT4G34760	MYB12	0.347	0.447	-0.551	0.640	0.670	-0.474	1.531	0.369	-0.902
AT4G36110	SAUR9	0.314	0.962	0.158	-0.272	1.291	-0.308	1.036	0.322	-0.153
AT1G04240	SHY2	0.288	0.143	-0.010	0.551	0.867	-0.051	0.226	0.568	-0.447

AT5G25890	IAA28	0.267	-0.091	0.364	0.196	0.906	0.558	0.928	0.469	0.844
AT1G18570	MYB51	0.222	0.735	0.215	-0.111	0.265	0.322	-0.799	0.286	-0.324
AT4G38840	SAUR14	0.221	0.084	-0.251	0.383	0.211	-0.778	1.068	0.114	-0.513
AT5G54490	PBP1	0.192	0.559	0.261	-0.200	0.509	0.313	-0.486	0.099	-0.207
AT5G18030	SAUR21	0.182	1.302	0.023	0.419	1.701	-0.208	1.490	1.120	-0.756
AT1G74840	N/A	0.157	0.398	-0.047	0.100	0.612	-0.042	0.570	0.261	0.081
AT3G01220	HB20	0.140	0.258	0.137	-0.154	0.600	0.268	0.860	0.496	0.517
AT2G22670	IAA8	0.126	0.014	0.118	0.168	0.085	-0.043	-0.452	-0.060	0.031
AT3G23250	MYB15	0.114	0.639	0.468	-0.372	0.956	0.852	-1.477	0.194	-0.759
AT5G50760	SAUR55	0.112	2.635	-0.087	0.227	1.956	0.128	0.809	0.654	0.542
AT5G07990	TT7	0.106	-0.237	0.100	0.837	-0.254	0.337	0.235	0.250	0.246
AT5G01490	CAX4	0.102	1.141	0.719	0.557	1.918	0.888	0.581	0.028	0.373
AT1G04250	AXR3	0.098	0.042	0.424	0.299	0.740	0.496	0.698	0.530	1.027
AT2G47000	ABCB4	0.087	0.584	0.300	-0.177	0.551	-0.025	0.609	0.253	0.493
AT3G07390	AIR12	0.082	0.437	-0.072	0.018	0.138	0.175	-0.920	0.172	-0.323
AT3G04730	IAA16	0.032	0.693	-0.084	0.102	0.763	0.065	0.665	0.556	-0.084
AT1G28130	GH3.17	-0.011	0.449	-0.050	-0.164	0.242	-0.162	0.587	-0.044	0.086
AT4G31320	SAUR37	-0.026	-0.918	0.754	0.308	0.476	0.511	0.995	0.692	1.636
AT4G29940	PRHA	-0.057	-0.110	-0.082	-0.044	-0.083	0.249	0.294	-0.121	0.094
AT4G32551	LUG	-0.068	-0.058	0.051	-0.059	-0.101	0.010	-0.248	-0.237	0.007
AT5G45710	RHA1	-0.079	0.227	-0.038	-0.135	0.424	-0.327	-0.657	0.161	-0.137
AT1G17520	N/A	-0.134	0.296	-0.260	-0.177	0.150	-0.004	0.381	0.011	-0.128
AT5G02840	LCL1	-0.292	0.959	-0.031	-0.185	0.854	-0.139	-0.110	0.264	-0.029
AT4G37610	BT5	-0.294	0.474	-0.323	-0.210	0.863	-0.670	-0.754	0.458	-0.394
AT1G76520	PILS3	-0.298	-0.052	-0.057	-0.104	0.020	-0.347	-0.374	0.001	-0.108
AT5G57560	TCH4	-0.356	0.702	-0.394	-0.330	0.994	-0.290	-1.097	0.374	-0.026
AT4G11280	ACS6	-0.619	0.879	0.236	-0.865	0.588	0.403	-1.320	0.597	-0.292
AT2G17500	PILS5	-0.681	0.648	0.033	-0.558	0.627	-0.335	0.378	0.110	0.388
AT3G12830	SAUR72	-0.791	-0.479	-0.452	-0.819	-0.218	-0.527	0.353	0.128	-0.170

Figure 3.11. Differential expression of Extensin (EXT) genes in wild type and auxin mutant whole seedlings. Extensin genes regulated in Col-0 (wild type), *tmk 1,3,4/+* and *axr1-3* treated with *Microbacterium* DAB 1A, *Microbacterium* DAB 33B, or 1 µM IAA. Each value represents the log2 ratio of the treated plant vs the sterile control plant. Color indicates degree of up- (red) or down- regulation (blue).

DAB 1A			DAB 33B			1 µM IAA				
Col-0	*tmk 1,3,4/+*	*axr1-3*	Col-0	*tmk 1,3,4/+*	*axr1-3*	Col-0	*tmk 1,3,4/+*	*axr1-3*		
0.251	-0.531	0.805	-0.322	-0.379	0.481	0.117	-0.884	0.049	At1G76930	EXT1
0.565	-1.494	1.561	-0.969	0.251	0.125	-0.510	-0.949	0.805	At3G54590	EXT2
0.178	-0.509	0.409	-0.087	0.639	0.094	0.274	-0.400	0.062	AT1G21310	EXT3
1.178	-1.200	2.779	-0.648	0.540	1.313	-1.314	-0.900	0.236	AT2G24980	EXT6
1.196	-0.495	3.541	-0.543	0.514	2.005	-0.429	-0.633	1.114	AT5G06640	EXT10
1.369	-0.946	2.635	-0.401	0.379	1.444	-0.806	-0.758	1.570	AT4G13390	EXT12
1.007	-1.484	1.766	-0.666	0.433	0.339	-0.501	-0.562	0.197	AT5G35190	EXT13

Figure 3.12. Functional enrichment analysis of RNA-Seq on wild type and auxin mutant roots. Pathways significantly regulated in Col-0 (wild type) and *axr1-3* roots. Plants were treated with *Microbacterium* DAB 1A, *Microbacterium* DAB 33B, or 1 µM IAA. Enrichment score indicates statistical strength of the enrichment relative to the sterile control, with red indicating upregulation and blue indicating downregulation. Split cells indicate significant enrichment of the pathway's genes among both up- and down-regulated genes.

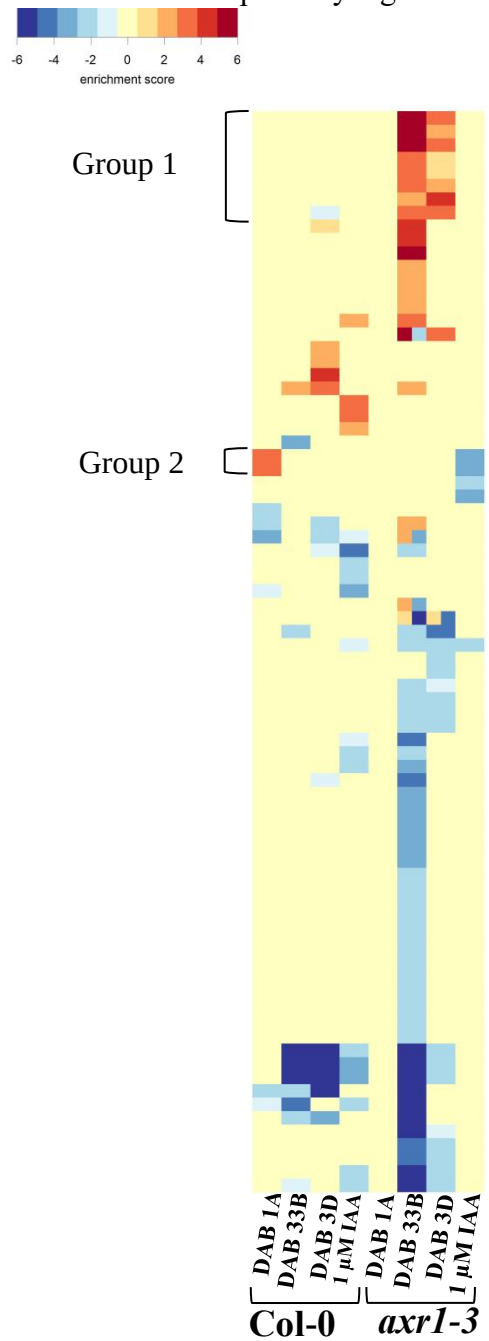

Figure 3.13. Differential expression of GH3.2, Extensin 12 and SAUR26 genes in wild type seedlings. Transcript levels of GH3.2 (AT4G37390), SAUR 26 (AT3G03850) and Extensin 12 (AT4G13390) were compared in Col-0 using reverse transcriptase-polymerase chain reaction (RT-PCR), with Actin as an endogenous control. Col-0 was treated with *Bacillus* DAB 3D, *Microbacterium* DAB 1A*, Microbacterium* DAB 33B, or exogenous 1 µM IAA and separated into vegetative (V) and root (R) sections.

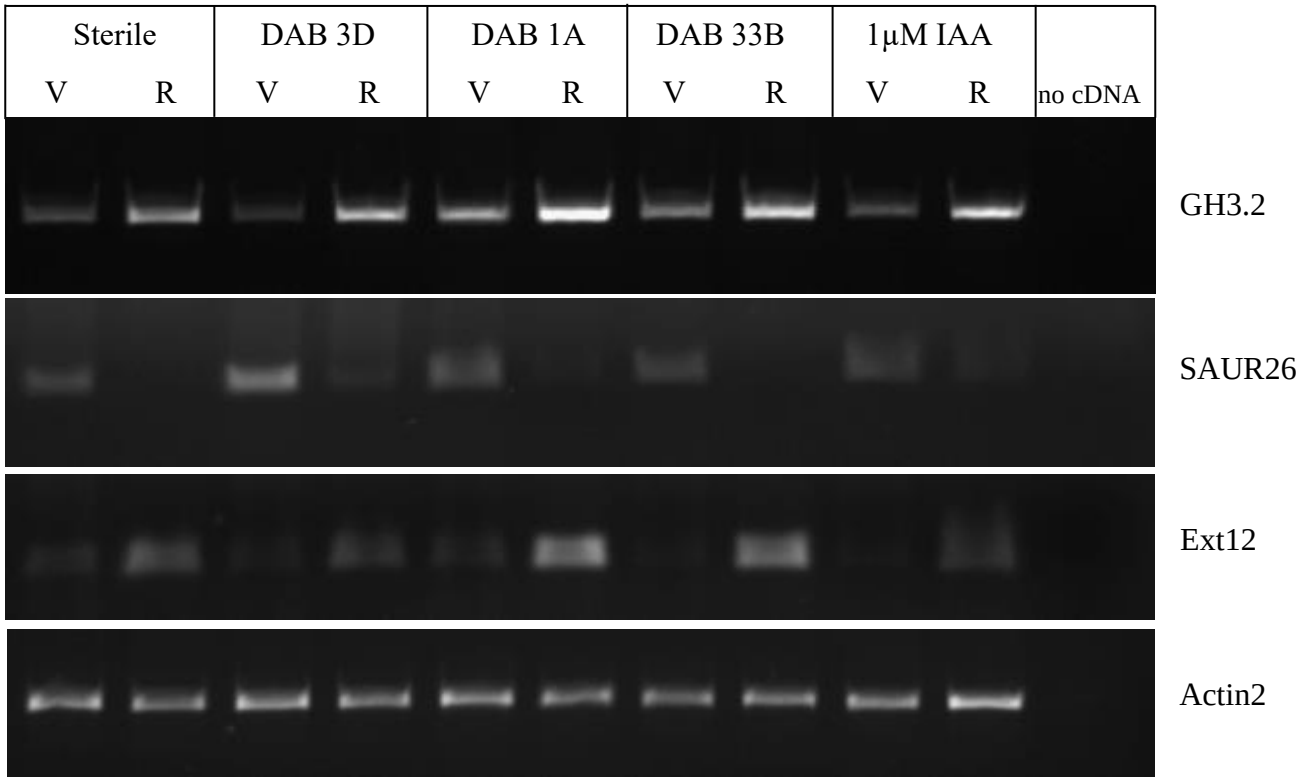

Figure 3.14. Relative quantity of GH3.2 transcripts in wild type and auxin mutant plants by RT-qPCR. Quantification of GH3.2 expression in vegetative tissue of A) Col-0 (wild type) and B) *axr1-3* using reverse transcriptase-quantitative polymerase chain reaction (RT-qPCR). Data represents the mean relative quantity (RQ) relative to the sterile control and error bars represent the RQ min and RQ max. Student's T-test ($P<0.05$) was performed (A) n=3, B) n=5) and an asterisk indicates significant difference compared to the sterile control.

A)

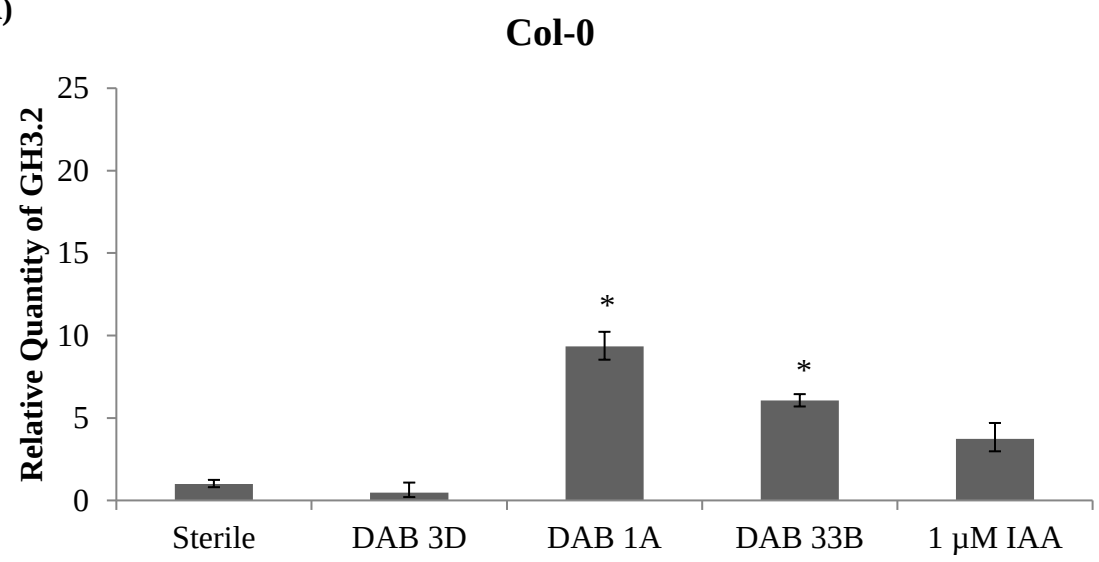

B)

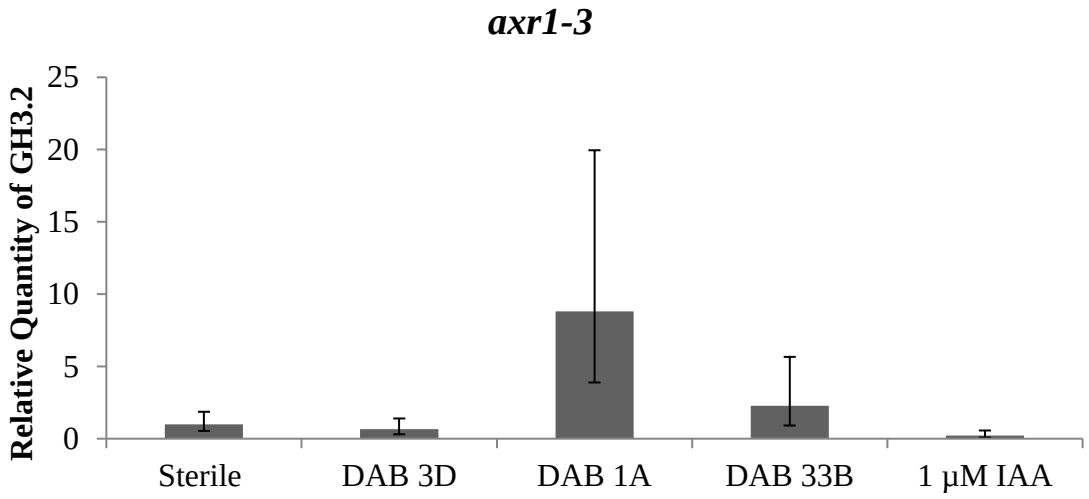

CHAPTER 4

Bacteria interaction and *Arabidopsis thaliana* host response via the auxin pathway

4.1 Abstract

Indole-3 acetic acid (IAA), a plant auxin that is produced by both plant growth promoting bacteria (PGPB) and pathogens, is involved in various aspects of plant development. Although the individual interactions between IAA-producing bacterium and its plant host have been extensively studied, the functionality of IAA in a plant associated bacterial community remains unclear. Thus, using our diverse collection of duckweed endophytes that produce various indole related compounds such as IAA, we used binary association assays to inform selection of tripartite interactions with the model plant, *A. thaliana*. We found an interaction between indole-3-lactic acid-producing *Herbaspirillum* strain DAB 5E and IAA-producing *Microbacterium* strain DAB 1A that results in suppression of a short root phenotype and reduction in bacteria colonization on plant tissues. Furthermore, DAB 5E decreased the amount of exogenous levels of IAA in culture, which appears to be associated with its ability to produce indole lactic acid (ILA), and it reduced the plant's response to IAA as demonstrated using the DR5:GFP reporter system. In the presence of DAB 5E, the plant transcriptome showed enrichment of bacteria defense pathways, which was suppressed in the presence of both DAB 5E and exogenous 1 μM IAA. This suggests a potential role of IAA in masking the plant defense response induced by DAB 5E. Altogether, these findings imply multiple roles of IAA in plant microbiome interactions.

4.2 Introduction

Interest in utilizing synthetic bacterial communities to improve plant health necessitates a functional understanding of plant microbiome assembly. The plant microbiome has been categorized into separate compartments, the phyllosphere (above ground), rhizosphere (surrounding soil) and endophytic (between or within cells) regions. The microbiome undergoes a decrease in diversity from the rhizosphere to the endophytic compartment, where strains become either enriched or depleted (Lundberg et al., 2012). Various studies have shown that in addition to the plant immune system, microbial members themselves can shape the plant microbiome by suppressing pathogens (Berg and Koskella, 2018; Helfrich et al., 2018; Rudrappa et al., 2008). However, the mechanisms of enrichment and exclusion by the host immune system or interactions between microbes are poorly understood in a variety of plant systems and under various environments.

We aim to understand mechanisms of signaling between bacterial endophytes and *A. thaliana* via the auxin pathway. In Chapter 3, the strains capable of producing indole related compounds were inoculated onto *A. thaliana* in binary-association assays to screen for an auxin phenotype. *Microbacterium* strain DAB 1A caused a short root phenotype in *Arabidopsis* whereas *Herbaspirillum* strain DAB 5E caused the inverse phenotype of a long primary root and short lateral roots. In this Chapter, we used the binary-association assays to inform selection of which strains to co-inoculate in tripartite experiments. Co-inoculation of DAB 1A and DAB 5E resulted in suppression of the short root phenotype normally with DAB 1A alone. Location of the strains on plant tissue was determined by confocal microscopy to observe degree of association. Using a

combination of molecular, biochemical, and –omics techniques, we propose a mechanism of endophyte competition by *Herbaspirillum* strain DAB 5E via the auxin pathway.

4.3 Methods

4.3.1 Bacterial Strains and Media

Bacillus sp. RU 3D (DAB 3D), *Microbacterium sp.* RU 1A (DAB 1A), *Microbacterium sp.* RU 19A (DAB 19A), and *Herbaspirillum sp.* RU 5E (DAB 5E) were isolated from *Spirodela polyrhiza*, *Lemna minor*, *Lemna japonica/minor,* and *Lemna minor,* respectively, as described in Gilbert et al. 2018. Bacterial strains were stored at -80°C in LB (Miller's, CA, USA) and supplemented with 40% sterilized glycerol. To isolate single colonies, bacteria from a glycerol stock was spread onto a LB agar plate using a sterile loop and then stored at 28ºC for 2 days or until single colonies were grown. Liquid cultures were made by taking a single colony using a pipet tip and placing the pipet tip in 6 mL of LB. Cultures were grown for 1 day at 28ºC and 240 rpm.

4.3.2 Arabidopsis Growth Assay

The *A. thaliana* growth assay was performed in a similar manner for observation of root lengths and morphology, qPCR, microscopy, and RNA isolation. For each assay, 200 *Arabidopsis thaliana* seeds were sterilized using 50% (v/v) bleach solution (0.3% sodium hypochlorite) in a 1.5 mL microcentrifuge tube for 4 minutes with continuous shaking using a vortex (Fisher Genie 2) shake setting 6. The bleach solution was removed and the seeds were washed four times in 1 mL of sterile water. After removing the water, the seeds were suspended in 0.1% (w/v) Difco Agar, Granulated (Becton Dickinson, MD, USA). Seeds were placed onto circular 100 x 15 mm plates containing 0.5x Murashige & Skoog (MS) Modified Basal Medium with Gamborg Vitamins (Phyto Technology

Laboratories, KS, USA), 1% sucrose, pH 5.7, 0.25% phytagel (Sigma-Aldrich, MO, USA). The seeds were vernalized at 4°C in the dark for 2 days and then stored vertically in a growth chamber at 22 °C under 100 µmol m^{-2} s^{-1} of 12 h light. After 6 days, previously grown bacterial cultures were prepared by taking 1 mL of culture and centrifuging at 12,000 rpm for 5 min. The supernatant was discarded and the bacterial pellet was suspended in sterile water to an OD_{600}/cm of 0.7. Bacterial cultures for heat killed samples were autoclaved for 15 minutes, centrifuged at 8,000 rpm for 5 min and the pellet diluted to an OD_{600}/cm of 0.7 before plating 100 µL onto an LB plate to confirm no growth. 100 µL of heat killed or living bacterial solution (or sterile water as a negative control) was spread onto square 100 x 15 mm plates containing 0.5x MS, pH 5.7, 0.5% Gellan Gum powder (Phyto Technology Laboratories, KS, USA). Co-inoculated samples contain 100 µL of both treatments. Plates containing IAA (Gibco Laboratories, USA) were previously prepared by adding IAA dissolved in DMSO (Sigma-Aldrich, MO, USA) directly to the media before pouring and solidifying. Six to 12 seedlings (depending on the assay) were transferred onto each plate, which were then sealed with self-adherent wrap, 3M, Micropore surgical tape (Coban, USA). Plates were then placed in the same growth chamber as germination and under the same temperature and light conditions for 5 days or 7 days, depending on the experiment. Pictures of plants were taken with a Nikon D5200 camera and roots were measured using ImageJ. Water was prepared from Millipore Synergy 185 and sterilized using a 0.2 micron polyethersulfone syringe filter.

4.3.3 Bacterial Localization on Arabidopsis

Confocal Microscopy

Five whole seedlings of Col-0 were each placed in a 1.5 mL microcentrifuge tube containing 1 mL of 4% paraformaldehyde. The tissue was fixed overnight at room temperature and then the solution was removed followed by washing twice with 1 mL of sterile phosphate buffer saline (1.37M NaCl, 26mM KCl, 10mM Na_2HPO_4•$7H_20$, 17.6mM KH_2PO_4,pH 7.4) and then storing at 4°C. Images were acquired by EMSL (Richland, WA) using a Zeiss LSM 710 scanning confocal microscope. The channels used were blue (Calcofluor White), green (Sybrgold DNA), red (chlorophyll autofluorescence) and grey (transmitted light).

DNA Extraction

Col-0 seedlings were grown as previously described in the growth assay method. After 7 days of treatment, 3 Col-0 seedlings per replicate were washed in a 1.5 mL eppendorf tube with sterile Rinse Solution (0.1% Triton-X, 137 mM NaCl, 2.7 mM KCl, 10 mM Na_2HPO_4•$7H_20$, 1.8 mM KH_2PO_4, 0.5 mM $MgSO_4$, 1 mM $CaCl_2$, pH 7.4) for 20 min using Fisher Vortex Genie 2, shake setting 3, and then decanted. The seedlings were washed twice with 1 mL of sterile water. Starter cultures for bacterial strains were grown from a single colony in 6 mL of LB supplemented with 5 mM L-tryptophan for 24 h at 28 °C and 240 rpm. The starter cultures were used to inoculate 6 mL of LB, supplemented with 5 mM L-tryptophan, to an OD_{600}/cm of 0.01. Co-inoculated cultures contained the same volume of each inoculum as their respective individual culture. After 24 h at 28 °C and 240 rpm, 4 mL of culture was centrifuged at 14,000 rpm for 5 min to collect the pellet.

Plant and bacterial DNA was isolated by grinding using HT 6™ (OPS Diagnostics, NJ, USA) at 4000 rpm for 8, 30 sec intervals in a 2 mL tube with 1 g of 100

µm silica beads, 0.5 g of 1.7 mm zirconium beads, a 4 mm silica bead, 300 µL of CTAB buffer (100 nM Tris-HCl pH 8.0, 1.4 M NaCl, 20 mM EDTA, 2% CTAB), 60 µL of 2-mercaptoethanol and 300 µL of phenol 25:24:1 chloroform isoamyl alcohol (Sigma-Aldrich, MO, USA).The extract was centrifuged at 16,000 g for 10 min. 200 µL of supernatant was transferred to a 1.5 mL centrifuge tube and 100 µL of 7.5 M ammonium acetate and 750 µL of 100% ethanol was added. The samples were stored overnight at 4° C and centrifuged at 16,000 g for 30 min at 4° C. Twice the supernatant was removed, 500 µL of 75% ethanol was added and samples were centrifuged at 16,000 g for 10 min at 4° C. After removing the supernatant, the pellet was air dried for 10 min and then suspended in 30 µL of sterile water. Concentration and quality of DNA was determined with a Nanodrop-1000 UV/Vis Spectrophotometer (Thermo Scientific, Waltham, MA) and then by running an aliquot of the sample on a 1% agarose gel with ethidium bromide followed by visualization on a transilluminator, respectively.

qPCR

Primer sequences were generated using Primer Express 3.0.1. A standard curve and melt curve analysis was performed on each primer set to calculate efficiency and ensure specificity. Five 1:5 dilutions were used for Actin2 and RU1A. Efficiencies and primer sequences are located in Table 4.1. qPCR was performed using 3 µL of sterile autoclaved water, 1 µL of forward primer, 1 µL of reverse primer, 10 µL of Power SYBR Green Master Mix (Thermo Scientific, MA, USA), and 5 µL of cDNA (diluted 1:100). The PCR condition was Stage 1 at 95° C for 10 min and Stage 2 (40 cycles) at 95° C for 15 s and 60° C for 1 min. For melt curve analysis, there was an added Stage 3 at 95° C for 15 s, 60° C for 1 min and 95° C for 15 sec. For plant samples, relative gene

expression was calculated with StepOne Software v2.2.2 using comparative C_T analysis. Actin2 was used as an endogenous control and the Col-0 treated with DAB 1A was used as a reference. Data is presented as the mean relative quantity (2^-ddCt). For bacteria samples, a standard curve was generated using four 1:10 dilutions of 65 ng/µL DAB 1A DNA. Data represents the mean concentration of DAB 1A. Each sample was analyzed using three technical replicates, and four biological replicates for Col-0 samples and six biological replicates for bacteria samples. One-way ANOVA and Fisher's LSD was performed using dCt values to determine significant difference.

4.3.4 Bacterial Growth Assay

To create the filtrates, a starter culture was made by inoculating 5 mL of LB supplemented with 5mM L-typtophan from a single bacterial culture. After 48 h, the starter culture was used to create a 50 mL culture at an OD_{600}/cm of 0.01. After 24 h, the culture was filtered with a 0.2 micron Nalgene Rapid-Flow sterile disposable filter (Thermo Scientific, MA, USA). 100 µL was streaked onto an LB plate and grown at 28° C for 48 h to confirm no growth. Filtrates were stored at 4° C overnight until use.

To create the inoculum, a starter culture was made by inoculating 5 mL of LB supplemented with 5mM L-typtophan from a single bacterial culture. After 48 h, 1 mL of culture was centrifuged at 12,000 rpm for 5 min and the pellet diluted with sterile LB to an OD_{600}/cm of 0.01. 25 µL of the culture was used to inoculate 3 mL of the previously prepared filtrates and a sterile LB control. The OD_{600}/cm was recorded after 10 h, 22 h, 32 h, and 47 h.

4.3.5 Quantification of Indole Related Compounds by LC/MS

Extraction of Indole Related Compounds

For each bacterial strain, a single colony was used to inoculate a starter culture of 6 mL of LB supplemented with 5 mM L-tryptophan. After 24 h of growth at 28°C with shaking at 240 rpm, the starter culture (of living or heat-treated bacteria) was used to make a 60 mL culture of LB, supplemented with 5 mM L-tryptophan, at OD_{600} 0.01. 20 ng/µL and 40 ng/µL IAA spike samples were made by first preparing IAA in DMSO and then diluting into either sterile LB (to calculate the percent recovery), living DAB 5E culture or heat-treated DAB 5E culture. The 60 mL cultures were grown at 28°C and 240 rpm for 24 h. The supernatant was collected at 8,000 g for 5 min at 4°C. Supernatants were acidified to pH 3.0 with 1N HCl and then aliquoted into 20 mL for triplicates.

A Sep-Pak C18 cartridge (360 mg sorbent, 55-105 µm particle size) was prepared for each sample by washing with 10 mL of 100% acetonitrile followed by 10 mL of water. 20 mL of the acidified supernatant was passed through the C18 cartridge. The C18 cartridge was then washed with 10 mL of water and eluted with 5 mL of 80% (v/v) acetonitrile. The eluate was centrifuged at 12,000 rpm for 5 min at 4°C to remove solid particles. A standard curve was generated by making IAA and ILA solutions of 0.5 ng/µL, 1 ng/µL, 10 ng/µL and 20 ng/µL in 100% acetonitrile. Acetonitrile of HPLC grade and HCl of ACS grade was used for the experiment and water was prepared from Millipore Synergy 185.

Using the external standard of IAA and ILA, we calculated the concentration of free IAA and free ILA in the samples using the peak area of UV280 in single ion chromatograms at positive ionization and subtracting the peak area of UV280 appearing at the same retention time of the LB medium only samples. To calculate the concentration in the original culture, the concentration was then divided by four to

account for the original culture volume being 20 μL and the final elution volume being 5 μL.

LC-MS

Samples were separated and analyzed by a UPLC/MS system including the Dionex® UltiMate 3000 RSLC ultra-high pressure liquid chromatography system, consisting of a workstation with ThermoFisher Scientific's Xcalibur v. 4.0 software package combined with Dionex®'s SII LC control software, solvent rack/degasser SRD-3400, pulseless chromatography pump HPG-3400RS, autosampler WPS-3000RS, column compartment TCC-3000RS, and photodiode array detector DAD-3000RS. After the photodiode array detector the eluent flow was guided to a Q Exactive Plus Orbitrap high-resolution high-mass-accuracy mass spectrometer (MS). Mass detection was full MS scan with low energy collision induced dissociation (CID) from 100 to 1000 m/z in positive ionization mode with electrospray (ESI) interface. Sheath gas flow rate was 30 arbitrary units, auxiliary gas flow rate was 7, and sweep gas flow rate was 1. The spray voltage was 3500 volts (-3500 for negative ESI) with a capillary temperature of 275°C. The mass resolution was 140,000 and the isolation window was 0.4 mDa. Substances were separated on a Phenomenex™ Kinetex C8 reverse phase column, size 100 x 2 mm, particle size 2.6 mm, pore size 100 Å. The mobile phase consisted of 2 components: Solvent A (0.5% ACS grade acetic acid in LCMS grade water, pH 3-3.5), and Solvent B (100% Acetonitrile, LCMS grade). The mobile phase flow was 0.20 ml/min, and a gradient mode was used for all analyses. The initial conditions of the gradient were 95% A and 5% B; for 30 minutes the proportion reaches 5% A and 95% B which was kept for the next 8 minutes, and during the following 4 minutes the ratio was brought to initial

conditions. An 8 minutes equilibration interval was included between subsequent injections. The average pump pressure using these parameters was typically around 3,900 psi for the initial conditions.

Putative formulas of IAA metabolites were determined by performing isotope abundance analysis on the high-resolution mass spectral data with Xcalibur v. 4.0 software and reporting the best fitting empirical formula. Database searches were performed using reaxys.com (RELX Intellectual Properties SA) and SciFinder (American Chemical Society).

4.3.6 Bacterial Genome Analysis

Whole genome sequencing of strains, DAB 3D, DAB 1A, and DAB 19A were performed by the DOE Joint Genome Institute (Project ID 1055648). Whole genome sequencing of DAB 5E was performed by BGI (San Jose, CA) using Illumina HiSeq 4000 PE150. Read quality was checked with FastQC version 0.11.7 (https://www.bioinformatics.babraham.ac.uk/projects/fastqc/). A draft genome assembly was generated using SPAdes version 3.13.0 at default settings (http://cab.spbu.ru/software/spades/). Scaffolds less than 200 bp were removed. QUAST version 5 was used to assess the genome assembly (http://quast.sourceforge.net/quast). Gene prediction was performed using GeneMark (http://opal.biology.gatech.edu/GeneMark/). Genome was uploaded to NCBI under accession number VBQF00000000. Analysis of complete genome sequences of DAB 5E was performed with KEGG Mapper and RAST annotation service (Aziz et al., 2008; Overbeek et al., 2013; Brettin et al., 2015).

4.3.7 Fluorescent Microscopy of IAA Response

IAA response in the plant was observed using DR5:GFP seedlings. After 5 to 7 days of treatment described previously in the *A. thaliana* growth assay method, 3 roots were placed on a microscope slide. 50 µL of Calcofluor White (Sigma-Aldrich, MO, USA) and 50 µL of 3M KOH were placed on each root for 1 min. The stain was removed and 100 µL of water was used to wash the root. The roots were observed using the 10x objective lens of Olympus FSX100 epifluorescence microscope (green filter of 460-495 nm excitation/510-550 nm emission and blue filter of 360-370 nm excitation/420-460 nm emission).

4.3.8 Transcriptome Analysis

RNA Isolation

Total RNA isolation was performed on 6 Col-0 seedlings using a modified protocol of the mirVana miRNA Isolation kit (Thermo Scientific, MA, USA). Tissue was placed into a 2 mL polypropylene disruption tube containing 1.0 g of 100 µm silica beads, 0.5 g of 1.7 mm zirconium beads, and a single 14 mm silica bead. Tissue was disrupted by adding 1 mL of lysis buffer, supplied by the RNA isolation kit, and grinding at 4°C for 2-16 min, until homogenized, at 4000 rpm using HT Mini (OPS Diagnostics LLC, NJ, USA). Tubes were left on ice for 5 min and then 100 µL of Homogenenate Additive, supplied by the RNA isolation kit, was added. After 10 min on ice, the tubes were centrifuged at 10,000 rpm for 5 min at 4°C. The supernatant was removed and used for the remaining extraction following the RNA isolation kit manual. RNA was eluted with 50 µL of elution buffer, supplied by the RNA isolation kit, and stored at -20°C for short-term use or -80°C for long-term.

Concentration and quality of RNA was determined with a Nanodrop-1000 UV/Vis Spectrophotometer (Thermo Scientific, MA, USA) and then by running an aliquot of the sample on 2100 Bioanalyzer (Agilent Technologies, Inc., USA). Samples were then treated with TURBO DNA-free kit (Thermo Scientific, MA, USA).

RNA-Seq

Sequencing and analysis with DeSeq2 were performed by EMSL (Richland, WA) on 3 biological replicates. DeSeq2 was used to calculate the $\log_2$ change of the treated samples vs. the sterile control. Functional enrichment analysis was performed to illustrate pathways that are enriched among up and down regulated genes. Principal coordinate analysis was performed to evaluate the similarity between biological replicates.

4.4 Results

4.4.1 Co-inoculation of DABs on Arabidopsis

Of the bacteria isolated from duckweed that were able to produce indole containing compounds in culture (Gilbert et al. 2018), we observed strains that were capable of inhibiting the primary root length of *A. thaliana* and those that were not. In particular, two *Microbacterium* strains, DAB 1A and DAB 19A, derived from the duckweed genus *Lemna,* caused the short root phenotype. *Herbaspirillum* strain DAB 5E also derived from the duckweed genus *Lemna,* was previously detected to produce a higher ratio of free indole-lactic acid (ILA) to free IAA in culture (Gilbert et al., 2018) and did not cause a short root phenotype. We asked whether the short root phenotype would still be observed when co-inoculating the strains. Co-inoculation of DAB 1A + DAB 5E resulted in suppression of the short root phenotype (Figure 4.1). However, co-inoculation of DAB 1A + *Bacillus* strain DAB 3D, which does not produce indole related

compounds, did not result in suppression (Figure 4.1), indicating a specific interaction between DAB 5E and the *Microbacterium* DAB 1A.

4.4.2 DAB 5E Localization on Arabidopsis

We asked whether DAB 5E colonizes the endophytic region of Col-0 leaves and roots similar to DAB 1A, which was demonstrated in Chapter 3. Confocal microscopy was used to localize the site(s) of attachment for DAB 5E. DAB 5E showed endophytic colonization on the leaves and roots, however apparently at lower abundance compared to DAB 1A (Figure 4.2).

Since both DAB 1A and DAB 5E showed endophytic colonization on Col-0, we asked whether DAB 5E reduces the amount of DAB 1A present in the endophytic region, to explain the mechanism of suppression of the short root phenotype. Using bacterial strain-specific primers in qPCR reactions, we first quantified the amount of DAB 1A present in LB liquid cultures with and without DAB 3D or DAB 5E. The growth of DAB 1A was reduced by DAB 5E and more so by DAB 3D (Figure 4.3A). We then quantified the amount of DAB 1A present on detergent treated *A. thaliana* with and without DAB 3D or DAB 5E. DAB 1A that was co-inoculated with DAB 5E showed a decrease in abundance relative to DAB 1A inoculated alone, but no decrease in abundance when co-inoculated with negative control strain, DAB 3D (Figure 4.3B). Thus, there appears to be growth competition between DAB 1A and DAB 5E upon inoculation onto *A. thaliana* tissues.

4.4.3 Bacterial Growth Assay

In order to determine the mechanism of interaction between DAB 1A and DAB 5E, we asked whether DAB 5E grow in the filtered supernatant (filtrate) of DAB 1A.

Filtrates of DAB 1A and DAB 5E were prepared by growing the DAB in LB medium supplemented with 5 mM L-tryptophan for 24 h before filtering to remove bacterial cells. DAB 5E grew poorly in its own filtrate, but it showed significant growth in the filtrate of DAB 1A (Figure 4.4). DAB 1A in LB medium showed a similar growth curve to DAB 5E in LB medium, however it did not grow in 5E filtrate or in its own filtrate (Figure 4.4). This suggests that DAB 5E improves its growth under nutrient poor conditions by using the products of DAB 1A metabolism that are absent in its own filtrate.

4.4.4 Co-inoculation of DAB 5E and IAA on Arabidopsis

Since high levels of IAA were previously detected in the supernatant of DAB 1A (Gilbert et al., 2018), we next asked whether a functional interaction between DAB 5E and DAB 1A could be revealed via effects on an auxin-dependent pathway. Upon treatment of Col-0 with DAB 5E + 1 µM IAA, we observed suppression of the auxin-dependent root stunting phenotype, and with DAB 5E + 20 µM IAA, we observed a partial suppression (Figure 4.5). Therefore, suppression of the root phenotype is dependent on IAA concentration. Furthermore, this suggests that DAB 5E may be suppressing the phenotype of *Microbacterium* strains through the auxin pathway. After killing DAB 5E with heat, we no longer observed suppression of the auxin root phenotype, indicating the bacterium is either modifying the plant's response to auxin or reducing the amount of auxin that is present.

4.4.5 Quantification of Indole Related Compounds by LC-MS

We next asked whether IAA was being converted to another indole related compound, oxidized or possibly degraded by DAB 5E. We spiked cultures of DAB 5E with two concentrations of IAA to detect increasing concentrations of the IAA-derived

product, if any. The supernatant was screened by LC-MS. In the supernatant of DAB 5E, we detected a high ratio of ILA to IAA as previously observed (Gilbert et al., 2018). In the supernatant of DAB 5E with 20 ng/µL IAA and 40 ng/µL IAA, we detected a decrease in IAA and a decrease in ILA compared to the respective concentrations of LB medium spiked with IAA and heat killed 5E medium spiked with IAA (Figure 4.6). This indicates that DAB 5E may be degrading IAA and reducing endogenous IAA and ILA production upon addition of exogenous IAA. No IAA derivatives were detected, indicating IAA is not being converted to a related product at detectable levels.

4.4.6 Genome Analysis of IAA Degradation Genes

We asked whether DAB 5E contains any genes for IAA degradation. The IAA degradation operon, iac, has been previously studied in *Paraburkholderia phytofirmans* PsJN and contains 10 genes (iacA, iacB, iacC, iacD, iacE, iacF, iacG, iacH, iacI and iacY) (Donoso et al., 2016). When the 10 genes were blasted against the DAB 5E genome, we were able to detect 8 of the 10 genes (excluding iacI and iacY) with a percent identity of at least 50% and located within 1 kb proximity of each other, which we labeled as ‘hotspot 3’ (Table 4.2). The presence of this iac gene cluster suggests that DAB 5E may be capable of degrading IAA.

4.4.7 IAA Response in Arabidopsis

To determine whether there is an IAA response in the plant upon treatment with DAB 5E and exogenous IAA, we used the DR5:GFP reporter system to observe localized IAA response in plant roots. GFP fluorescence was detected in the elongation region of sterile roots and in the meristem and mature region of roots treated with 20 µM IAA (Figure 4.7). Upon treatment with DAB 5E, GFP fluorescence was observed in the

meristem region. Treatment with DAB 5E + 20 µM IAA resulted in reduced GFP fluorescence, as well as less lateral root formation, compared to IAA treatment alone. In the upper root region, GFP fluorescence was reduced, however still present, by treatment with DAB 5E + 1 µM IAA compared to IAA alone (Figure 4.8). Thus, in the presence of DAB 5E there is reduced plant response to exogenous IAA, as demonstrated biochemically by the DR5 reporter system and morphologically by lateral root formation.

4.4.8 Transcriptome of Arabidopsis in Response to DABs

We asked to what extent the plant showed a transcriptomic response when treated with DAB 5E + 1 µM IAA. Functional enrichment analysis of RNA-Seq was performed to show which pathways were significantly upregulated and downregulated. Based on the pattern of regulation, we clustered the pathways into five groups (Figure 4.9). Group 1 contains pathways that were upregulated in response to IAA and DAB 5E+ IAA but not so much in DAB 5E alone. It primarily contains pathways related to the ribosome, suggesting that treatment with IAA increased plant protein synthesis. Group 2, which contains pathways that were upregulated by only IAA and suppressed in the presence of DAB 5E treatment, is related to cell division. This corresponds with the observation of an IAA-induced short root phenotype that is inhibited by the presence of DAB 5E. Group 3 and Group 5 contain pathways in which the effect of DAB 5E appears to be inhibited by the presence of IAA. These pathways are related to oxidative stress and response to bacterium, suggesting the IAA response is masking the plant's response to DAB 5E. Lastly, Group 4 pathways are downregulated by both IAA and 5E and are primarily related to photosynthesis. Thus, the plant appears to be reallocating its resources away from photosynthesis and to other pathways when treated with IAA and/or bacteria.

To further understand the effect of IAA on the plant's defense response to DAB 5E, we looked at the $\log_2$ change of genes within the 'response to bacterium' pathway. We clustered the genes into three groups based on the pattern of regulation (Figure 4.10). Group 1 contains genes that were upregulated by IAA, thus demonstrating that IAA plays a role in the plant's response to bacteria. Group 3 contains genes that were upregulated by DAB 5E but downregulated by IAA alone and DAB 5E+ IAA, which may indicate that a response to IAA in the plant could be advantageous for DAB 5E to avoid activating the plant immune system. However, a subset of genes in Group 2 was upregulated by DAB 5E and DAB 5E + IAA, and thus not affected by the interaction between DAB 5E and IAA.

Based on the findings that DAB 5E suppresses the auxin short root phenotype of IAA in a concentration dependent manner, we expected to see a reduction, yet not a complete reversal, of IAA response in the plant. Transcriptomics was consistent with this hypothesis in that the presence of DAB 5E+ IAA still caused a significant activation of the auxin response pathway in the plant (Figure 4.9). However, a set of eight small auxin-upregulated RNA (SAUR) genes showed strong upregulation by DAB 5E + IAA, that was not detected in treatment with DAB 5E or IAA individually, suggesting their synergistic modulation by the interaction between DAB 5E and IAA (Figure 4.11).

4.5 Discussion

In this work, binary association assays were used to inform selection of strains for co-inoculating *A. thaliana*. *Herbaspirillum* strain DAB 5E suppressed the short root phenotype caused by our IAA-producing *Microbacterium* strains and its presence decreased the amount of DAB 1A strongly attached to the plant. Future work is needed to

determine whether the suppressed phenotype causes or results in the decrease in DAB 1A's association with the plant. A similar study reported suppression of a short root phenotype by a single bacterial genus, *Variovorax*, in a synthetic community suggesting that our findings may be reproducible in a complex community (Finkel et al., 2019).

DAB 5E also suppressed the auxin short root phenotype of exogenous IAA. We speculate that DAB 5E degrades IAA in a concentration dependent manner to use as an energy source, which is advantageous to the bacterium under nutrient limited conditions. Since DAB 5E produces a small amount of IAA itself, this suggests that the bacterium needs to be induced to degrade IAA. Additionally, the mechanism is associated with DAB 5E's ILA production, since we observed a decrease in endogenous ILA in the presence of spiked IAA. The presence of the iac gene operon in DAB 5E suggests it may be degrading IAA, though many mechanisms of IAA degradation by bacteria have been proposed and few *Herbaspirillum* strains have been reported to degrade IAA (Leveau and Gerards, 2008; Dhungana and Itoh, 2019).

We propose that DAB 5E is reducing the amount of IAA in a concentration dependent manner, causing the plant to still respond to low levels of IAA. Treatment with DAB 5E + IAA caused a reduction of IAA response in the root meristem and the upper root section of DR5:GFP seedlings, indicating that the plant still responds to reduced levels of auxin. Furthermore, despite the difference in root phenotype of IAA and DAB 5E + IAA treated plants, transcriptome response was overall similar. One notable difference was that a subset of small auxin upregulated RNA (SAUR) genes showed stronger upregulation by treatment with DAB 5E + IAA suggesting a synergistic interaction between the DAB 5E and IAA response pathways. However, the family of

SAUR genes in *A. thaliana* is known to have many roles including cell elongation, response to hormones and response to stress (Ren and Gray, 2015). SAUR 26, SAUR27, SAUR28, and SAUR29, which had the highest upregulation by treatment with DAB 5E + IAA, show sequence similarity and have been found to be involved in thermo-responsive growth in *A. thaliana* (Wang et al., 2019).

Transcriptomics indicates that DAB 5E caused upregulation of the oxidative stress pathway in the plant, indicating a pattern-triggered immunity (PTI) response (Jones and Dangl, 2006). However, treatment with both DAB 5E and exogenous 1µM IAA caused downregulation of bacterial response genes, suggesting that maintenance of the plant's response to IAA may be advantageous for DAB 5E to escape plant detection. It has been reported that *A. thaliana* can downregulate auxin signaling to decrease susceptibility to pathogens such as *Pseudomonas syringae*, yet this seems to not be the case with DAB 5E (Navarro et al., 2006; Spaepen and Vanderleyden, 2011). To conclude, *Herbaspirillum* strain DAB 5E appears to utilize IAA as an energy source, as competition with endophytic *Microbacterium* strains and to escape the plant's defense response. These findings are useful for understanding the role of IAA in plant microbiome ecology and for identifying genes involved in this process.

4.6 Tables and Figures

Table 4.1. Primer sequences and percent efficiency for qPCR. Primer sequences and percent efficiency used in quantitative polymerase chain reaction (qPCR) on Actin2 and DAB 1A specific genes. Actin2 was used as an endogenous control.

Primer	Polarity	Sequence	% Efficiency
Actin2	Forward	GATTCAGATGCCCAGAAGTCTTG	96.53
	Reverse	TGGATTCCAGCAGCTTCCAT	
RU1A	Forward	GGTAGAAGTCGCAGCCGTATG	95.7
	Reverse	CCGTGTACAGCGCCATCAT	

Table 4.2. Percent identity of iac genes in Hotspot 3 of the DAB 5E genome. Genes iacA, iacB, iacC, iacD, iacE, iacF, iacG, iacH, iacI and iacY from *Paraburkholderia phytofirmans* PsJN were blasted against the DAB 5E genome. Genes iacA-H were found in one copy within a 1 kb region labeled "Hotspot 3".

Gene in Hotspot 3	% Identity
iacA	65.6
iacB	70.9
iacC	71.2
iacD	54.8
iacE	59.9
iacF	52.5
iacG	60.8
iacH	58.0
iacI	Not found
iacY	Not found

Figure 4.1. Effect of co-inoculated DABs on *Arabidopsis* root length. Box plot for change in primary root length of Col-0 in millimeters (mm) after 7 days. Horizontal lines represent the median, with the box representing the 25th and 75th percentiles, the whiskers representing the minimum and maximum. Student's T-test ($P<0.05$) was performed (n=18) and asterisks indicate significant differences compared to the sterile control.

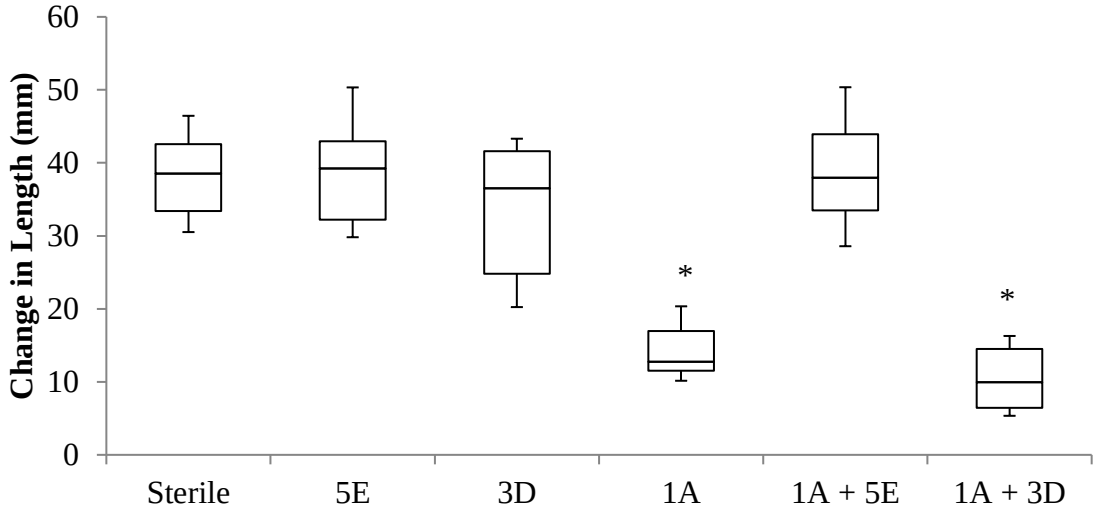

Figure 4.2. Localization of DAB 5E on *Arabidopsis* tissue. Confocal microscopy showing A) 3D structure and B) orthogonal view of Col-0 roots colonized with endophyte DAB 5E in low abundance. The microscopy channels are blue (Calcofluor White), green (Sybrgold DNA), red (chlorophyll autofluorescence) and grey (transmitted light). White arrows indicate bacteria location.

A) **B)**

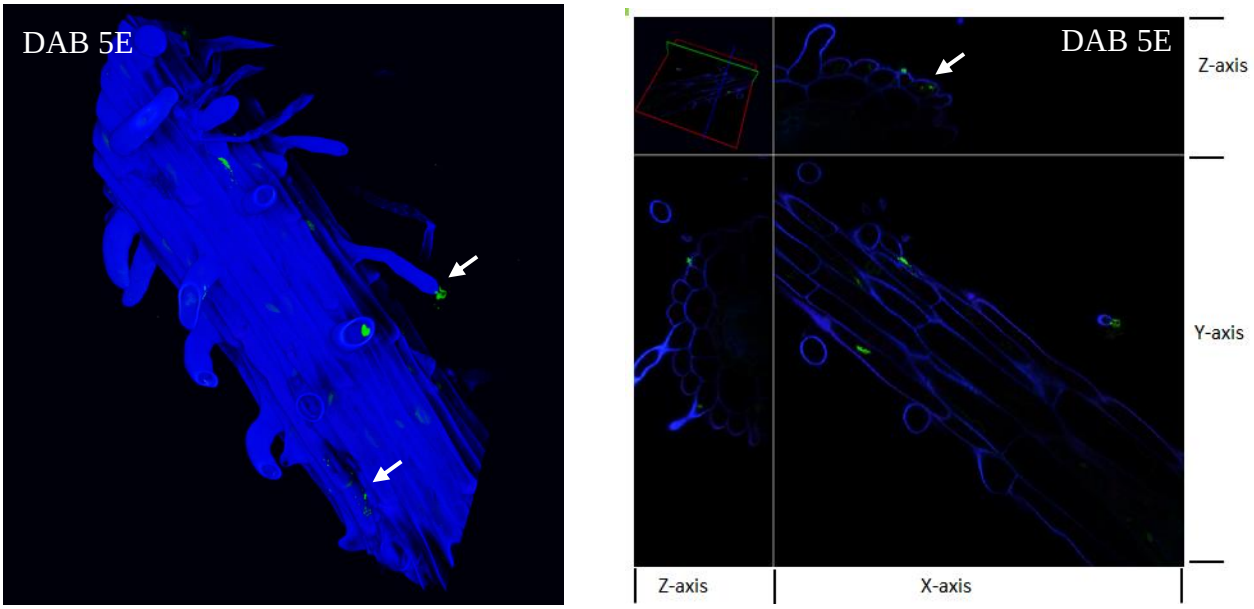

Figure 4.3. Effect of DAB 1A growth by DABs 3D and 5E. A) Mean concentration of 1A in LB co-cultures and SE (n=6). Bars with different letters are significantly different (One-way ANOVA p-value = 6.71 E-06, Fisher's LSD = 30.7). **B)** Mean percent relative quantity (RQ) of 1A in plant co-inoculums relative to the Col-0_1A control. Error bars represent the RQ min and RQ max (n=4). Bars with different letters are significantly different (One-way ANOVA p-value = 8.7 E-03, Fisher's LSD = 0.98).

A)

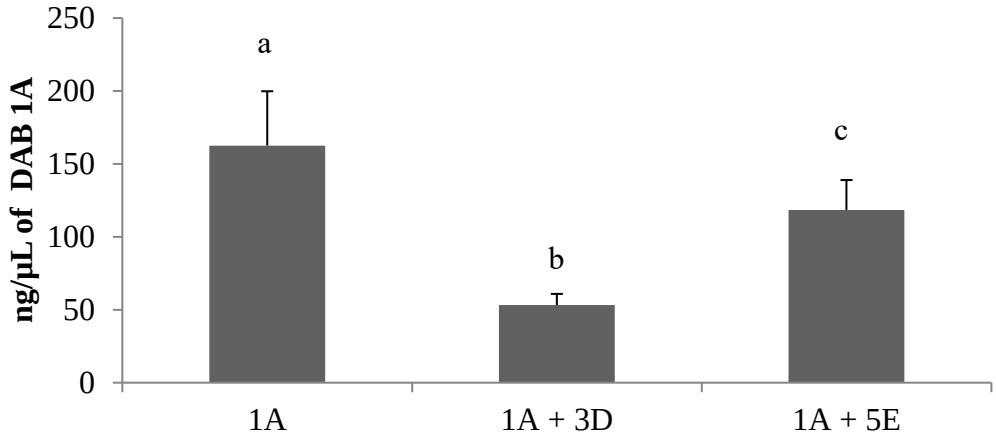

B)

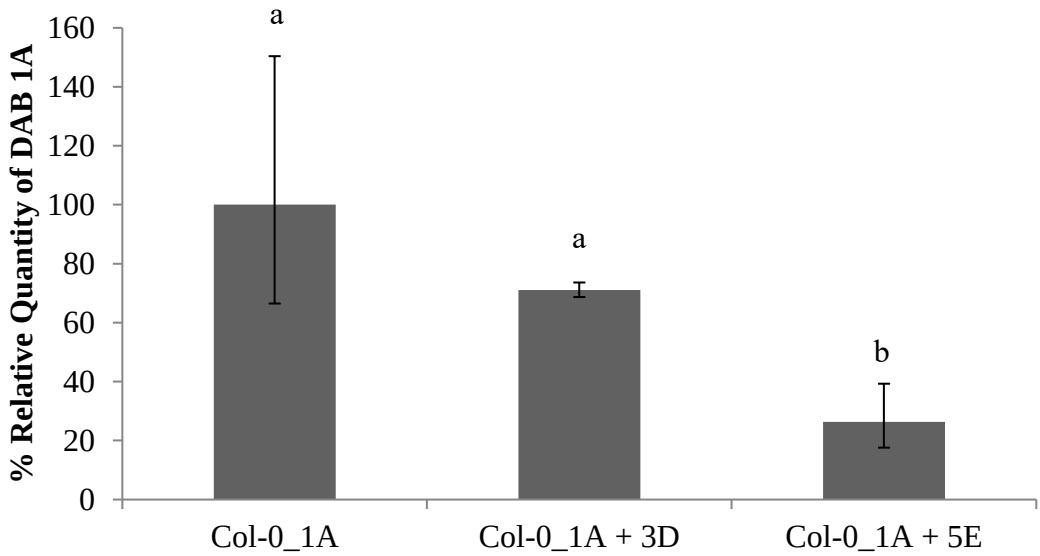

Figure 4.4. Growth curve of DABs in bacterial filtrate. DABs 5E and 1A were grown in LB medium and bacterial filtrates and the optical density (OD) at 600 nm was recorded from 10 h to 47 h. Data represents the mean OD_{600} and SE (n=3).

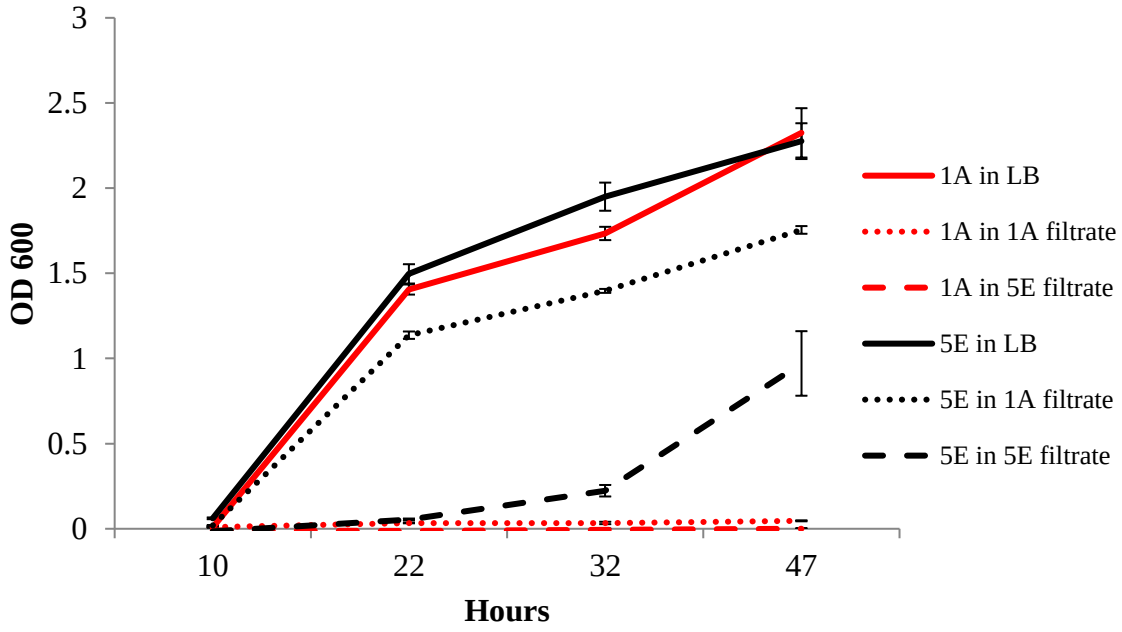

Figure 4.5. Effect of DAB 5E on *Arabidopsis* root length when co-inoculated with IAA. Box plot for change in primary root length of Col-0 in millimeters (mm) after 7 days. Horizontal lines represent the median, with the box representing the 25th and 75th percentiles, the whiskers representing the minimum and maximum. HT= Heat treated. Student's T-test ($P<0.05$) was performed (n=6) and an asterisk indicates significant difference compared to the sterile control.

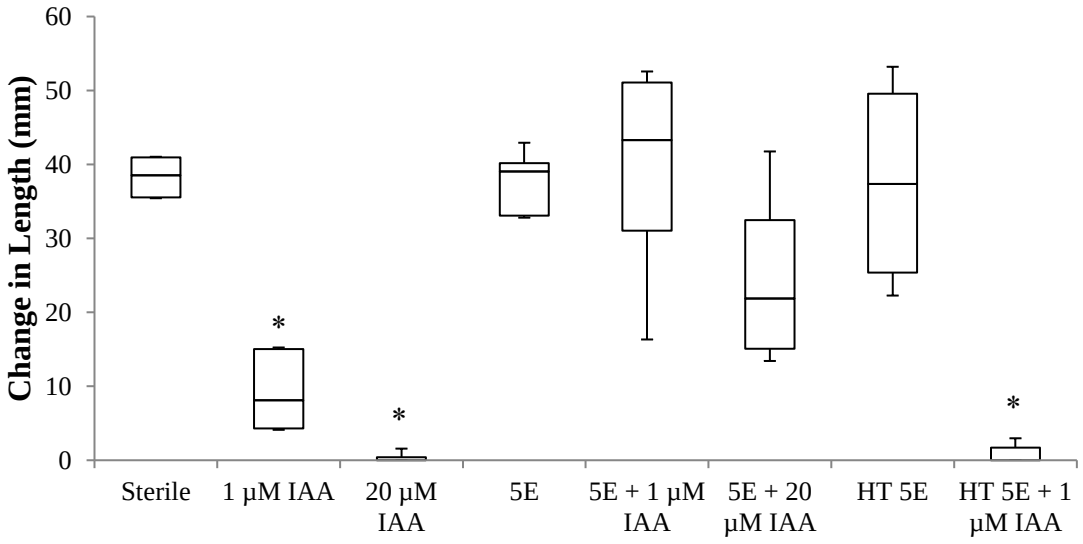

Figure 4.6. Quantification of indole related compounds with LC-MS. LC-MS quantification of **A)** IAA and **B)** ILA, present in the supernatant of DAB 5E with and without increasing quantity of spiked IAA. HT= Heat treated. Data represent mean concentration (ng/µL) and SE (n=3). Bars with different letters are significantly different ([A] One-way ANOVA p-value = 3.6 E-06, Fisher's LSD = 2.6 [B] One-way ANOVA p-value = 7.1 E-07, Fisher's LSD = 5.5).

A)

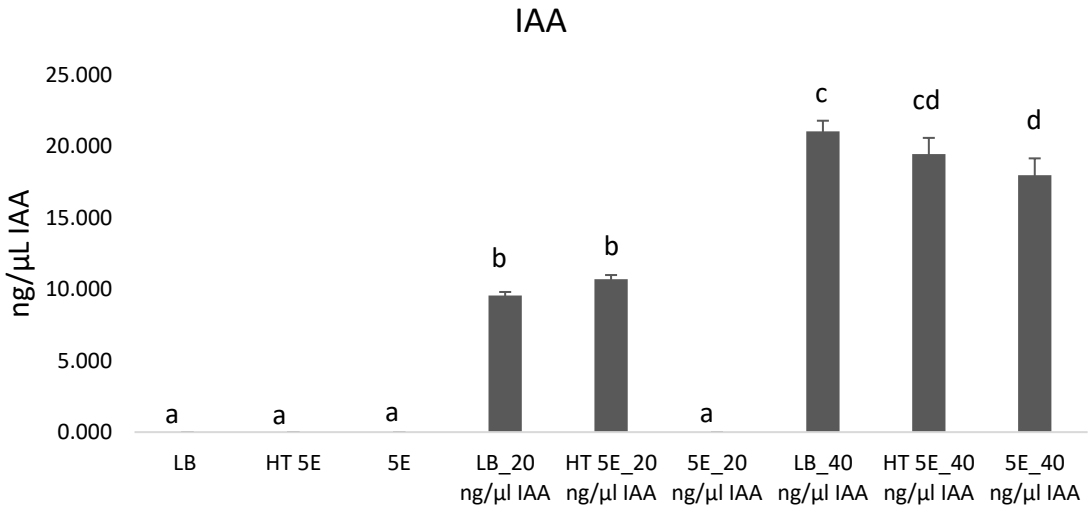

B)

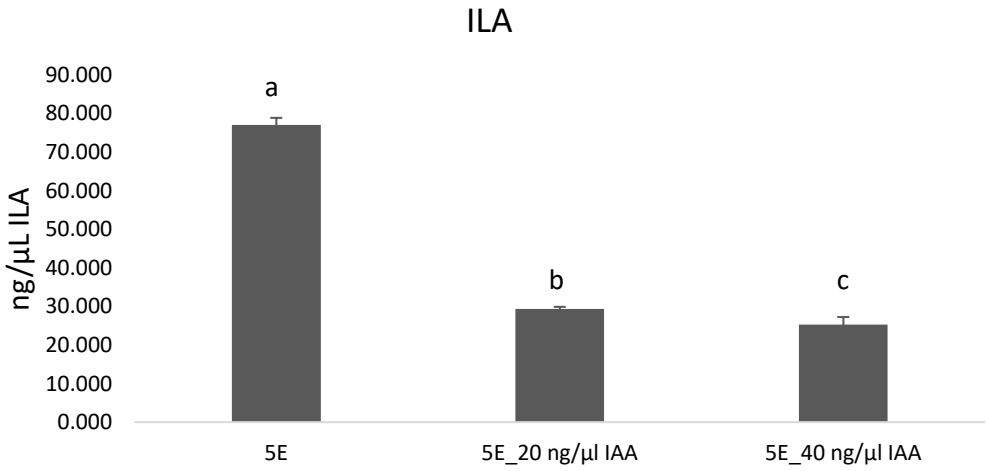

Figure 4.7. Auxin response in DR5:GFP root meristem after 7 days. GFP expression is represented by green fluorescence at ½ sec exposure and Calcofluor staining is represented by blue fluorescence at 1/4000 sec exposure. Size bar indicates 153 µm. White arrow indicates location of GFP fluorescence. Basal level GFP fluorescence was observed in the elongation zone of sterile roots and increased GFP fluorescence was observed in the mature and meristem regions of 20 µM IAA treated roots. GFP fluorescence was observed in the meristem region of DAB 5E treated roots. Plants treated with both DAB 5E and 20 µM IAA had reduced levels of GFP fluorescence relative to IAA treatment alone.

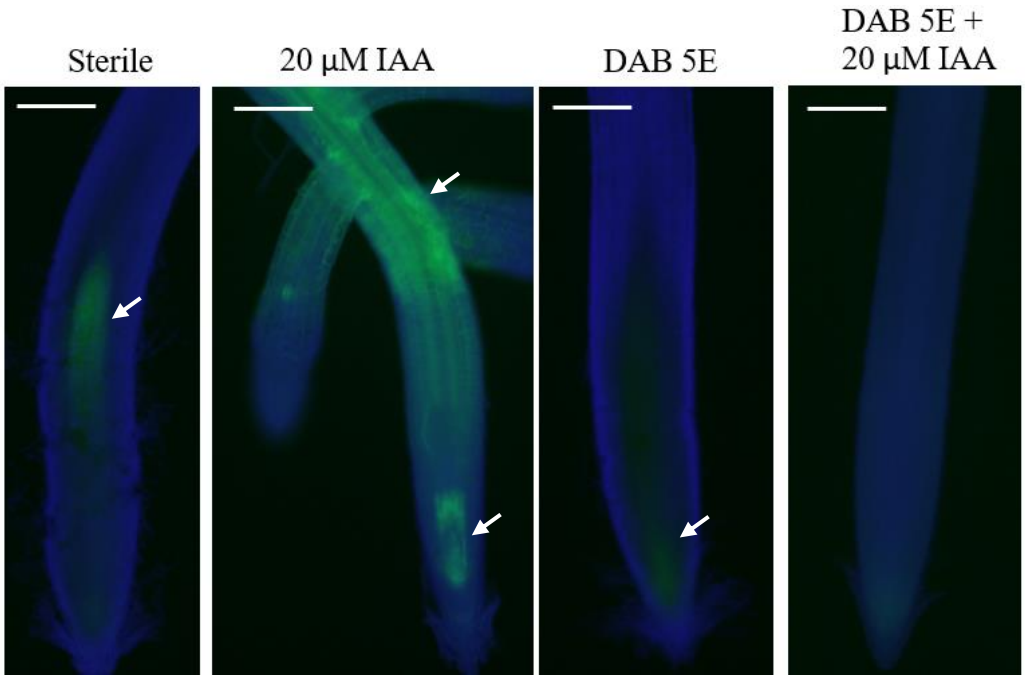

Figure 4.8. Auxin response in DR5:GFP upper roots after 5 days. GFP expression is represented by green fluorescence at 1/5.5 sec exposure and Calcofluor staining is represented by blue fluorescence at 1/500 sec exposure. Size bar indicates 153 µm. GFP fluorescence is observed in the upper roots upon treatment with 1 µM IAA, however it is reduced, yet still present, upon treatment with DAB 5E + 1 µM IAA. White arrow indicates location of GFP fluorescence.

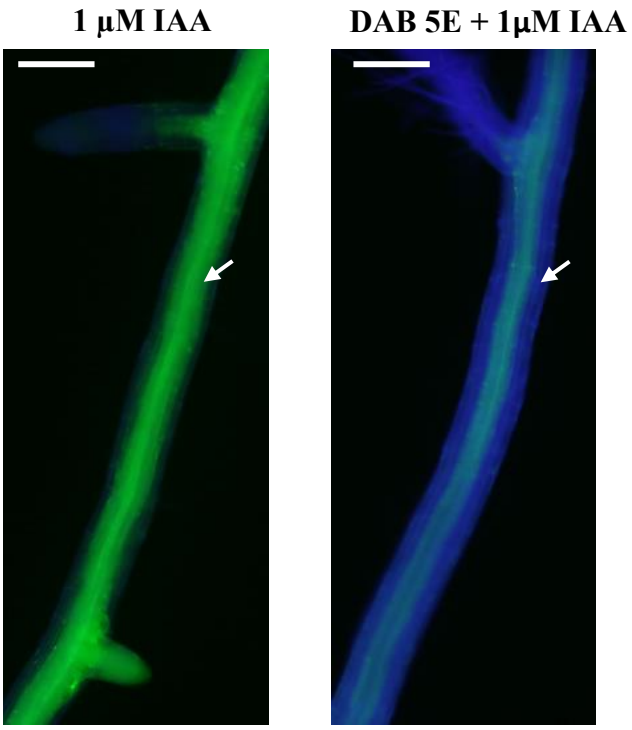

Figure 4.9. Functional enrichment analysis of RNA-Seq. Pathways significantly regulated in Col-0 treated with DAB 5E, 1 µM IAA, and DAB 5E + 1 µM IAA compared to the sterile control. Enrichment score indicates statistical strength of the enrichment, with red indicating upregulation and blue indicating downregulation. Split cells indicate significant enrichment of the pathway's genes among both up- and down-regulated genes.

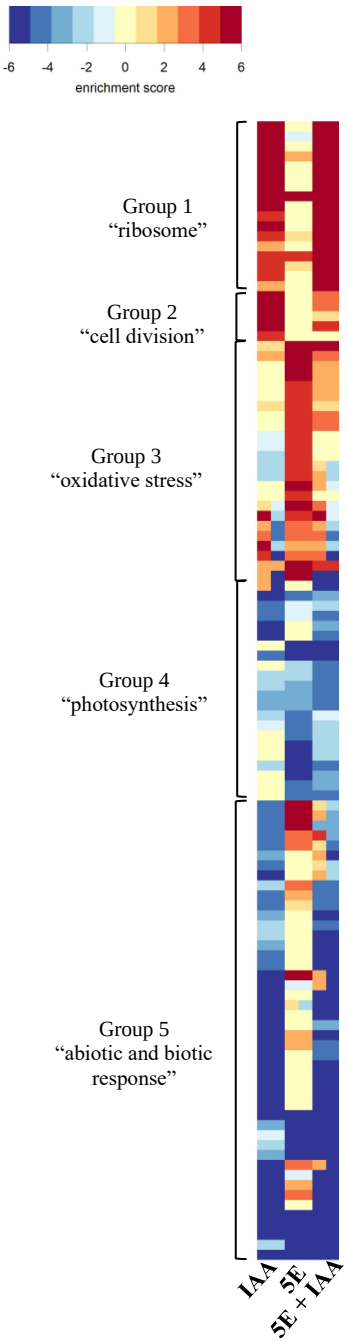

Figure 4.10. Differential expression of bacterial response genes. Response to bacterium genes regulated in Col-0 treated with 1 µM IAA, DAB 5E, and DAB 5E + 1 µM IAA, compared to the sterile control. Each column represents the log2 ratio of the treated plant vs the sterile control plant. Color value indicates degree of up- (red) or down- regulation (blue). Genes are grouped based on the pattern of regulation.

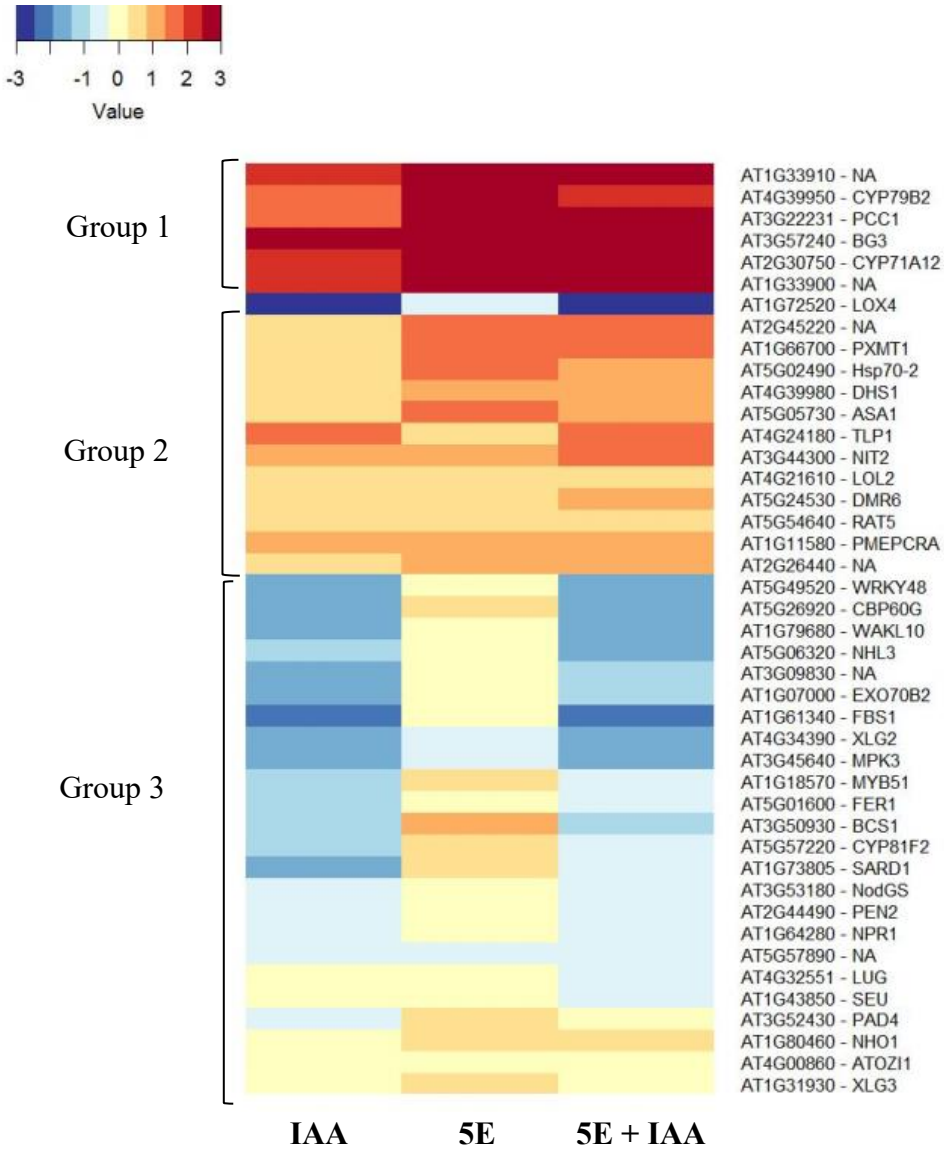

Figure 4.11. Differential expression of SAUR genes. SAUR genes significantly regulated in Col-0 treated with 1 µM IAA, DAB 5E, and DAB 5E + 1 µM IAA, compared to the sterile control. Each column represents the log2 ratio of the treated plant vs the sterile control plant. Color value indicates degree of up- (red) or down- regulation (blue).

IAA	5E	5E + IAA		
1.561	1.362	1.819	SAUR9	AT4G36110
1.034	-0.036	1.664	SAUR15	AT4G38850
1.068	0.478	2.757	SAUR19	AT5G18010
0.985	-0.451	2.790	SAUR20	AT5G18020
-0.166	0.249	0.120	SAUR21	AT5G01830
0.287	-0.393	2.220	SAUR22	AT5G18050
0.061	-0.378	1.110	SAUR23	AT5G18060
0.745	0.057	1.978	SAUR24	AT5G18080
0.998	-0.041	3.118	SAUR26	AT3G03850
2.458	1.318	4.336	SAUR27	AT3G03840
0.617	0.090	3.184	SAUR28	AT3G03830
0.990	-0.222	2.975	SAUR29	AT3G03820
1.216	0.793	1.491	SAUR36	AT2G45210
0.046	-1.214	1.291	SAUR68	AT1G29510
0.963	0.000	1.021	SAUR75	AT5G27780

CHAPTER 5

Conclusion

The goal of this thesis was to understand biochemical, molecular and physiological interactions between duckweed associated bacteria and *A. thaliana,* in addition to interactions within the duckweed microbiome itself, with a focus on the auxin pathway. The specific aims were to 1) Characterize the duckweed microbiome by auxin production to identify potential growth promoting strains, 2) Determine the mechanisms of plant-bacteria interactions via the auxin pathway, and 3) Determine the mechanisms of auxin signaling within tripartite interactions.

The results from this work will enhance our knowledge of the duckweed microbiome which to date has not been well characterized. The Lam lab's collection of diverse duckweed clones from all over the world has provided a unique resource for studying duckweed associated bacteria (DABs). 47 strains of DABs were isolated from various duckweed clones, providing an excellent resource for this work and for future studies which may entail construction of synthetic bacterial communities for improved duckweed farming or understanding conserved mechanisms of plant microbiome assembly between aquatic plants such as duckweeds and land plants such as *A. thaliana*.

By characterizing the duckweed microbiome by auxin production, we identified 79% of DABs were capable of producing indole related compounds. Quantification of IAA in the bacterial supernatant by LC-MS did not correlate with results from the Salkowski assay due to the Salkowski's nonspecific detection of IAA. This assay has been commonly used to screen for production of IAA from plant associated bacteria, and thus it is advised to be used as a preliminary screen that is not conclusive. However, the

assay did reveal production of indole related compounds other than IAA, which was then confirmed by LC-MS to be indole-3-lactic acid and indole. Furthermore, DABs that produced indole, a compound known to be involved in biofilm production, were associated with being derived from the rootless duckweed genus, *Wolffia*. Whether indole plays a role in the bacterium's attachment to plant tissue remains unknown. The roles of these indole related compounds in plant-microbe interactions should be further studied.

Use of binary association assays to study the mechanisms of plant-bacteria interactions led to the discovery of two genetically similar *Microbacterium* strains that produce different physiological effects on *A. thaliana.* DAB 1A, capable of producing high levels of IAA, resulted in a short root phenotype whereas DAB 33B, capable of producing low levels of IAA, did not. Yet both strains caused enrichment of genes in the plant's auxin response pathway. This suggests the plant's ability to regulate auxin responsive genes independent of an auxin-related short root phenotype. Additionally, use of auxin mutants, *axr1-3* and *tmk 1,3,4/+,* revealed potential unknown roles of the AXR1 gene in bacterial response mechanisms.

Tripartite assays involving two DABs and *A. thaliana* were necessary to study auxin signaling within a more realistic scenario of a community context. Two strains, DAB 1A and DAB 5E, produced inverse root phenotypes on *A. thaliana,* and thus were the focus of this aim. We propose a mechanism in which *Herbaspirillum* strain DAB 5E interacts with *Microbacterium* strain DAB 1A. DAB 5E suppressed the short root phenotype caused by DAB 1A and reduced the amount of strongly attached DAB 1A to the plant tissues. In nutrient limited culture, DAB 5E grew well on the filtered supernatant of DAB 1A, indicating its ability to utilize the other bacterium's products as

an energy source. This may be through IAA since DAB 5E contains the iac locus involved in IAA degradation and moreover, we detected a loss of IAA when spiked into DAB 5E cultures. This mechanism appears to be associated with its ability to produce ILA. It also appears to be induced in a concentration dependent manner, which may explain DAB 5E production of low levels of IAA and the plant's persistent response to IAA when co-inoculated with DAB 5E and IAA. Treatment with IAA downregulated the expression of genes involved in the plant's response to bacterium whereas treatment with DAB 5E created a pattern-triggered immunity (PTI) response in the plant. Thus, DAB 5E appears to degrade IAA when at high levels, which improves its growth and competition with other strains, while maintaining IAA response in the plant to escape detection.

The initial chemical screening of indole related compounds informed selection of binary association assays which then informed selection of tripartite experiments, resulting in successfully characterizing the duckweed microbiome via the auxin pathway and revealing mechanisms of bacterial interactions. The findings presented here will impact how bacteria are used in agriculture, particularly by improving our knowledge of plant microbiome assembly for proper construction of synthetic bacterial communities. Hopefully this thesis will be a step upwards in the monumental effort to enhance plant health for feeding and sustaining our growing population.

References

Appenroth, K. J., Sree, K. S., Böhm, V., Hammann, S., Vetter, W., Leiterer, M., et al. (2017). Nutritional value of duckweeds (Lemnaceae) as human food. *Food chemistry* 217, 266-273.

Aziz, R. K., Bartels, D., Best, A. A., DeJongh, M., Disz, T., Edwards, R. A., et al. (2008). The RAST server: rapid annotations using subsystems technology. *BMC Genomics* 9,75.

Bai, Y., Müller, D. B., Srinivas, G., Garrido-Oter, R., Potthoff, E., Rott, M., et al. (2015). Functional overlap of the Arabidopsis leaf and root microbiota. *Nature 528,* 364.

Baker, G. C., Smith, J. J., and Cowan, D. A. (2003). Review and re-analysis of domain-specific 16S primers. *J. Microbiol. Methods*, 55 (3), 541–555.

Bashan, Y., and de-Bashan, L. E. (2010). How the plant growth-promoting bacterium *Azospirillum* promotes plant growth - a critical assessment. *Adv. Agron*. 108, 77–136.

Berendsen, R. L., Pieterse, C. M., & Bakker, P. A. (2012). The rhizosphere microbiome and plant health. *Trends in plant science* 17, 478-486.

Berg, M., & Koskella, B. (2018). Nutrient-and dose-dependent microbiome-mediated protection against a plant pathogen. *Current Biology* 28, 2487-2492.

Bianco, C., Imperlini, E., Calogero, R., Senatore, B., Amoresano, A., Carpentieri, A., et al. (2006). Indole-3-acetic acid improves *Escherichia coli's* defences to stress. *Arch. Microbiol*. 185, 373–382.

Borisjuk, N., Chu, P., Gutierrez, R., Zhang, H., Acosta, K., Friesen, N., et al. (2015). Assessment, validation and deployment strategy of a two-barcode protocol for facile genotyping of duckweed species. *Plant Biol.* 1, 42–49.

Brettin, T., Davis, J. J., Disz, T., Edwards, R. A., Gerdes, S., Olsen, G. J., et al. (2015). RASTtk: a modular and extensible implementation of the RAST algorithm for building custom annotation pipelines and annotating batches of genomes. *Sci. Rep.* 5:8365.

Broek, A. V., Lambrecht, M., Eggermont, K., & Vanderleyden, J. (1999). Auxins upregulate expression of the indole-3-pyruvate decarboxylase gene in Azospirillum brasilense. *Journal of Bacteriology* 181, 1338-1342.

Bulgarelli, D., Rott, M., Schlaeppi, K., Ver Loren van Themaat, E., Ahmadinejad, N., Assenza, F., et al. (2012). Revealing structure and assembly cues for Arabidopsis root-inhabiting bacterial microbiota. *Nature* 488, 91–95.

Chakravorty, S., Helb, D., Burday, M., Connell, N., and Alland, D. (2007). A detailed analysis of 16S ribosomal RNA gene segments for the diagnosis of pathogenic bacteria. *J. Microbiol. Methods* 69, 330–339.

Chaw, S. M., Chang, C. C., Chen, H. L., and Li, W. H. (2004). Dating the monocot-dicot divergence and the origin of core eudicots using whole chloroplast genomes. *J. Mol. Evol.* 58, 424–441.

Cheng, J. J., and Stomp, A.-M. (2009). Growing duckweed to recover nutrients from wastewaters and for production of fuel ethanol and animal feed. *Clean Soil Air Water* 37, 17–26.

Dai, N., Wang, W., Patterson, S. E., & Bleecker, A. B. (2013). The TMK subfamily of receptor-like kinases in Arabidopsis display an essential role in growth and a reduced sensitivity to auxin. *PLoS One* 8, e60990.

Dhungana, S. A., & Itoh, K. (2019). Effects of Co-Inoculation of Indole-3-Acetic Acid-Producing and-Degrading Bacterial Endophytes on Plant Growth. *Horticulturae* 5, 17.

Donoso, R., Leiva-Novoa, P., Zúñiga, A., Timmermann, T., Recabarren-Gajardo, G., & González, B. (2017). Biochemical and genetic bases of indole-3-acetic acid (auxin phytohormone) degradation by the plant-growth-promoting rhizobacterium Paraburkholderia phytofirmans PsJN. *Appl. Environ. Microbiol.* 83, e01991-16.

Duca, D., Lorv, J., Patten, C. L., Rose, D., & Glick, B. R. (2014). Indole-3-acetic acid in plant–microbe interactions. *Antonie Van Leeuwenhoek* 106, 85-125.

Eckert, M., & Kaldenhoff, R. (2000). Light-induced stomatal movement of selected Arabidopsis thaliana mutants. *Journal of Experimental Botany* 51, 1435-1442.

Edwards, J., Johnson, C., Santos-Medellin, C., Lurie, E., Podishetty, N. K., Bhatnagar, S., et al. (2015). Structure, variation and assembly of the root-associated microbiomes of rice. *Proc. Natl. Acad. Sci. U.S.A.* 112, E911–E920.

Finkel, O. M., Salas-González, I., Castrillo, G., Law, T. F., Conway, J. M., Jones, C. D., & Dangl, J. L. (2019). Root development is maintained by specific bacteria-bacteria interactions within a complex microbiome. *BioRxiv* 645655.

Gilbert, S., Xu, J., Acosta, K., Poulev, A., Lebeis, S., & Lam, E. (2018). Bacterial production of indole related compounds reveals their role in association between duckweeds and endophytes. *Frontiers in chemistry* 6, 265.

Glickmann, E., and Dessaux, Y. (1995). A critical examination of the specificity of the Salkowski Reagent for indolic compounds produced by phytopathogenic bacteria. *Appl. Environ. Microbiol.* 61, 793–796.

Gordon, S. A., and Weber, R. P. (1951). Colorimetric estimation of indoleacetic acid. *Plant Physiol.* 26, 192–195.

Greenhut, I. V., Slezak, B. L., & Leveau, J. H. (2018). iac gene expression in the indole-3-acetic acid-degrading soil bacterium Enterobacter soli LF7. *Appl. Environ. Microbiol.* 84, e01057-18.

Haney, C. H., Samuel, B. S., Bush, J., and Ausubel, F. M. (2015). Associations with rhizosphere bacteria can confer an adaptive advantage to plants. *Nat. Plants*. 1:15051.

He, Z. H., He, D., & Kohorn, B. D. (1998). Requirement for the induced expression of a cell wall associated receptor kinase for survival during the pathogen response. *The Plant Journal* 14, 55-63.

Helfrich, E. J., Vogel, C. M., Ueoka, R., Schäfer, M., Ryffel, F., Müller, D. B., ... & Vorholt, J. A. (2018). Bipartite interactions, antibiotic production and biosynthetic potential of the Arabidopsis leaf microbiome. *Nature microbiology* 3, 909.

Jones, J. D., & Dangl, J. L. (2006). The plant immune system. *Nature* 444, 323.

Landolt, E., & Kandeler, R. (1987). The Family of Lemnaceae—A Monographic Study (Volume 2). *Veroff. Geobot. Inst. ETH* 95.

Kamilova, F., Kravchenko, L. V., Shaposhnikov, A. I., Azarova, T., Makarova, N., and Lugtenberg, B. (2006). Organic acids, sugars, and L-tryptophane in exudates of vegetables growing on stonewool and their effects on activities of rhizosphere bacteria. *Mol. Plant-Microbe Interact*. 19, 250–256.

Korner, S., and Vermaat, J. E. (1998). The relative importance of *Lemna gibba* L., bacteria and algae for the nitrogen and phosphorus removal in duckweed-covered domestic wastewater. *Water Res.* 32, 3651–3661.

Lee, J. H., and Lee, J. (2010). Indole as an intercellular signal in microbial communities. *FEMS Microbiol. Rev*. 34, 426–444.

Leveau, J. H., & Gerards, S. (2008). Discovery of a bacterial gene cluster for catabolism of the plant hormone indole 3-acetic acid. *FEMS microbiology ecology* 65, 238-250.

Li, Y., Kurepa, J., & Smalle, J. (2013). AXR1 promotes the Arabidopsis cytokinin response by facilitating ARR5 proteolysis. *The Plant Journal* 74, 13-24.

Lincoln, C., Britton, J. H., & Estelle, M. (1990). Growth and development of the axr1 mutants of Arabidopsis. *The Plant Cell* 2, 1071-1080.

Lincoln, C., & Estelle, M. (1991). The axr1 Mutation of Arabidopsis is Expressed 10 Booth Roots and Shoots. *Journal of the Iowa Academy of Science: JIAS* 98, 68-71.

Lui, P., and Nester, E. W. (2006). Indoleacetic acid, a product of transferred DNA, inhibits *vir* gene expression and growth of *Agrobacterium tumefaciens*C58. *Proc. Natl. Acad. Sci. U.S.A.* 103, 4658–4662.

Lundberg, D. S., Lebeis, S. L., Paredes, S. H., Yourstone, S., Gehring, J., Malfatti, S., et al. (2012). Defining the core *Arabidopsis thaliana* root microbiome. *Nature* 488, 86–90.

Mano, Y., & Nemoto, K. (2012). The pathway of auxin biosynthesis in plants. *Journal of experimental Botany* 63, 2853-2872.

Martino, P. D., Fursy, R., Bret, L., Sundararaju, B., and Phillips, R. S. (2003). Indole can act as an extracellular signal to regulate biofilm formation of *Escherichia coli* and other indole-producing bacteria. *Can. J. Microbiol.* 49, 443–449.

Meier, S., Ruzvidzo, O., Morse, M., Donaldson, L., Kwezi, L., & Gehring, C. (2010). The Arabidopsis wall associated kinase-like 10 gene encodes a functional guanylyl cyclase and is co-expressed with pathogen defense related genes. *PloS one* 5, e8904.

Melotto, M., Underwood, W., Koczan, J., Nomura, K., & He, S. Y. (2006). Plant stomata function in innate immunity against bacterial invasion. *Cell* 126, 969-980

Michael, T. P., Bryant, D., Gutierrez, R., Borisjuk, N., Chu, P., Zhang, H., et al. (2017). Comprehensive definition of genome features in *Spirodela polyrhiza*by high-depth physical mapping and short-read DNA sequencing strategies. *Plant J.* 89, 617–635.

Navarro, L., Dunoyer, P., Jay, F., Arnold, B., Dharmasiri, N., Estelle, M., ... & Jones, J. D. (2006). A plant miRNA contributes to antibacterial resistance by repressing auxin signaling. *Science* 312, 436-439.

Oldroyd, G. E., Harrison, M. J., & Paszkowski, U. (2009). Reprogramming plant cells for endosymbiosis. *Science* 324, 753-754.

Ona, O., Van Impe, J., Prinsen, E., & Vanderleyden, J. (2005). Growth and indole-3-acetic acid biosynthesis of Azospirillum brasilense Sp245 is environmentally controlled. *FEMS Microbiology Letters* 246, 125-132.

Overbeek, R., Olson, R., Pusch, G. D., Olsen, G. J., Davis, J. J., Disz, T., et al. (2013). The SEED and the rapid annotation of microbial genomes using subsystems technology (RAST) *Nucleic Acids Res.* 42, D206–D214.

Paredes, S. H., Gao, T., Law, T. F., Finkel, O. M., Mucyn, T., Teixeira, P. J. P. L., et al. (2018). Design of synthetic bacterial communities for predictable plant phenotypes. *PLoS biology* 16, e2003962.

Ristova, D., Carré, C., Pervent, M., Medici, A., Kim, G. J., Scalia, D., et al. (2016). Combinatorial interaction network of transcriptomic and phenotypic responses to nitrogen and hormones in the Arabidopsis thaliana root. *Sci. Signal.* 9, rs13-rs13.

Rudrappa, T., Czymmek, K. J., Paré, P. W., & Bais, H. P. (2008). Root-secreted malic acid recruits beneficial soil bacteria. *Plant physiology* 148, 1547-1556.

Santoyo, G., Moreno-Hagelsieb, G., Orozco-Mosqueda, M. C., and Glick, B. R. (2016). Plant growth-promoting bacterial endophytes. *Microbio. Res*. 183, 92–99.

Spaepen, S., and Vanderleyden, J. (2011). Auxin and plant-microbe interactions. *Cold Spring Harb. Perspect. Biol.* 3, a001438.

Spaepen, S., Vanderleyden, J., and Remans, R. (2007). Indole-3-acetic acid in microbial and microorganism-plant signaling. *FEMS Microbiol. Rev*. 31, 425–448.

Suzuki, W., Sugawara, M., Miwa, K., and Morikawa, M. (2014). Plant growth-promoting bacterium *Acinetobacter calcoaceticus* P23 increases the chlorophyll content of the monocot *Lemna minor* (duckweed) and the dicot *Lactuca sativa* (lettuce). *J. Biosci. Bioeng.* 118, 41–44.

Tiryaki, I., & Staswick, P. E. (2002). An Arabidopsis mutant defective in jasmonate response is allelic to the auxin-signaling mutant axr1. *Plant physiology* 130, 887-894.

Wang, Z., Yang, L., Liu, Z., Lu, M., Wang, M., Sun, Q., et al. (2019). Natural variations of growth thermo-responsiveness determined by SAUR 26/27/28 proteins in Arabidopsis thaliana. *New Phytologist*.

Yamaga, F., Washio, K., and Morikawa, M. (2010). Sustainable biodegradation of phenol by *Acinetobacter calcoaceticus* P23 isolated from the rhizosphere of duckweed *Lemna aoukikusa*. *Environ. Sci. Technol.* 44, 6470–6476.